Novel signaling routes and molecular determinants for leukotriene biosynthesis

Dissertation

to fulfill the

Requirements for the Degree of

„doctor rerum naturalium“ (Dr. rer. nat.)

Submitted to the Council of the Faculty of

Biological Sciences

of the Friedrich Schiller University Jena

by Dipl.-Pharm. Erik Romp

born on July the 20th, 1990 in Arnstadt

1st Reviewer: Prof. Dr. Oliver Werz, FSU Jena
2nd Reviewer: Prof. Dr. Gerhard K. E. Scriba, FSU Jena
3rd Reviewer: Prof. Dr. Nils H. Schebb, BU Wuppertal

Date of submission: 19.12.2019

Date of defense: 16.07.2020

TABLE OF CONTENTS

ACKNOWLEDGEMENTS

Nachfolgend würde ich gern einigen ausgewählten Förderern und Wegbegleitern meinen Dank für ihre Unterstützung bei der Anfertigung dieser Dissertation aussprechen.

Zunächst möchte ich mich bei Prof. Dr. Oliver Werz für die bereitwillige Übernahme und Betreuung meiner Promotion, aber auch für meine gesamte universitäre und wissenschaftliche Ausbildung sowie für seine professionelle Unterstützung bei zahlreichen Projekten, Stipendien und Forschungsarbeiten bedanken.

Darüber hinaus gilt mein besonderer Dank Prof. Dr. Ulrike Garscha für ihre intensive fachliche Betreuung und die erfolgreiche Zusammenarbeit der letzten Jahre. In ihr habe ich nicht nur eine Mentorin in wissenschaftlichen Fragen, sondern auch eine Vertraute in allen Lebenslagen gefunden. Liebe Ulrike, ich danke Dir für deine ermutigenden Worte, die mir die Kraft und Motivation gegeben haben die Promotion abzuschließen und mich zudem in meiner Persönlichkeit gestärkt haben.

PD Dr. Lorena Tuchscherr und ihren Doktorandinnen Vandana Arakandy und Anke Siegmund danke ich für eine produktive Kooperation, den regen Wissensaustausch und die Bereitstellung von Tierproben sowie *S. aureus* Stämmen.

Weiterhin möchte ich einen Dank an Prof. Dr. Gerhard K. E. Scriba aussprechen, der bereits zu Studienzeiten immer mit einem Rat zur Stelle war und der mich auch im Laufe der Promotion nicht nur mit seinen zahllosen Gutachten stets unterstützte und motivierte.

Zahlreiche Experimente und Konferenzen wären zudem nicht durch eine entsprechende Finanzierung möglich gewesen. In diesem Sinne möchte ich mich für den Erhalt des Landesgraduiertenstipendiums der Graduiertenakademie Jena und des Landes Thüringen sowie für die Zuwendungen der Forschungsgemeinschaft RTG 1715 *Molecular Signatures of Adaptive Stress Responses* bedanken.

Mein ausdrücklicher Dank gilt aber meinen Weggefährten Markus Werner und Jana Fischer. Ohne euch als Freunde, Vertraute und Kollegen hätte ich sicher nicht das Promotionsziel erreicht. Ich danke euch für die unzähligen Gespräche und Ratschläge sowie für eure treue Freundschaft, die schon im Studium begann und als Leidensgenossen im Labor fortgeführt wurde, in guten wie in schlechten Zeiten.

Für die experimentelle und gleichzeitige freundschaftliche Zusammenarbeit sowie ihre tatkräftige Unterstützung danke ich weiterhin Nadja, Katrin, Petra, Stefanie K., Stefanie L., Konstantin L., Konstantin K., Helmut, Christian, Laura, Friedemann, Finja und Verena.

Neben dem genannten universitären Rahmen wäre diese Dissertation aber keinesfalls ohne die Unterstützung meines privaten Umfeldes möglich gewesen. Daher danke ich vor allem Anna und Benni für unsere tiefe Verbundenheit seit der Schulzeit und die Kraft, die ich aus eurem Beistand und aus unserem Trio ziehe. Außerdem möchte ich Maxi und Franzi für unsere gemeinsamen Erlebnisse und Gespräche danken, die mir geholfen haben im Laufe dieses turbulenten Lebensabschnittes nicht den Fokus auf das Wesentliche zu verlieren.

Abschießend jedoch gilt der größte Dank meiner Familie, für ihre Unterstützung in allen Lebenslagen, ihre Toleranz für all meine Entscheidungen und unseren bedingungslosen Zusammenhalt. Diese Promotionsarbeit, aber auch mein gesamter akademischer Werdegang, wäre ohne euch und ohne die persönlichen Werte und charakterlichen Eigenschaften, die ihr mir auf meinem Lebensweg vermittelt habt, nicht möglich gewesen. Ich danke und liebe euch!

Für dich!
A. Romp · 14.06.1920 – 23.02.2017

SUMMARY

Leukotrienes (LTs), originated from the enzymatic oxygenation of the *C-20:4* polyunsaturated arachidonic acid (AA) by 5-lipoxygenase (5-LOX) and its helper protein 5-lipoxygenase-activating protein (FLAP), are important mediators involved in inflammation (1). While cyclooxygenase-(COX)-derived prostaglandins (PGs) are mediating both physiological and pathophysiological functions, 5-LOX activation has primarily been associated to inflammatory conditions (2). However, to date the agents and receptors inducing 5-LOX activation and LT biosynthesis are not completely understood. In particular, how pathogenic bacteria elicit LT formation under infectious conditions is poorly characterized.

The molecular mechanism of bacteria-induced 5-LOX activity was studied in the first part of this thesis. Investigations with cell-free bacteria-conditioned medium (BCM) revealed bacterial exotoxins, primarily secreted by pathogenic strains, as crucial determinants for *in cellulo* 5-LOX activation in HEK293 cells and human neutrophils. Since *Staphylococcus* (*S.*) *aureus* infections and the concomitant rise of antibiotic resistant strains are a common threat to human (3,4), this study focused on staphylococcal toxins and their impact on lipid mediator (LM) biosynthesis. While 5-LOX, stably co-transfected with FLAP in non-immunocompetent HEK293 cells, could be activated by both staphylococcal phenol-soluble modulins (PSMs) and α-hemolysin, LT formation in neutrophils was exclusively induced by amphipathic α-helical PSM peptides. Incubations with BCM of genetically modified *S. aureus* devoid of PSM expression substantiated PSMs as key activators of LT biosynthesis in neutrophils. Interestingly, other branches of the AA pathway (*e.g.* COX, 12- or 15-LOX) appeared to be stimulated by other exotoxins apart from PSMs. Supporting this data, we found altered LT biosynthesis *in vivo* after infection of mice paws with *S. aureus* USA300Δ*psm*αβ compared to the corresponding wildtype bacteria, whereas the biosynthesis of COX-derived mediators was independent of PSM presence. Moreover, PSM-induced LT formation of neutrophils was mediated via the G_i-protein-coupled formyl peptide receptor 2 (FPR2), and selective inhibition of FPR2 by the synthetic peptide WRW4 prevented LM biosynthesis. PSMs thereby provoked an intracellular Ca^{2+} increase and activation of the extracellular-signal regulated protein kinase ERK1/2, both known to induce 5-LOX activity (5-7). Accordingly, LT formation in neutrophils upon PSM challenge was decreased after Ca^{2+}-chelation or inhibition of ERK1/2 activation. Taken together, our findings underline the impact of bacterial exotoxins as inducers of LT biosynthesis, particularly PSMs acting via the FPR2 during *S. aureus*-induced infections, which should be considered as prospective strategy for the treatment of inflammatory/infectious disorders.

Targeting 5-LOX and/or FLAP displays a common strategy to modulate LT biosynthesis (5,8). While the direct 5-LOX inhibitor zileuton is applied in asthmatic diseases (9,10) and numerous natural products affect 5-LOX activity (11), only few FLAP inhibitors have been studied in clinical trials and none could reach the pharmaceutical market so far (8,10). Moreover, although an interaction of 5-LOX and FLAP appeared to be crucial for LT biosynthesis (12), the structural requirements for the assembly of a LT-synthetic complex at the nuclear membrane remained elusive. Thus, the second part of this thesis focused on the mutagenesis of FLAP to deepen the knowledge about 5-LOX/FLAP interaction and subsequent LT

formation. Modifications within the second cytosolic loop (C2) of nuclear membrane-bound FLAP significantly altered FLAP-mediated 5-LOX activity in a HEK293 cell model, while variations of residues located on other FLAP-domains did not notably affect 5-LOX product formation. In detail, mutagenesis, or deletion of Ser^{108} (and minorly Tyr^{112}) entirely prevented the *in situ* interaction of 5-LOX and FLAP and diminished the FLAP-supported formation of leukotriene A_4 (LTA_4) from its precursor 5-hydroperoxyeicosatetraenoic acid (5-HpETE). Simultaneously, 5-LOX subcellular translocation and co-localization with FLAP were found to be unaffected from FLAP mutagenesis and independent of the location of mutated residues. However, it remains to be clarified whether structural modification of loop C2 directly disrupts a physical 5-LOX/FLAP interaction by steric hindrance or rather alters the presentation of AA and 5-HpETE to the active site of 5-LOX by FLAP. Nevertheless, our data reveal the C2-loop of FLAP as potential molecular target for novel FLAP inhibitors to pharmacologically modulate LT biosynthesis. Besides, we discussed Ser^{108} as putative phosphorylation site of FLAP. Although striking effects on 5-LOX product formation were found for the FLAP mutant carrying a phosphomimetic *S108D*, we failed to demonstrate FLAP as target for cellular kinases by phospho-proteomic approaches with HEK_5-LOX/FLAP cells and human neutrophils. However, phosphoregulation of MAPEG-proteins (membrane-associated proteins in eicosanoid and glutathione metabolism) as it was recently reported for leukotriene C_4 synthase (LTC_4S) (13) should be explored in future studies for elucidating the molecular regulation of LM biosynthesis. In summary, our data provide new insights into the role of distinct FLAP residues during the formation and activity of the LT-biosynthetic 5-LOX/FLAP protein complex.

ZUSAMMENFASSUNG

Die enzymatische Oxidation der *C-20:4* ungesättigten Fettsäure Arachidonsäure (AA) durch 5-Lipoxygenase (5-LOX) im Zusammenspiel mit dem zellulären Helfer 5-Lipoxygenase-aktivierendes Protein (FLAP) resultiert in der Bildung und Freisetzung von Leukotrienen (LTs). Diese stellen bedeutsame para- und autokrine Botenstoffe dar und sind in zahlreiche inflammatorische Erkrankungen involviert (1). Während durch Cyclooxygenasen (COX) gebildete Prostaglandine (PG) sowohl pro- als auch anti-inflammatorische Funktionen ausüben, wurde eine Aktivierung von 5-LOX weitestgehend mit entzündlichen Prozessen assoziiert (2). Bis heute jedoch sind die Faktoren pathogener Mikroorganismen und die Rezeptoren, die zur Bildung von LTs im Verlauf einer Infektion führen, noch immer nicht vollständig aufgeklärt.

Im ersten Teil der vorliegenden Arbeit sollte zunächst der molekulare Mechanismus einer bakteriell-induzierten 5-LOX-Aktivierung identifiziert werden. Unsere Untersuchungen mit steril-filtrierten Kulturmedien (BCM) pathogener Bakterien zeigten dabei die Notwendigkeit von mikrobiell-sekretierten Toxinen für die *in cellulo* Stimulation von 5-LOX, sowohl in einem nicht-immunkompetenten HEK293 Zellmodel als auch in humanen Neutrophilen. Im weiteren konzentrierten sich unsere Experimente auf das Bakterium *Staphylococcus* (*S.*) *aureus*, das wiederholt mit lebensbedrohlichen Infektionen, aber auch mit einer zunehmenden Resistenz gegen gängige Antibiotika in Verbindung gebracht wird (3,4). Dabei untersuchten wir zunächst den Zusammenhang zwischen der Expression von *Staphylococcus*-Toxinen und ihrem Einfluss auf die Lipidmediator-(LM)-Synthese. Während sowohl α-Hemolysin als auch Phenol-soluble moduline (PSMs) die mit FLAP co-transfizierte 5-LOX in HEK293 Zellen aktivierten, konnten 5-LOX-Translokation und LT-Biosynthese in Neutrophilen ausschließlich durch PSMs induziert werden. Zusätzlich unterstrichen Untersuchungen mit genetisch modifizierten *S. aureus* LS1 Stämmen die sekretierten PSMs als Schlüsselfaktoren für die LT-Bildung in neutrophilen Leukozyten. Andere LM-bildende Enzyme (z.B. COX, 12- oder 15-LOX) schienen dabei jedoch durch andere Exotoxine beeinflusst zu werden. Darüber hinaus zeigte ein *in vivo* Mausmodell verminderte LT-Gewebskonzentrationen nach subkutaner Infektion mit einem *S. aureus* USA300Δ*psm*αβ Knockout-Stamm im Vergleich zur Wildtyp-Kontrolle, obwohl die Abwesenheit von PSMs gleichzeitig keinen Einfluss auf die COX-vermittelte Bildung von PGs und Thromboxan ausübte. In Übereinstimmung mit aktuellen Veröffentlichungen identifizierten wir außerdem den G_i-Protein-gekoppelten Formyl Peptide Rezeptor 2 (FPR2) als molekulares Target für PSMs in humanen Neutrophilen. Entsprechend konnte die PSM-induzierte LT-Bildung nahezu vollständig durch den selektiven Antagonismus an FPR2 durch das synthetische Peptid WRW4 verhindert werden. Zudem konnten wir die PSM-vermittelte LM-Biosynthese auf eine Erhöhung der intrazellulären Ca^{2+}-Konzentration und auf die Stimulierung der Extrazellulär-Signal-regulierten Proteinkinase ERK1/2 zurückführen. Beide Faktoren sind als Induktoren der 5-LOX-Aktivität bekannt (5-7), und sowohl die Komplexierung freier Ca^{2+}-Ionen als auch die Hemmung der zellulären ERK1/2-Aktivität führten zur Reduktion der PSM-abhängigen LT-Bildung in unseren Experimenten. Zusammenfassend unterstreichen unsere Daten die Sekretion von Exotoxinen und die Aktivierung des FPR2 Rezeptors durch *S. aureus* PSMs als wichtige Induktoren der 5-LOX-Aktivität. Diese Erkenntnisse sollten zukünftig

Eingang in die Behandlung infektiös-entzündlicher Erkrankungen erhalten.

Eine verbreitete Strategie zur pharmakologischen Beeinflussung der LT-Biosynthese ist die Modulation von 5-LOX und/oder FLAP (5,8). Während mit dem Hydroxyharnstoff Zileuton ein direkter 5-LOX-Inhibitor therapeutischen Einsatz bei asthmatischen Erkrankungen findet (9,10) und auch für zahlreiche Naturprodukte eine Hemmung der 5-LOX-Aktivität beschrieben werden konnte (11), wurden bisher nur wenige FLAP-Inhibitoren in klinischen Studien untersucht und kein einziger Kandidat wurde zur Marktreife entwickelt (8,10). Obwohl gezeigt werden konnte, dass die direkte Interaktion von 5-LOX und FLAP entscheidend für die LT-Biosynthese ist (12), wurden bisher keine genauen Aminosäuren oder strukturelle Erfordernisse für die Formation des LT-synthetisierenden Proteinkomplexes diskutiert. Der zweite Teil dieser Dissertation beschäftigt sich daher mit der Modifikation ausgewählter Strukturelemente im FLAP, um so die bisherigen Erkenntnisse der Interaktion mit 5-LOX und der damit verbundenen LT-Synthese zu ergänzen. Dabei konnten wir zeigen, dass Variationen in der zweiten zytosolischen Schleife (C2) des integralen Membranproteins deutlich die 5-LOX-Aktivität in HEK293-Zellen beeinflussten, während Mutationen von Aminosäuren anderer FLAP-Domänen kaum Änderungen gegenüber der Wildtyp-Form verursachten. Im Detail resultierte der Austausch bzw. die Entfernung von Ser^{108} (und geringfügig von Tyr^{112}) in der vollständigen Prävention der *in situ* 5-LOX/FLAP Interaktion und verringerte die FLAP-vermittelte Synthese von Leukotrien A_4 (LTA_4). Gleichzeitig zeigte keine der getesteten Mutationen einen Einfluss auf die zelluläre 5-LOX-Translokation und Co-Lokalisierung mit FLAP, unabhängig von der Lokalisation der abgewandelten Aminosäuren im Protein. Zwar konnte hier nicht vollständig geklärt werden, ob eine strukturelle Modifikation des C2-Loops direkt die physische Wechselwirkung von 5-LOX und FLAP durch eine sterische Hinderung oder vielmehr durch einen veränderten Transfer von AA und/oder 5-HpETE zum aktiven Zentrum der 5-LOX bedingt. Dennoch identifizieren unsere Daten die zweite zytosolische Schleife des FLAP-Proteins als potentielle neuartige Bindestelle für Inhibitoren zur pharmakologischen Modulation der LT-Bildung. Darüber hinaus vermuten wir Ser^{108} als mögliche Phosphorylierungsstelle innerhalb FLAPs. Obwohl deutliche Veränderungen der 5-LOX Produktbildung für die phosphomimetische FLAP-Isoform *S108D* auftraten, gelang kein finaler Beweis einer zellulären Phosphorylierung durch Phosphoproteom-Analysen an HEK_5-LOX/FLAP-Zellen oder humanen Neutrophilen. Dennoch sollte die Möglichkeit der Regulation von MAPEG-Proteinen (Membran-assoziierte Proteine im Eikosanoid- und Glutathion-metabolismus) durch zelluläre Proteinkinasen für zukünftige Studien der LM-Biosynthese in Betracht gezogen werden, da erst kürzlich ein derartiger Mechanismus auch für die FLAP-verwandte Leukotrien C_4 Synthase (LTC_4S) veröffentlicht wurde (13). Zusammenfassend geben unsere Daten einen neuartigen Einblick in die Rolle verschiedener FLAP-Domänen bei der Bildung und Aktivität des LT-synthetisierenden Proteinkomplex mit 5-LOX.

LIST OF ABBREVIATIONS

The following abbreviations are indicated once and continuatively utilized in the text, except for the chapters *Summary* and *Zusammenfassung*:

^{3}H-AA	[5,6,8,9,11,12,14,15-^{3}H(N)]-Arachidonic acid
5-LOX	5-Lipoxygenase
AA	Arachidonic acid
ADAM-10	A disintegrin and metalloproteinase domain-containing protein 10
agr	Accessory gene regulator
AIP	Autoinducing peptide
ATP	Adenosine triphosphate
BCM	Bacteria-conditioned medium
BHI	Brain heart infusion broth
BSA	Bovine serum albumin
C5a	Complement component 5a
CFU	Colony-forming units
CHIPS	Chemotaxis inhibitory protein of *S. aureus*
CLP	Coactosin-like protein
COX	Cyclooxygenase
cPLA$_2$	Cytosolic (Ca^{2+}-dependent) phospholipase A_2
CTR	Conjugate in tissue regeneration
CYP	Cytochrome P450
cysLT	Cysteinyl leukotriene
DAPI	4',6-diamidino-2-phenylindole
DHA	Docosahexaenoic acid
DiHETE	Dihydroxyeicosatetraenoic acid
DiHETrE	Dihydroxyeicosatrienoic acid
E. coli	*Escherichia coli*
EET	Epoxyeicosatrienoic acid
EPA	Eicosapentaenoic acid
eLOX-3	Epidermal LOX-3
ERK	Extracellular-signal regulated kinase
FA	Fatty acid
FCS	Fetal calf serum
FLAP	5-LOX-activating protein
FLIPr	FPRL1 inhibitory protein
fMLP	N-formylmethionyl-leucyl-phenylalanine
FPR	Formyl peptide receptor
FPRL1	FPR-like 1
GGT	γ-Glutamyl transferase
GM-CSF	Granulocyte-macrophage colony-stimulating factor
GPCR	G-protein-coupled receptor

GSH	Glutathione
HEK	Human embryonic kidney
HDHA	Hydroxydocosahexaenoic acid
HEPE	Hydroxeicosapentaenoic acid
HETE	Hydroxyeicosatetraenoic acid
HpDHA	Hydroperoxydocosahexaenoic acid
HpETE	Hydroperoxyeicosatetraenoic acid
HPLC	High-performance liquid chromatography
IF	Immunofluorescence
IL	Interleukin
LDH	Lactate dehydrogenase
LM	Lipid mediator
LOX	Lipoxygenase
LPS	Lipopolysaccharides
LT	Leukotriene
LTA_4H	LTA_4 hydrolase
LTC_4S	LTC_4 synthase
LX	Lipoxin
MAPEG	Membrane-associated proteins in eicosanoid and glutathione metabolism
MAPK	Mitogen-activated protein kinase
MAPKAP	MAPK-activated protein kinase
Mar	Maresin
MBD	Membrane-bound dipeptidase
MGST	Microsomal glutathione-S-transferase
mPGES-1	Microsomal prostaglandin E synthase-1
MS	Mass spectrometry
NB	Nutrient broth
NES	Nuclear export signal
NET	Neutrophil extracellular trap
NFκB	Nuclear factor κ-light-chain-enhancer of activated B ells
NLS	Nuclear localization signal
NSAID	Nonsteroidal anti-inflammatory drug
PAF	Platelet-activating factor
PAMP	Pathogen-associated molecular pattern
PC	Phosphatidylcholine
PCA	Principle component analysis
PD	Protectin
PFT	Pore-forming toxin
PG	Prostaglandin
PGDS	PGD_2 synthase
PGES	PGE_2 synthase
PGFS	$PGF_{2\alpha}$ synthase
PGIS	PGI_2 synthase

TBXAS1	TXA_2 synthase-1
PI3K	Phosphoinositide 3-kinase
PKA	Protein kinase A
PKC	Protein kinase C
PL	Phospholipase
PLA	Proximity ligation assay
PMNL	Polymorphonuclear leukocyte
PRR	Pattern recognition receptor
PSM	Phenol-soluble modulin
PVL	Panton-Valentine leukocidin
RAP	RNAIII activating protein
RCA	Rolling circle amplification
Rot	Repressor of toxins
RPMI	Roswell Park Memorial Institute
RT	Room temperature
Rv	Resolvin
S. aureus	*Staphylococcus aureus*
SAA	Serum amyloid A
sarA	Staphylococcal accessory regulator A
SDS	Sodium dodecyl sulfate
sEH	Soluble epoxide hydrolase
SEM	Standard error of the mean
SPE	Solid-phase extraction
SPM	Specialized pro-resolving mediator
SRS-A	Slow-reacting substance of anaphylaxis
TFA	Trifluoroacetic acid
TGF-β	Transforming growth factor β
TLR	Toll-like receptor
TNFα	Tumor necrosis factor α
TX	Thromboxane
unstim	Unstimulated
UPLC	Ultra-performance liquid chromatography
VEGF	Vascular endothelial growth factor
wt	Wildtype
w/o	Without

1 INTRODUCTION

1.1 Inflammation

1.1.1 Infection-induced inflammation

Inflammation is characterized as adaptive response to homeostatic imbalances within the human body, and various factors have been discussed to induce inflammatory processes. Microbial infection and tissue injury are thereby the most prominent and best described inflammatory inducers. In general, inflammation aims to restore homeostasis by resolving infections or repairing tissue damages (14,15).

The underlying mechanisms of inflammatory responses are well characterized for infection-induced inflammation and can partially be transferred to other inflammatory states. Infections are caused by microbial factors that can be separated into pathogen-associated molecular patterns (PAMPs) and virulence factors. The formers are defined molecular structures that can be detected by specific receptors of the host and are shared by various microorganisms, independent of their pathogenicity. In contrast, virulence factors are restricted to pathogenic microbes and execute their activities in a widely receptor-independent way, although depending on the presence of specialized sensors in some cases (15).

Tissue-resident cells such as macrophages, dendritic cells or mast cells are responsible for the recognition of microorganisms at the first site of infection. After being challenged with invading microbes, these cells induce and release a plethora of mediators including cytokines, vasoactive amines and peptides, chemokines, proteolytic enzymes, fragments of complement factors, and lipid mediators (LM) to create a local environment of inflammation (15,16). Subsequently, resulting from the activities of the indicated mediators, neutrophils circulating in the blood are recruited to the inflamed tissue (17). After extravasation, neutrophils are aiming to kill microbes by either phagocytosis, degranulation and subsequent release of antimicrobial peptides, or formation of neutrophil extracellular traps (NETs) (17). However, besides the local response to environmental changes by the innate immune system, intercellular communication of leukocytes can further activate systemic reactions and adaptive immune responses (18).

Finally, inflammatory processes are leading to the cardinal signs of an acute inflammation that were already described in ancient medicine: heat (*calor*), pain (*dolor*), redness (*rubor*), swelling (*tumor*) and loss of function (*functio laesa*), respectively (19).

While acute inflammation and its resolution are crucial control mechanisms to adequately respond to environmental challenges, several diseases are related to pronounced or unresolved inflammatory conditions (20). For instance, atherosclerosis, rheumatoid arthritis, chronic lung or liver diseases, sepsis, neurodegeneration, gastrointestinal and skin diseases, or even cancer and diabetes are characterized by increased levels of inflammatory cytokines, predominantly interleukins (ILs) such as IL-1β. Accordingly, widely applied pharmaceuticals in the therapy of these disorders are targeting inflammatory processes and thereby underline the necessity to explicitly understand the course of inflammation (20).

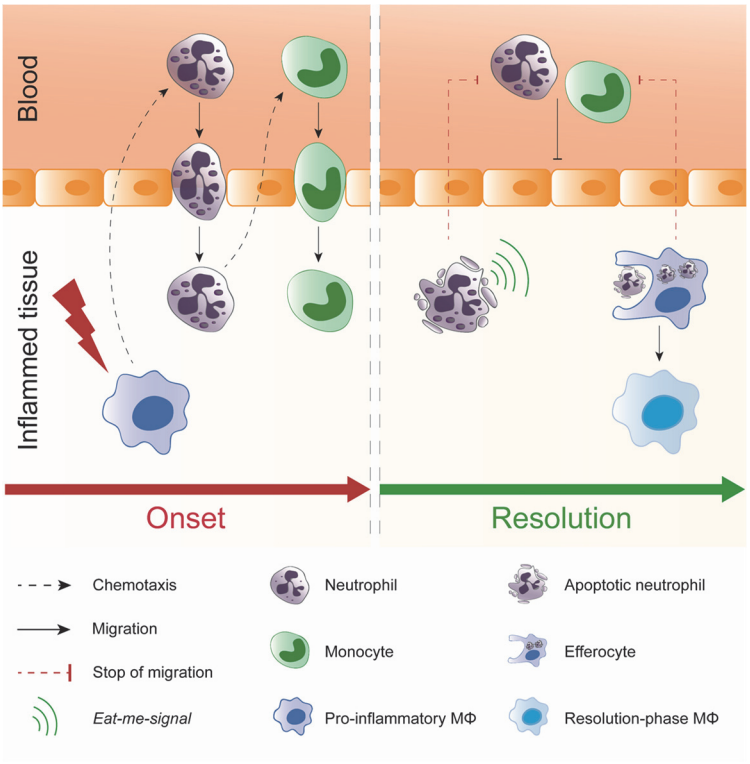

Fig. 1.1 Onset and resolution of inflammation. Adapted from Ortega-Gomez et al. 2013 (21). As soon as tissue-resident cells including pro-inflammatory macrophages (MΦ) recognize homeostatic alterations, chemotactic mediators are released, and neutrophils and monocytes start to invade. While neutrophils rapidly migrate to the site of infection and subsequently release an own subset of chemotactic agents, monocyte migration was found to be delayed in this respect. The resolution of inflammatory conditions is initiated by neutrophil apoptosis and the liberation of *eat-me-signals* to induce efferocytosis by macrophages, and to terminate further leukocyte extravasation. Moreover, macrophages transform into a resolution-phase phenotype in order to restore homeostasis within inflamed tissues.

1.1.2 Resolution of inflammation

Although acute inflammation is essential to initiate the recovery of homeostasis upon damage, unlimited and prolonged inflammatory reactions might lead to a permanent tissue disturbance and result in chronic diseases. Under normal conditions, the initial step of resolution is related to decreasing levels of chemokines and subsequent reduction of infiltrating neutrophils (21-23). Both, capturing and entrapment of chemotactic agents by decoy receptors and enhanced chemokine cleavage have been described in this respect (21,24). Additionally, apoptosis of neutrophils is induced after they have executed their anti-microbial activities and apoptotic cells are digested by macrophages. Neutrophil efferocytosis thereby drives the maturation of macrophages towards the M2-like phenotype with anti-inflammatory properties (**Fig. 1.1**) (21,25). Those macrophages mediate the resolution process by releasing anti-inflammatory mediators such as IL-10, transforming growth factor-(TGF)-β, vascular endothelial growth factor (VEGF) or specialized pro-resolving mediators (SPMs, discussed under *Eicosanoids and related lipid mediators*) (16,21). However, the termination of inflammation as an active process is still not fully understood but displays a potential strategy to manipulate inflammatory disorders (21).

1.2 Eicosanoids and related lipid mediators (LMs)

1.2.1 Biosynthetic pathways and roles of LMs

Among the group of inflammatory mediators, LMs derived from arachidonic acid (AA) and related polyunsaturated fatty acids (FAs) execute crucial functions upon physiological and pathologic conditions (26,27). Eicosanoids are characterized as oxygenated metabolites of AA and other polyunsaturated C-*20* FAs by either specific enzymes or non-enzymatic reactions (27). More recently, related FAs such as the ω3 C-*22:6* docosahexaenoic acid (DHA) were shown to be an analogue source for bioactive mediators, termed as docosanoids (27,28).

In line with their outstanding activities in the course of inflammation, a majority of eicosanoids is biosynthesized in innate immune cells including neutrophils, macrophages and dendritic cells (2). Once released from the cell, eicosanoids mediate their effects by targeting membrane G-protein-coupled receptors (GPCRs) in an auto- or paracrine manner (2).

Within the AA cascade, three branches of enzymes have been discussed (**Fig. 1.2**): (I) cyclooxygenases (COXs) convert AA into the prostaglandin H_2 (PGH_2) that is further metabolized into various prostanoids, (II) cytochrome P450 (CYP) enzymes generate epoxyeicosatrienoic (EETs) or hydroxyeicosatetraenoic acids (HETEs), and (III) lipoxygenases (LOXs) dioxygenate AA into hydroperoxyeicosatetraenoic acids (HpETEs). In this context, 5-lipoxygenase (5-LOX) uniquely catalyzes a second conversion step to form leukotriene A_4 (LTA_4) that represents a precursor for the downstream biosynthesis of leukotrienes (LTs) including LTB_4 and cysteinyl LTs (cysLTs) (1,2,29,30). However, while LTs are predominantly produced under inflammatory conditions, PGs execute both inflammatory and homeostatic functions and their biosynthesis was found to be almost ubiquitous (2). Accordingly, the present thesis focusses on the formation of LTs, although a wide spectrum of eicosanoids and docosanoids have been analyzed in several experiments (see *Materials and methods* and *Results*). Thus, enzymes involved in the biosynthesis of the detected mediators are shortly discussed below (**Table 1.1**, **Fig. 1.2**, and **Fig 1.3**).

1.2.2 Enzymes involved in the biosynthesis of LMs

Polyunsaturated FAs are naturally esterified and stored within phospholipids of cellular membranes (27,31). Thus, the release of AA is prerequisite for LM formation and is regulated by phospholipases (PLs). Besides Ca^{2+}-independent PLA_2 ($iPLA_2$) that is mainly responsible for homeostatic FA release and membrane remodeling, cytosolic Ca^{2+}-dependent PLA_2 ($cPLA_2$) and secreted PLA_2 ($sPLA_2$) are thought to liberate FAs under specific stimulatory conditions (27). It is generally excepted that the formation of PGs and LTs is strongly related to $cPLA_{2\alpha}$ activity (1,32). The 85 kDa enzyme is ubiquitously expressed and located within the cytosol under resting conditions. Upon cell stimulation, $cPLA_{2\alpha}$ Ca^{2+}-dependently translocates to the nuclear membrane or endoplasmic reticulum and subsequently mediates the selective hydrolysis of AA from the *sn-2* position of phospholipids (1,33,34). Notably, the subcellular localization of $cPLA_{2\alpha}$ regulates the eicosanoid profile by generating high local concentrations

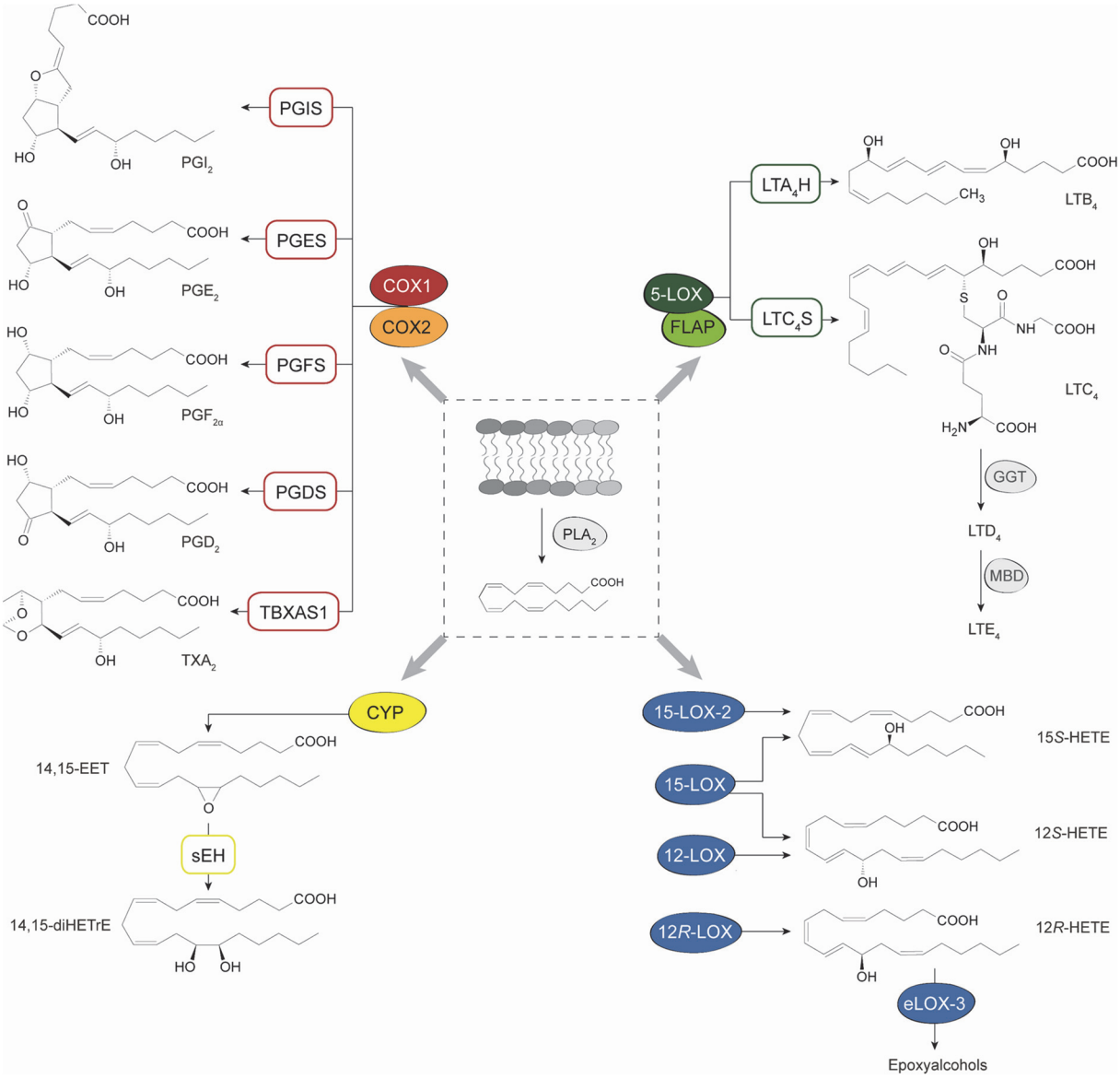

Fig. 1.2 AA-derived eicosanoid formation. Adapted and modified from Dennis et al. 2015, Lone et al. 2013, and Kuhn et al. 2015 (27,35,36). AA released from cellular phospholipids is converted into bioactive lipid mediators by distinct enzymatic branches including COXs, LOXs, and CYPs, and further metabolized by a subset of downstream enzymes. The biosynthesis of lipoxins and resolvins is presented in **Fig. 1.3**. COX – cyclooxygenase, CYP – cytochrome P450, DiHETrE – dihydroxyeicosatrienoic acid, EET – epoxyeicosatrienoic acid, eLOX-3 – epidermal LOX-3, FLAP – 5-LOX-activating protein, GGT – γ-glutamyl transferase, HETE – hydroxyeicosatetraenoic acid, LOX – lipoxygenase, LT – leukotriene, LTA_4H – LTA_4 hydrolase, LTC_4S – LTC_4 synthase, MBD – membrane-bound dipeptidase, PG – prostaglandin, PGDS – PGD_2 synthase, PGES – PGE_2 synthase, PGFS – $PGF_{2\alpha}$ synthase, PGIS – PGI_2 synthase, PL – phospholipase, sEH – soluble epoxide hydrolase, TBXAS1 – TXA_2 synthase-1.

of FAs in close proximity to enzymes involved in LM biosynthesis (27). As described above, PGs are formed via the COX-pathway. Two isoforms of COXs (COX-1 and COX-2) with about 60% structural identity have been reported and extensively discussed before (37). Human COX-1 and COX-2 consist of 576 and 581 amino acid residues, respectively, and are located at the lumenal side of endoplasmic reticulum membranes. Both isoenzymes perform a dioxygenation of AA resulting in PGG_2 and PGH_2 that act as substrates for downstream-synthases creating the bioactive prostaglandins PGE_2, PGD_2, $PGF_{2\alpha}$ and PGI_2 and

thromboxane (TX) TXA_2 (29,37,38). While COX-1 is constitutively expressed in a wide range of tissues, COX-2 expression is predominantly induced under inflammatory conditions (37,39).

Beside the COX pathway, six human LOXs convert AA into hydroperoxides with distinct biologic activities. Corresponding to their stereospecific reaction and FA metabolism, 15-, 12-, 12*R*-, and 5-LOX as well as 15-LOX-2 and epidermal LOX-3 have been described (40). Although sharing a high overall structural identity, distinctions within their substrate cavity are responsible for unique position- and stereoselectivity. Moreover, the expression of LOXs is diverse and was related to both physiological and pathophysiological conditions (40). However, according to the prominent role during inflammation, LTs produced by 5-LOX have primarily been in the focus of research and are therefore discussed in more detail in this thesis (see *5-Lipoxygenase* and *5-Lipoxygenase-activating protein*).

CYPs represent the third branch of AA metabolizing enzymes and consist of 400-500 amino acids and a central heme moiety. Besides their fundamental activities in the biotransformation of xenobiotics, CYPs were likewise found to metabolize endogenous compounds including FA substrates (30,41). While members of the CYP4A and CYP4F family generate pro-inflammatory HETEs (predominantly 20-HETE), CYP2C and CYP2J were shown to convert AA into EETs with vasodilatory and anti-inflammatory properties (30,42). EETs are degraded by the soluble epoxide hydrolase (sEH) by water addition and the subsequent formation of dihydroxyeicosatrienoic acids (DiHETrEs) with altered biological activities (43).

Noteworthy, besides diverse expression levels and subcellular localization, the distribution of the emphasized enzymes might be a key determinant for eicosanoid formation, represented by the fact that the number of biosynthetic enzymes is usually restricted within a certain cell type (27). Thus, the interplay of enzymes located in distinct cells, referred to as transcellular eicosanoid biosynthesis, might define the spectrum of LMs under resting and inflammatory conditions. For instance, co-incubations of neutrophils with red blood cells, platelets or endothelial cells resulted in increased levels of LTs such as LTB_4 or LTC_4, respectively, originating from the expression of the downstream enzymes LTA_4 hydrolase (LTA_4H) or LTC_4 synthase (LTC_4S) that utilize neutrophil-derived LTA_4 as substrate (see below) (44). Furthermore, a cell-cell transfer of eicosanoids or its unstable intermediates allows the biosynthesis of more complex FA metabolites by increasing the number of enzymes participating in their formation. In this context, co-incubations of neutrophils and platelets or endothelial cells resulted in the biosynthesis of 5*S*,6*R*,15*S*-trihydroxy-eicosa-7,9,13-*trans*-11-*cis*-tetraenoic acid (termed as lipoxin A_4) and analogues (22,44). The formation of such multiple hydroxylated eicosanoids is related to the resolution of inflammation and will therefore be discussed below.

1.2.3 Specialized pro-resolving mediators (SPMs)

In general, LTs and PGs mediate acute inflammation and chronic inflammatory disorders. LTB_4 acts as one of the most potent chemoattractant, cysLTs regulate vascular permeability and bronchoconstriction, and PGs such as PGE_2, PGI_2 and $PGF_{2\alpha}$ affect the local blood flow

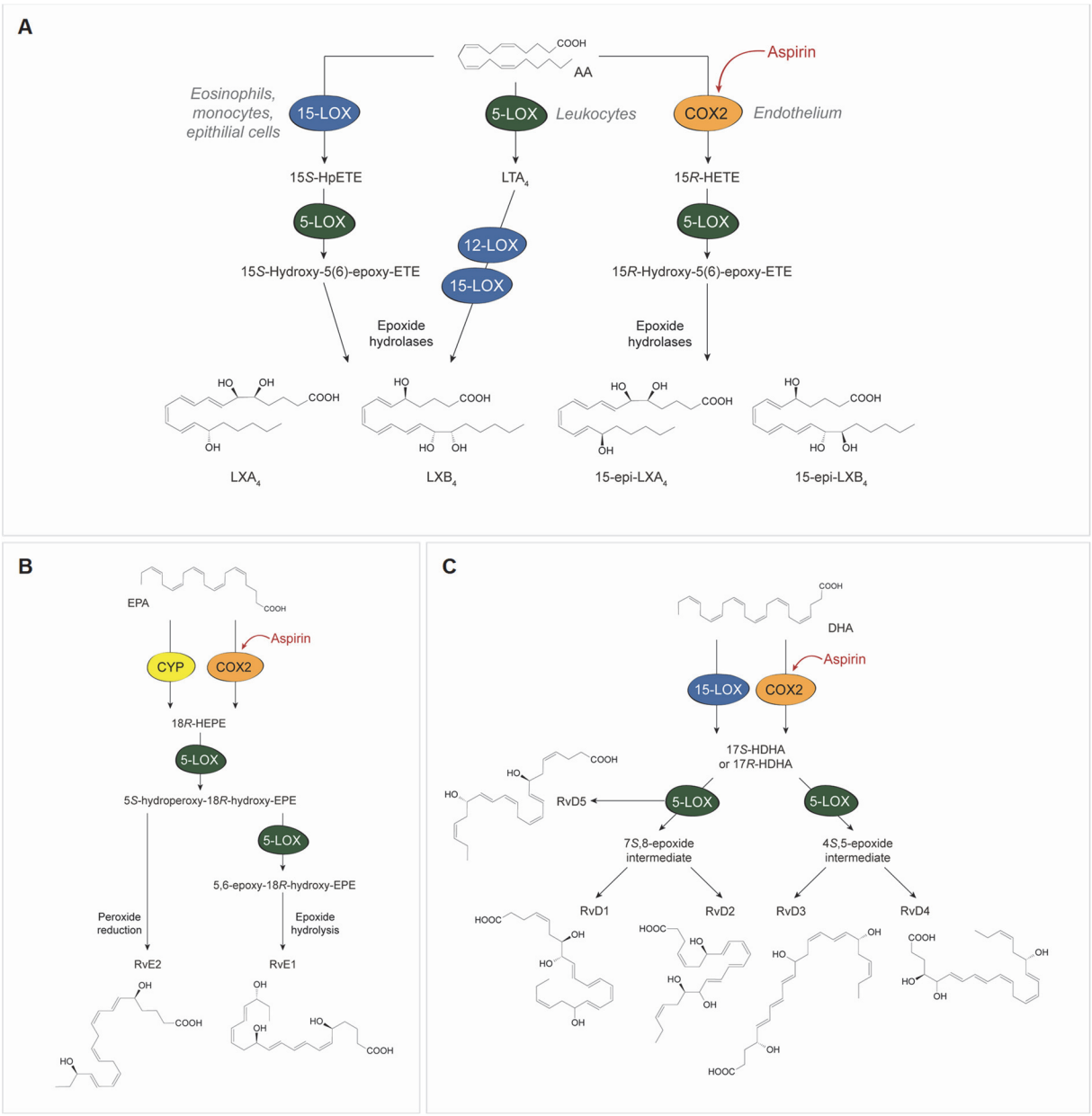

Fig. 1.3 The biosynthesis of SPMs derived from AA, EPA, and DHA. Adapted and modified from Bannenberg et al. 2010, Stables et al. 2011, and Lopez-Vicario et al. 2016 (22,38,45). **A** LX formation is related to three main pathways, each involving different cell types and enzymes: (I) 15-LOX expressed in eosinophils, monocytes or epithelial cells generates 15*S*-hydroperoxyeicosatetraenoic acid (15*S*-HpETE) that is transferred to neutrophils and converted by 5-LOX yielding LXA_4 or LXB_4, respectively; (II) LTA_4 biosynthesized by 5-LOX in neutrophils or monocytes is used as substrate for 12-LOX to generate LXs in platelets; (III) acetylated COX-2, resulting from aspirin treatment, was shown to convert AA into 15*R*-HpETE with subsequent conversion into epimeric "aspirin-triggered" LXA_4 by leukocyte 5-LOX. **B** E-series Rvs were found to be a transcellular product of neutrophil 5-LOX and either aspirin-treated COX-2 of endothelial cells, or CYP enzymes, respectively. **C** The formation of D-series Rvs requires a 15-LOX activity by either aspirin-triggered COX-2 or 15-LOX, and subsequent conversion by 5-LOX in neutrophils. Moreover (not shown here), PDs derived from DHA are converted uniquely by 15-LOX, involving 17*S*-hydroperoxydocosahexaenoic acid (17*S*-HpDHA) formation followed by epoxygenation and hydrolysis in leukocytes. By contrast, maresins are thought to be exclusively biosynthesized from DHA by human 12-LOX including the sequential conversion to 14*S*-HpDHA and final formation of 7,14*S*-dihydroxylated products. AA – arachidonic acid, COX – cyclooxygenase, DHA – docosahexaenoic acid, EPA – eicosapentaenoic acid, HDHA – hydroxydocosahexaenoic acid, (H)EPE – (hydroxy)eicosapentaenoic acid, (H)ETE – (hydroxy)eicosatetraenoic acid, LOX – lipoxygenase, LT – leukotriene, LX – lipoxin.

and induce the cardinal signs of inflammation (see *Infection-induced inflammation*) (22,27,46). However, after intense investigations of these pro-inflammatory mediators, an additional focus was set on LMs formed during the resolution phase. Along these lines, SPMs were described, including lipoxins (LX) derived from AA, resolvins (Rv) from eicosapentaenoic acid (EPA) (E-series Rvs) or DHA (D-series Rvs), as well as protectins (PD) and maresins (Mar, macrophage mediator in resolving inflammation) from DHA (22). More recently, sulfido-conjugated SPMs originated from resolvins, protectins and maresins were discovered and termed as conjugates in tissue regeneration (CTRs) according to their tissue repairing properties (47,48). These SPMs act as immunoresolvents and promote an active process of resolution (49) by reducing neutrophil infiltration and extravasation, improving macrophage phagocytosis and controlling tissue regeneration (22,48,50-52). However, in contrast to pro-inflammatory mediators, biosynthesis of polyhydroxylated SPMs generally requests the interplay of multiple enzymes and transcellular pathways and is therefore dependent on temporal cell recruitment into the inflamed tissue (22) (**Fig. 1.3**). The participation of differentially regulated enzymes such as COXs, LOXs, CYPs or downstream synthases and hydrolases might therefore allow a distinct regulation of LM by inflammatory stimuli and/or pharmacological agents.

Table 1.1 AA-derived LM and their bioactivities. Selected mediators that have been analyzed in this study are presented below. All information is adopted from Dennis et al. 2015 (27). BLT – LTB_4 receptor, COX – cyclooxygenase, CYP – cytochrome P450, CysLT – cysteinyl leukotriene receptor, DiHETE – dihydroxyeicosatetraenoic acid, DP – PGD_2 receptor, EP – PGE_2 receptor, EET – epoxyeicosatrienoic acid, FP – $PGF_{2\alpha}$ receptor, FPR2 – formyl peptide receptor 2, HETE – hydroxyeicosatetraenoic acid, IP – PGI_2 receptor, LOX – lipoxygenase, LT – leukotriene, LX – lipoxin, PG – prostaglandin, PPAR – peroxisome-proliferator activated receptor, TP – thromboxane receptor, TRPV1 – transient receptor potential vanilloid 1, TX – thromboxane.

Biosynthetic pathway	Lipid mediator	Receptor	Biochemical effects (selected)
COX	PGE_2	EP1-4	Vasodilation, vascular leakage, hyperalgesia, fever
	PGD_2	DP1-2	Mast cell maturation, eosinophil recruitment
	$PGF_{2\alpha}$	FP	Smooth muscle contraction (airways, blood vessels, uterus)
	PGI_2	IP, PPARΔ	Decreased platelet aggregation, vasodilation
	TXA_2	TP	Increased platelet aggregation
5-LOX	LTB_4	BLT1-2, PPARα	Neutrophil recruitment, vascular leakage
	LTC_4, LTD_4, LTE_4	CysLT1-2	Bronchoconstriction, neutrophil extravasation, vascular leakage
8-/12-/15-LOX	HpETEs, HETEs, diHETEs	PPARα, PPARγ, TRPV1	Expression of FA translocase (CD36), hyperalgesia
CYP	EETs	PPARα and PPARγ	Antihyperalgesia, decreased COX2 expression
LOX-LOX or LOX-COX	LXA_4, 15-epi-LXA_4, LXB_4, 15-epi-LXB_4	FPR2	Increased efferocytosis, decreased neutrophil recruitment

1.3 5-Lipoxygenase (5-LOX)

1.3.1 Protein expression and crystal structure of 5-LOX

Among the family of LOXs, 5-LOX acts as key regulator of inflammatory processes and plays a unique role in LT biosynthesis (40). While genes for all other lipoxygenases can be found on chromosome 17, *ALOX5* encoding for 5-LOX is located on chromosome 10 (53). Mammalian 5-LOX is exclusively expressed in myeloid cells including granulocytes, monocytes, macrophages, mast cells, dendritic cells, and B-lymphocytes, and DNA methylation within the promotor region was shown to prevent transcription of *ALOX5* in other tissues (1,54). However, enzyme expression in bone marrow-derived cells is strongly regulated by several cytokines and increased in presence vitamin D_3, granulocyte-macrophage colony-stimulating factor (GM-CSF) or IL-3 (1,55-57).

Monomeric 5-LOX consists of 673 amino acids with a molecular weight of 78 kDa (58). A high resolution 2.4 Å crystal structure for human 5-LOX was first described in 2011, when Gilbert et al. were able to stabilize the enzyme by distinct modifications, mainly by replacing Lys-rich segments within the C-terminus with an analogue sequence of 8*R*-LOX from the black sea rod

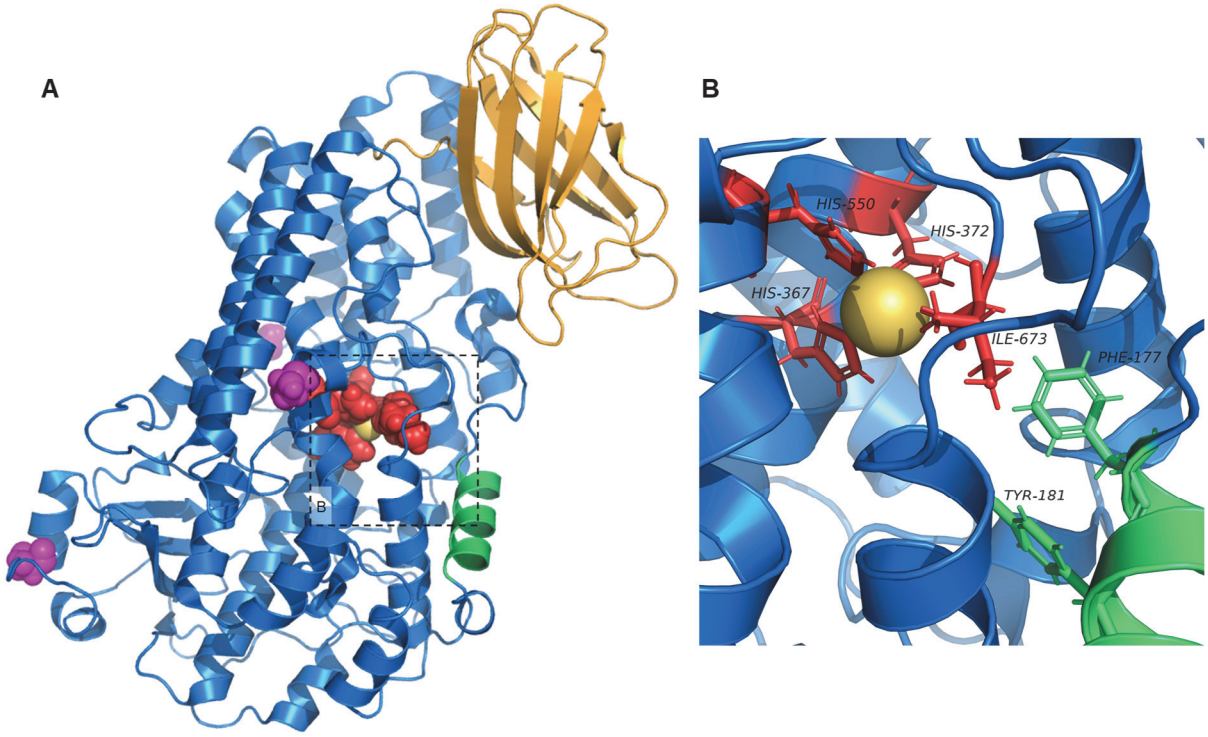

Fig. 1.4 A Crystal structure of monomeric, human *stable-5-LOX* (PDB accession number: 3o8y) according to Gilbert et al. 2011 (59). The N-terminal C2-like domain is depicted in bright orange and the α-helical C-terminal catalytic domain is colored in blue. The non-heme iron (yellow), located at the active site of the enzyme, is positioned by His^{367}, His^{372}, His^{550}, and Ile^{673} (red spheres), and shielded by the characteristic three-turn α-helix (green cartoon) that distinguishes 5-LOX from other mammalian lipoxygenases. Phosphorylation sites (Ser^{271}, Ser^{523} and Ser^{663}) are highlighted as magenta spheres. **B** View into the active site of 5-LOX with iron-stabilizing residues shown as red sticks. Phe^{177} and Tyr^{181} („FY-cork“) are presented as green sticks and limit the access of substrates to the catalytic cavity.

Plexaura homomalla, referred to as *stable-5-LOX* (59). In detail, 5-LOX consists of a N-terminal C2-like domain and an α-helical catalytic domain including a non-heme iron within the active site of the enzyme (**Fig. 1.4A**). The iron is stabilized by three histidines (His^{367}, His^{372}, and His^{550}) and the C-terminal carboxylate group of isoleucine (Ile^{673}) (**Fig. 1.4B**) (59). Moreover, the crystal structure of 5-LOX unveiled a unique characteristic compared to related LOXs. In contrast to 8*R*- and 15*S*-LOX from rabbit reticulocytes that were often used to study human 5-LOX structures in the past, the active site of 5-LOX is shielded by a three-turn α-helix containing tyrosine (Tyr^{181}) and phenylalanine (Phe^{177}) that limit the access of substrates to the catalytic cavity (**Fig. 1.4B**) (59). The mechanism of substrate entrance and concurrent uncapping of this designated FY-cork is still under investigation, although a recent study indicated the participation of the 5-LOX-activating protein (FLAP) in this respect (60). In brief, uncapping the cork would favor an entrance of AA with its carboxy-end first, whereas an access with the ω-end first might be explainable from the opposite site of the catalytic cavity (59). Noteworthy, *stable-5-LOX* lacks important residues within the N-terminal domain that were shown to be responsible for Ca^{2+} and membrane binding and nuclear translocation upon stimulation, respectively (see *Subcellular organization of enzymes involved in LT biosynthesis*) (7,61). Moreover, 5-LOX was recently shown to form dimers, although dimerization apparently did not affect catalytic activity and LT formation (62).

1.3.2 Reaction mechanism of 5-LOX-mediated LT formation

As common for all LOX reactions, 5-LOX catalyzes the insertion of molecular oxygen and hence can be classified as dioxygenase enzyme (**Fig. 1.5**) (1). Enzymatic activity of 5-LOX requires an active, ferric form (Fe^{3+}) of the catalytic iron. Thus, hydroperoxides within the cellular milieu both activate and control the activity of 5-LOX by regulating the redox tone and oxidizing the ferrous ion (Fe^{2+}) into its active state (1,53). C-*20:4* polyunsaturated ($\Delta^{5,8,11,14}$) AA was found to be the main substrate that is converted in a two-step radical reaction (1,63). First, homolytic cleavage of the pro-*S* hydrogen at C-7 results in a delocalized radical and is followed by rearrangement of the double bond from Δ^5 to Δ^6 position and an antarafacial oxygen insertion at C-5, generating 5*S*-hydroperoxy-6-*trans*-8,11,14-*cis*-eicosatetraenoic acid (5-HpETE). In a second step, 5-LOX mediates the formation of LTA_4 by pro-*R* hydrogen abstraction at C-10, subsequent $\Delta^{7,9}$-*trans*-triene formation, and intramolecular 5,6-epoxide biosynthesis. Notably, this LTA_4 synthase activity has long been thought to be mediated by another enzyme, but was found to be an unique property of 5-LOX (1).

Instable LTA_4 can be non-enzymatically converted to dihydroxylated metabolites (LTB_4-isomers), or enzymatically metabolized by specific downstream enzymes into LTs. The notation of *leukotrienes* derives from early experiments with human *leuko*cytes that produced polar, dihydroxylated AA metabolites with distinct biological properties. LTA_4H converts LTA_4 into LTB_4 (5*S*,12*R*-dihydroxy-6,14-*cis*-8,10-*trans*-eicosatetraenoic acid), which plays crucial roles in neutrophil chemotaxis and enzyme release by targeting two GPCRs, BLT1 and BLT2 (1,64). Human LTA_4H consists of 610 amino acid residues with a molecular weight of 69 kDa and is ubiquitously expressed, although higher levels were found in neutrophils, monocytes,

lymphocytes and erythrocytes (65). By contrast, the 18 kDa membrane-embedded LTC_4S conjugates GSH to LTA_4, yielding LTC_4 (5*S*-hydroxy-6*R*-S-glutathionyl-7,9-*trans*-11,14-*cis*-eicosatetraenoic acid). LTC_4 is subsequently exported to the extracellular milieu, where the glutathione (GSH) moiety is cleaved by removing Glu and then Gly to yield LTD_4 and LTE_4, respectively (1,66). Collectively denoted as cysLTs, LTC_4, LTD_4 and LTE_4 mediate vascular permeability and smooth muscle contraction and exceed their activities by targeting two GPCRs, CysLT1 and CysLT2. Additionally, cysLTs were found to be identical to the "slow-reacting substance of anaphylaxis" (SRS-A) discovered at the very beginning of the LT history (1).

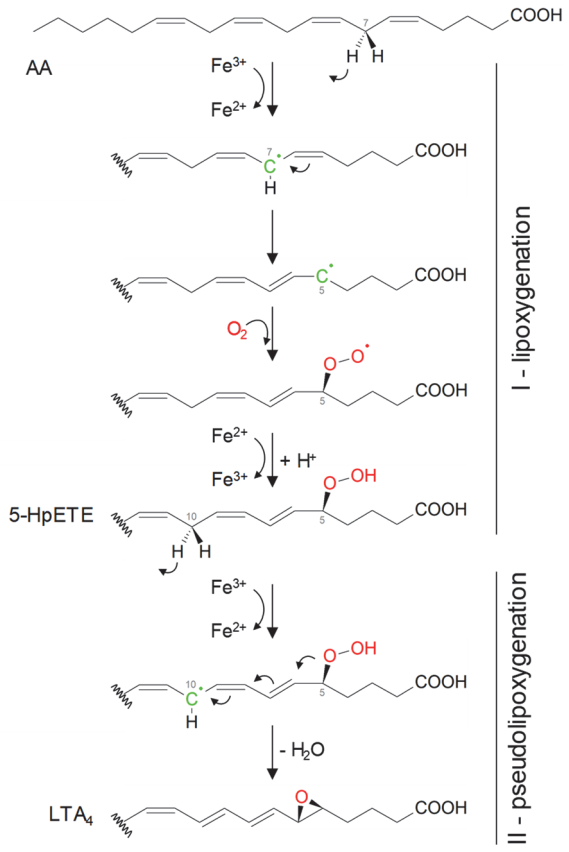

Fig. 1.5 Free radical reaction mechanism of 5-LOX according to Haeggstrom et al. 2011 (1). AA is converted into LTA_4 within a two-step conversion mediated by 5-LOX. Lipoxygenation results in 5-HpETE formation and is followed by pseudo-lipoxygenation and subsequent epoxide synthesis of the conjugated triene LTA_4.

1.3.3 Regulation of 5-LOX activity

Enzymatic activity of 5-LOX is regulated by the presence of several co-factors. *In vitro,* stimulation of 5-LOX is dependent on Ca^{2+}, adenosine triphosphate (ATP), phospholipid binding and the redox status required for iron activation. Additionally, in cellular systems, enzyme activity could be related to phosphorylation as well as subcellular translocation and co-localization with further enzymes and proteins (see *Subcellular organization of enzymes involved in LT biosynthesis*) (53).

Ca^{2+}-mediated 5-LOX activation appeared to play a superior role, as induction of LT formation was strongly related to increased intracellular Ca^{2+} levels *in cellulo* (5,7). 5-LOX binds Ca^{2+} at

a ratio of 1:2 and Asn^{43}, Asp^{44}, and Glu^{46} within the N-terminal C2-like domain were identified to cause binding of the bivalent cation (7,67). Interestingly, a comparison with other mammals revealed the presence of these residues only in 5-LOX analogues from rat, mouse, and hamster, but not in other lipoxygenases, thus explaining the pronounced Ca^{2+} sensitivity of 5-LOX (7). Additionally, Ca^{2+} mediates binding to phospholipids, mainly phosphatidylcholine (PC) species, by increasing the hydrophobicity of the enzyme (53). Interestingly, cell-stress induction by osmotic shock, heat shock, or genotoxic agents induces LT formation also in absence of Ca^{2+} (5,68).

Besides Ca^{2+} and PC binding, 5-LOX product formation is regulated by kinase activity and corresponding phosphorylation. Both phosphorylation at Ser^{271} by p38 dependent MAPKAP kinase (mitogen-activated protein kinase-activated protein kinase) MK-2/3 and at Ser^{663} mediated by ERK-1/2 (extracellular-signal regulated kinase) were shown to increase LT formation in neutrophils, whereas phosphorylation at Ser^{523} by protein kinase A (PKA) suppressed 5-LOX activity (6,53,69,70). However, whether the subcellular distribution is affected by phosphorylation is still under investigation and several, partly oppositional findings have been reported to date (53).

1.3.4 Subcellular organization of enzymes involved in LT biosynthesis

Cellular 5-LOX activity is strongly determined by its subcellular localization and the interaction with other proteins (**Fig. 1.6**). Under resting conditions, 5-LOX is located in soluble cell compartments of myeloid cells including nucleus or cytosol (71). However, subcellular localization of inactive 5-LOX is strongly cell-dependent and regulated by nuclear localization (NLS) and nuclear export signals (NES) (72,73). In human neutrophils, 5-LOX was found to be largely cytosolic but rapidly redistributed to the soluble parts of the nucleus after *in vitro* adherence to several surface materials (74).

Induction of LT formation was related to simultaneous Ca^{2+}-mediated translocation of $cPLA_2$ and 5-LOX to the nuclear envelope and the assembly of a multi-protein complex involving the membrane-embedded helper protein FLAP (see *5-Lipoxygenase-activating protein*) (75-77). Formation of this complex at either the inner or the outer membrane of the nucleus is supposed to determine the formation of LTB_4 or LTC_4, respectively, since soluble LTA_4H was found to be expressed within the nucleus and LTC_4S is exclusively inserted into the outer nuclear membrane (77). Furthermore, binding of 5-LOX to the actin regulating coactosin-like protein (CLP) and the RNA helicase *dicer* was reported and resulted in increased 5-LOX activity *in vitro* (53,78).

Taken together, subcellular organization of different enzymes might be a key mechanism in the regulation of LM biosynthesis and underlines the occurrence of a multifactorial, intricate mechanism. Based on these findings, stimulation of cellular 5-LOX product formation in line with subcellular translocation is achieved by a plethora of agents including the Ca^{2+}-mobilizing compound ionophore A23187, or naturally-occurring soluble factors like N-formylmethionyl-leucyl-phenylalanine (fMLP), complement component 5a (C5a), platelet-activating factor (PAF), IL-8 or zymosan (5,79-84). Noteworthy, endogenous AA release and LT formation is

very moderate upon stimulation with these physiological agents, although cell priming using GM-CSF, lipopolysaccharides (LPS) or tumor necrosis factor α (TNFα) could strongly increase LM biosynthesis (5).

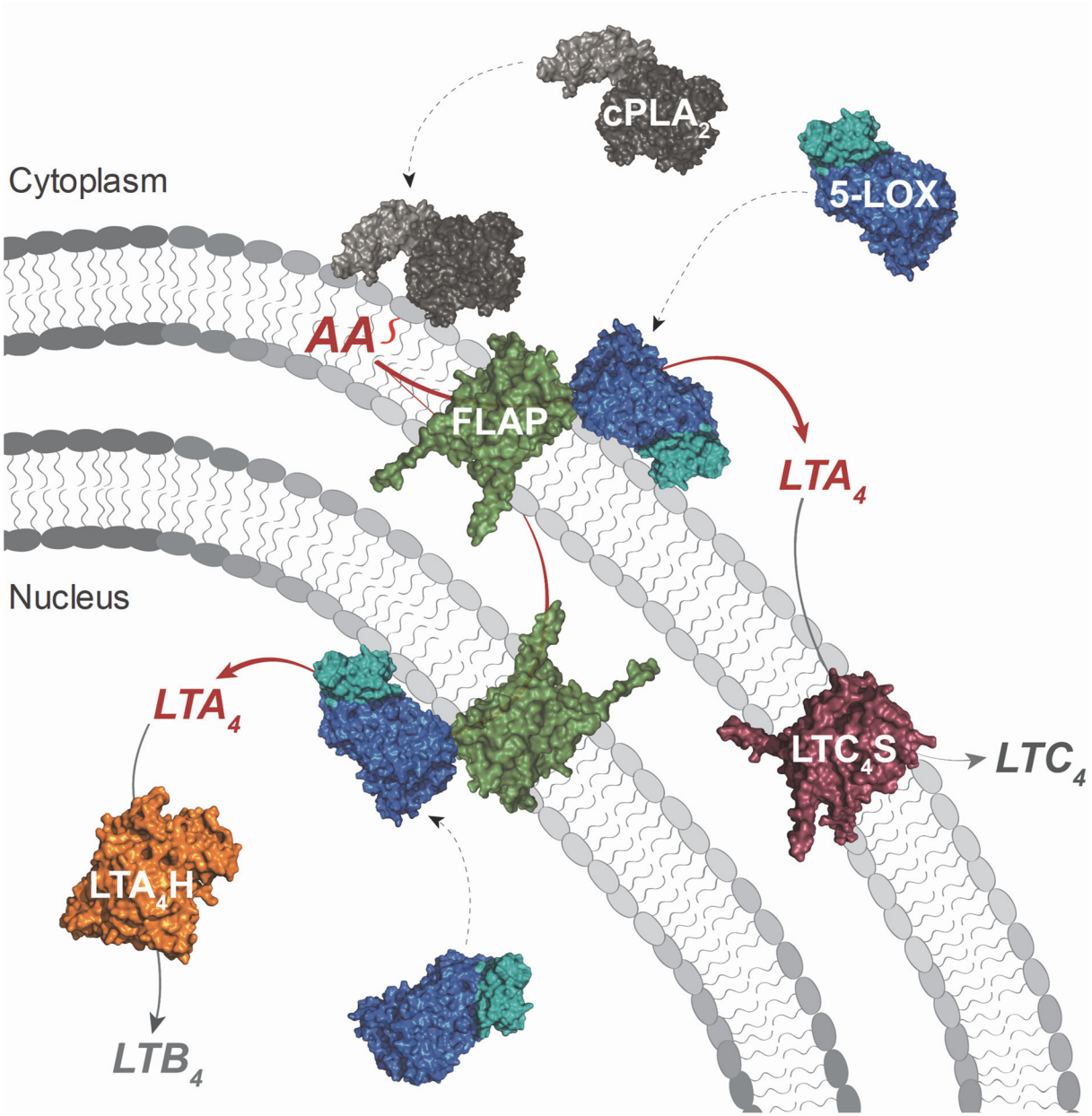

Fig. 1.6 Subcellular localization of LT-formatting enzymes (given as surface renderings, PDB accession numbers: (stable) 5-LOX, blue – 3o8y; FLAP, green - 2q7m; cPLA$_{2\alpha}$, dark grey – 1cjy; LTA$_4$H, orange – 1hs6; LTC$_4$S, red – 2pno), modified from Newcomer et al. 2010 (77). Upon cellular stimulation, 5-LOX and cPLA$_{2\alpha}$ translocate to the nuclear envelope with subsequent Ca^{2+}-mediated membrane binding by their N-terminal domains (depicted in light colors). AA is released by cPLA$_{2\alpha}$ and converted into LTA$_4$ by the 5-LOX/FLAP complex. Depending on cytosolic or nuclear localization of 5-LOX, LTA$_4$ is subsequently metabolized to the corresponding LTs by either LTC$_4$S or LTA$_4$H, respectively.

1.4 5-Lipoxygenase-activating protein (FLAP)

1.4.1 Protein expression and crystal structure of FLAP

As emphasized above, localization of 5-LOX at the nuclear envelope was described as a key determinant for endogenous substrate access and LT formation. Soon after the identification of 5-LOX and the mediated LT biosynthesis, 5-LOX was transfected to osteosarcoma cells and stimulated with A23187, however without apparent product formation (85). In parallel, the indole-based inhibitor MK886 (*L-663-539*) was shown to inhibit LT formation *in cellulo* without directly targeting 5-LOX activity (86). Based on these observations, a novel protein was isolated as MK886-binding protein and characterized by Miller et al. in 1990. In detail, neutrophil extracts were incubated with the MK886 competing ^{125}I-labIled photoaffinity probe L-669,083 to visualize a 18 kDa, membrane-associated protein subsequently termed as *5-lipoxygenase-activating protein (FLAP)* (87).

Besides microsomal glutathione-S-transferases (MGST1-3), LTC_4S, and microsomal prostaglandin E synthase-1 (mPGES-1), FLAP belongs to the MAPEG protein family (membrane-associated proteins in eicosanoid and glutathione metabolism) (88). Although a considerably sequence homology within the family was discussed, FLAP does not possess GSH binding sites and lacks any enzymatic activities, which is in clear contrast to the other MAPEG members that are involved in the biosynthesis of LMs and metabolism of xenobiotics (88). FLAP is encoded by the *ALOX5AP* gene located on chromosome 13 and is predominately expressed in bone marrow-derived cells, although minor protein levels were found in various other tissues including epithelia and brain cells (1,72). Similar to 5-LOX, FLAP expression could be increased by colony-stimulating factors, vitamin D_3 or IL-3 (55,57,72,89). Interestingly, *ALOX5* and *ALOX5AP* are not identical in their promoter regions and are located on distinct chromosomes, although their translation is restricted to almost identical cell types (72). However, 5-LOX knockout mice showed decreased expression of FLAP suggesting a correlation that is still elusive (90).

A 4.0 Å crystal structure of FLAP was obtained in presence of the inhibitor MK-591 by Ferguson et al. in 2007 (91). FLAP forms a homotrimer anchored within the phospholipid bilayer (**Fig. 1.7B**). Each monomer consists of four α-helices (α1-α4), spanning through the nuclear membrane, and a short lumenal helix at the N-terminus (αL). Moreover, a lumenal (L1) and two cytosolic (C1 and C2) loops serve as linker of the transmembrane helices, whereas both N- and C-terminal ends are facing the inner side of the nuclear double membrane (**Fig. 1.7A**). Interactions between the monomers were found for every subunit except of helix α3 and the lumenal loop L1 (91). Three cavities exposed to the lipid surface of FLAP are formed by proximate monomers and were shown to be responsible for inhibitor-binding, including van der Waals interactions by Val^{20}, Val^{21}, Gly^{24}, Phe^{25}, Ala^{27}, Ala^{63}, Tyr^{112}, Ile^{113}, Ile^{119}, Leu^{120}, and Phe^{123} as well as polar interplays by Asn^{23}, Asp^{62}, Thr^{66}, and Lys^{116} (91). Interestingly, an additional cavity within the trimer of FLAP was described. It is directed towards the lumenal side of the membrane and reaches from the bottom of the trimer to Pro^{65} that is located at the midpoint of the protein. Noteworthy, Pro^{65} is positioned at the characteristic bend of helix α2 (91). Proline- enriched distortions within transmembrane proteins are thereby discussed to be

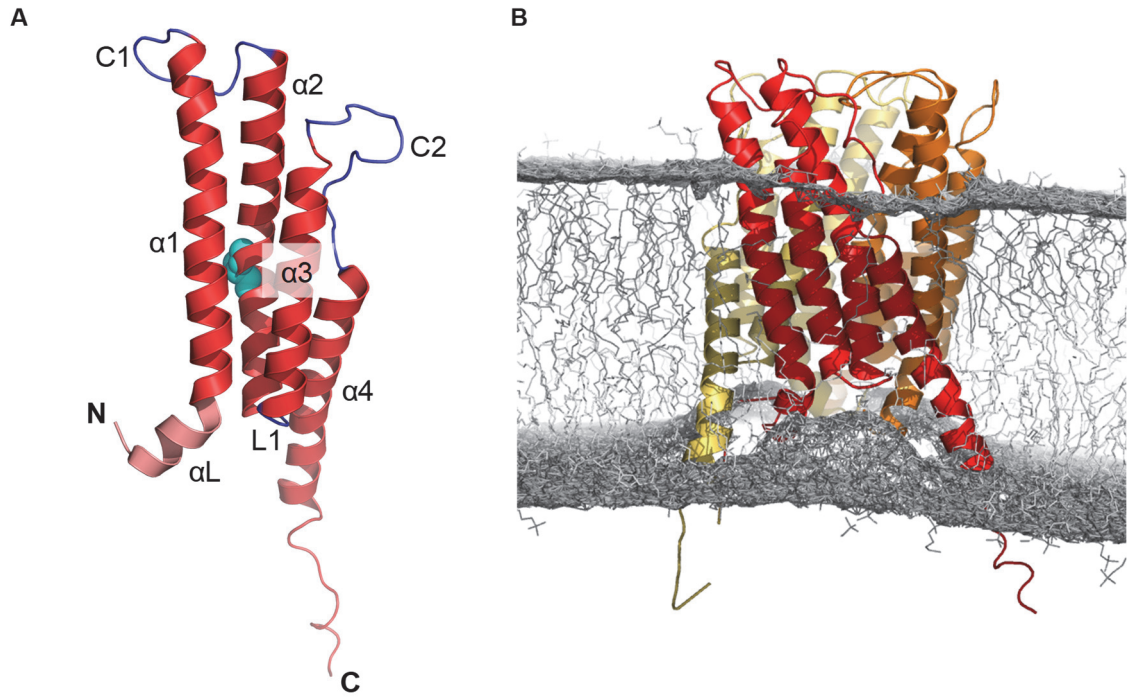

Fig. 1.7 Crystal structure of membrane-bound FLAP. A 3D-structure of a FLAP monomer according to Ferguson et al. 2007 (91), with helices shown in red and loops in blue (PDB accession number: 2q7r). Each monomer consist of a lumenal helix αL (residues 1-9, highlighted in light red), helix α1 (10-37), loop C1 (38-47), helix α2 (48-77) with a bend at Pro^{65} (presented as cyan spheres), loop L1 (78-80), helix α3 (81-101), loop C2 (102-115), helix α4 (116-138), and the extended C-terminus (139-161). **B** Membrane-embedded FLAP (PDB accession number: 2q7r) shown as homotrimer (cartoon presentation of monomers colored in red, orange, and yellow and phospholipids with polar headgroups depicted in light or dark grey lines, respectively) The given trimer is 60 Å long and 36 Å wide. The simulation inserting FLAP into a lipid bilayer is adopted from the free access MemProtMD database (http://memprotmd.bioch.ox.ac.uk/_ref/PDB/2q7r/ _sim/2q7r_default_dppc/) (Newport et al. 2019 (92)) and partially differs from the original opinions of Ferguson et al.

related to transmembrane signaling, that has not been described for FLAP yet (93). Moreover, although sharing an overall sequence homology of approximately 31% with LTC_4S, FLAP displays highly conserved structural differences that might explain its unique role in eicosanoid metabolism. In detail, FLAP is devoid of a fifth lumenal helix, whereas loop C2 and the intersection to helix α4 is extended, resulting in insufficient GSH binding. In addition, the conserved cytosolic loops within the structure of FLAP might be responsible for an interaction with 5-LOX that has not been reported for other MAPEG proteins so far (77,88).

1.4.2 Role of FLAP in LM biosynthesis and inflammatory diseases

Deficient in any enzymatic activity, the role of FLAP during LT biosynthesis has long been discussed. Early studies revealed its eminent functions in binding and transferring AA to the active site of 5-LOX and inhibitors such as MK886 were shown to directly compete with the substrate to bind FLAP (94). However, the presence of these inhibitors could not prevent AA release in neutrophils, thus disproving FLAP to have a proper lipase activity (87). Moreover, binding to FLAP was reported for several other FAs distinct from AA, although with lower affinities (95).

Soon after its identification, it was hypothesized that FLAP acts as 5-LOX anchor protein mediating 5-LOX translocation and association to the nuclear envelope (85,96), but proceeded studies demonstrated that 5-LOX redistribution upon stimulation is FLAP-independent and cannot be prevented by MK886 (12,97). A direct interaction of 5-LOX and FLAP was shown recently by making advantage of a proximity ligation assay (PLA) that detects *in situ* protein-protein interactions at closer proximities than 40 nm (12,60). However, amino acid residues involved in this process remain elusive for both proteins.

As mentioned before, LT formation was moderate when 5-LOX was transfected to intact cells alone, while co-expression with FLAP resulted in elevated amounts of 5-LOX products (85). The contribution of FLAP is eminent when LT biosynthesis is based on endogenous FA supply. In contrast, conversion of exogenous AA sources is supported by, but not exclusively depending on FLAP (53). In a recent study, FLAP appeared to play a major role in supporting the second step of 5-LOX catalysis by promoting the conversion from 5-HpETE to LTA_4 (98). Additionally, our group reported that FLAP inhibition specifically decreases LT formation in human macrophages treated with intact pathogenic *Escherichia (E.) coli* bacteria. However, pro-resolving mediators appeared to be increased in presence of MK886, pointing out FLAP as a promising pharmacological target for the treatment of inflammatory diseases (99).

Moreover, mice deficient in FLAP showed reduced inflammatory reactions and decreased LT formation in isolated peritoneal macrophages. In parallel, *ALOX5AP* knockout mice developed properly and healthy, suggesting FLAP's unique role in LT biosynthesis without affecting physiological processes (100). Expression of FLAP was also related to atherosclerosis and cerebral diseases. For instance, mice deficient in *ALOX5AP* or treated with FLAP inhibitors showed attenuated formation of atherosclerosis (101,102). Furthermore, genetic knockout of *ALOX5AP* ameliorated the neuropathology of Alzheimer's diseases implying a repeatedly discussed role of FLAP in the progression of neurological disorders and cerebral inflammation (40,103). Besides, a four-SNP haplotype of *ALOX5AP* was associated with an increased risk of stroke and myocardial infarcts in Iceland, apparently due to enhanced LTB_4 formation (104).

1.5 *Staphylococcus aureus* (*S. aureus*)

1.5.1 S. aureus in infectious diseases

As mentioned above, the most prominent inducers of inflammation and related bioactive mediator formation are microbial challenges (15). Among bacteria, the Gram-positive micrococcus S*taphylococcus* (*S.) aureus* is a frequent cause of both community- and hospital-acquired infections. The bacteria appear in characteristic clusters and are characterized by a coagulase activity and gold-pigmentated colonies during cultivation (105). As a commensal, 30 to 50 percent of the population is colonized with *S. aureus* without developing an infectious disease, but invading bacteria and interaction with the host immune system are often associated with life-threatening infections (4,105).

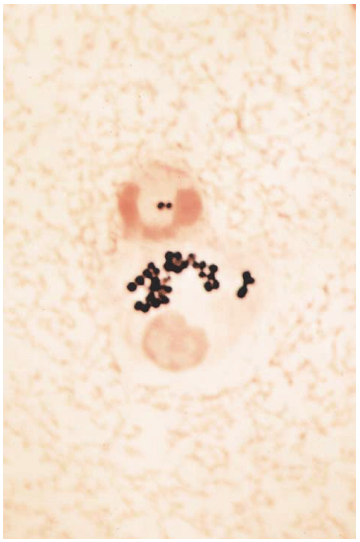

Fig. 1.8 Neutrophils challenged with *S. aureus,* microscopic image adopted from adopted from Lowy 1998 (105).

Accordingly, *S. aureus* can cause a multitude of diseases including pleuropulmonary, skin and soft tissue or osteoarticular infections as well as bacteremia or infective endocarditis (4). More recently, *S. aureus* biofilm formation was discussed to be a common risk factor when foreign devices are implanted in human (4,106). Noteworthy, staphylococcal infections are strongly related to leukocyte infiltration and frequently result in abscess formation (105). In this respect, granulocyte-depleted mice could not survive intravenous *S. aureus* infections, underlining a superior role of neutrophils during staphylococcal infection (107) (**Fig. 1.8**). However, the arsenal of factors participating in the pathogenesis of *S. aureus* is divers and remains far from complete understanding (105). It is well excepted that exotoxins secreted from *S. aureus* are involved in disease progression and vaccination with RNAIII activating protein (RAP) that regulates toxin formation was protective against cutaneous staphylococcal infections (108). Since RAP and RNAIII play crucial roles within a defined quorum-sensing system of *S. aureus,* the underlying regulation of exotoxin expression will be discussed in more detail within the following section.

1.5.2 Genomic regulation of staphylococcal exotoxin expression

Bacterial growth and cell density of *S. aureus* cultures are regulated by two key mechanism, termed as the accessory gene regulator (*agr*) and the LuxS system (109). The former is thought to be crucial for staphylococcal pathogenesis, since *agr* controls about 70 genes of which 23 have been related to the virulence of *S. aureus* to date (110).

The *agr* system consists of four proteins, ArgA, AgrB, AgrC, and AgrD, and their related genes, *agrA* to *agrD* (**Fig. 1.9**). AgrD, also referred to as autoinducing peptide (AIP), undergoes extracellular export by membrane-bound AgrB and subsequently activates the transmembrane kinase AgrC. AgrC in turn phosphorylates intracellular AgrA that finally binds to two distinct promoter regions, P2 and P3, and thereby controls the formation of RNAII and RNAIII, respectively. While RNAII is regulating the transcription of the *agr* genes, giving a positive feedback loop for the quorum-sensing system, RNAIII is involved in the expression of multiple

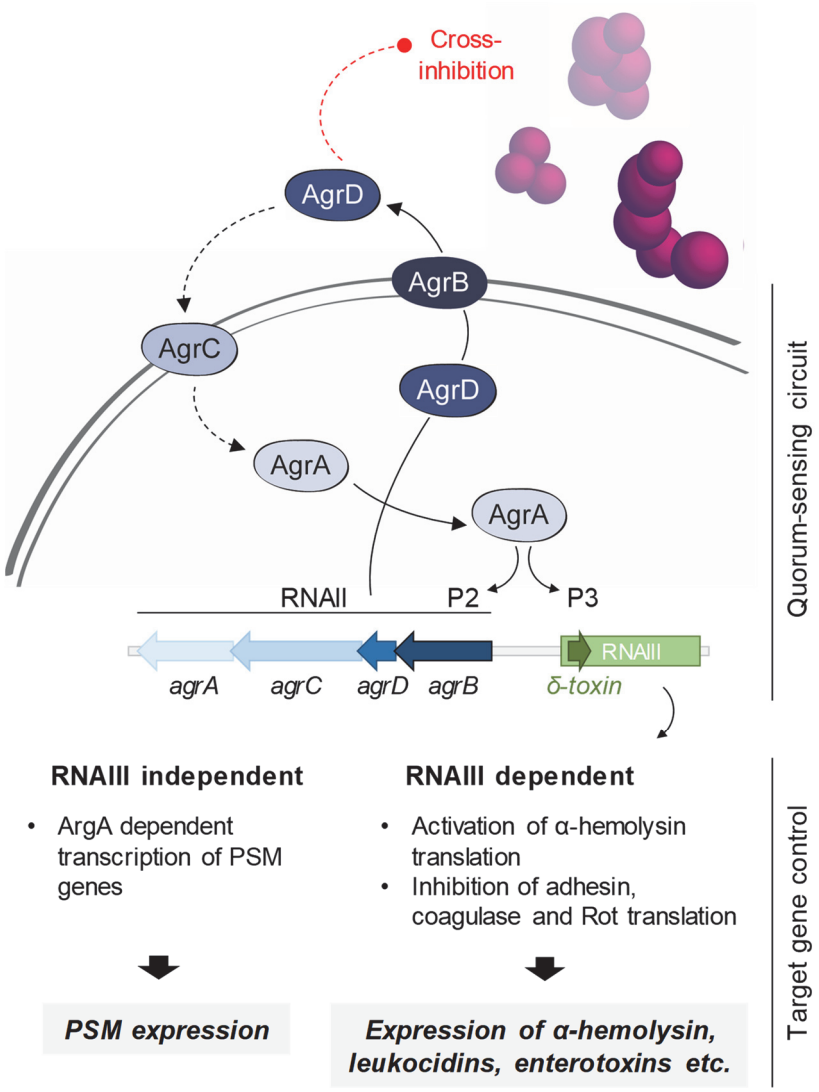

Fig. 1.9 Staphylococcal quorum-sensing is mediated by *agr*. The expression of Agr proteins is regulated by the corresponding genes *agrA* – *agrD*. AgrB mediates the release of AgrD which in turn can activate AgrC and AgrA, or cross-inhibit the growth of non-related staphylococci. Activated AgrA promotes the translation of *agr*-genes, thereby giving a feedback-regulation for quorum-sensing, and increases RNAIII transcription. Target genes including staphylococcal exotoxins and proteins are directly regulated by AgrA (PSMs, see **Fig. 1.10**) or dependent on RNAIII transcription, as indicated. The figure is adopted and modified from Le et al. 2015 (109).

staphylococcal proteins (109,110). On the one hand, RNAIII directly represents the mRNA for δ-hemolysin (δ-toxin) expression and stimulates the translation of α-hemolysin mRNA. On the other hand, RNAIII and its related antisense base pairing mechanism inhibits the expression of the repressor protein Rot (repressor of toxins), resulting in increased release of virulence factors (109). Besides, AgrA was shown to directly mediate the expression of phenol-soluble modulins (PSMs, see *Staphylococcal exotoxins*), independent of RNAII and RNAIII activation (111).

An additional key regulator in exotoxin expression, complementary to the *agr* system, is the staphylococcal accessory regulator A (*sarA*). SarA mediates the expression of *agr* genes under basal conditions by targeting the promotor region P2 (110,112). Moreover, sarA was shown to directly promote the expression of exotoxins such as α-hemolysin, independently of

agr, underlining the crucial role of *sarA* as second important global gene regulator in *S. aureus* (113). Noteworthy, *S. aureus* strains carrying mutations in either *agr* or *sarA* showed decreased virulence compared to the corresponding wildtype strains, whereas only the *agr/sarA* double deletion mutant was found to be completely avirulent (110).

1.5.3 Staphylococcal exotoxins

A multitude of *agr*-regulated exotoxins are secreted by *S. aureus*. These polypeptides can be separated into distinct classes with highly specific but generally membrane damaging properties: (I) α-hemolysin and bi-component leukocidins with pore-forming abilities; (II) β-hemolysins with sphingomyelinase activity; and (III) small amphipathic PSMs that were shown to be cytolytic for leukocytes as well, thus representing a novel group of staphylococcal leukocidins (114,115).

Among staphylococcal toxins, α-hemolysin belongs to the best described virulence factors and was associated to several *S. aureus* diseases (116-118). α-Hemolysin is of 33.4 kDa size and its expression is regulated RNAIII-dependently (109,119). The cytolytic activity of α-hemolysin relies on the ability to form homoheptameric, β-barrel transmembrane pores with an 14 Å diameter that disturb membrane composition and enable the transport of small molecules, especially the influx of Ca^{2+} ions and its subsequent cell death (114,119). Recently, ADAM-10 (A disintegrin and metalloproteinase domain-containing protein 10) was identified to interact with α-hemolysin and organizes pore formation (120). While ADAM-10 is responsible for toxin binding, caveolin-1 was identified as a second co-receptor mediating a conformational change and insertion of α-hemolysin into the lipid-bilayer (114,121). In this respect, human monocytes and lymphocytes showed higher cytolytic sensitivity compared to granulocytes (122).

Besides α-hemolysin, the subclass of staphylococcal pore-forming toxins (PFTs) is complemented by bi-component leukocidins. They consist of four subgroups: (I) γ-hemolysin, (II) Panton-Valentine leukocidins (PVLs), (III) leukocidin ED (LukED) and (IV) leukocidin AB (LukAB) (114). Each leukocidin is genetically regulated by the *agr*-Rot system and is built of two monomeric, 33 kDa subunits, one S and one F component (slow and fast migration during chromatographic analysis). Leukocidins are supposed to form heterooctameric pores within the membrane of leukocytes including monocytes, neutrophils, and macrophages. Pore-formation of leukocidins thereby involves the initial recognition of complement and chemokine receptors by the S component and subsequent attachment of a corresponding F component. Resulting β-barrel pores allow the influx of cations as described for α-hemolysin lead to cell lysis and cell death, respectively (123).

β-hemolysin exceeds a sphingomyelinase activity by hydrolyzing sphingomyelin into phosphorylcholine and ceramide. Thus, it is not considered as a pore-forming staphylococcal exotoxin (114). The translation of the corresponding *hlb* gene is regulated by Rot in a RNAIII-dependent manner, leading to the expression of β-hemolysin with a molecular weight of 35 kDa (124,125). The protein shows structural similarities to other bacterial sphingomyelinases from *Listeria ivanovii* and *Bacillus cereus* and was shown to be active against various human immune cells, albeit related studies are partly inconsistent in this respect (125,126). In addition,

the mechanism of β-hemolysin-related cytotoxicity remains poorly understood, although the influence on membrane fluidity might be a crucial determinant (114).

PSMs were first described in 1999 when Mehlin et al. performed hot phenol extraction of *S. epidermidis* cultures (127). PSMs consist of PSMα(1-4), PSMβ(1-2) and PSMγ. The latter was found to be equivalent to δ-hemolysin (115,127). Two groups of PSMs have been classified according to their protein size: PSMα and δ-hemolysin consist of 20-26 amino acids, while PSMβ are about 44 residues long (114). The expression of PSMα and PSMβ is directly regulated by AgrA, while δ-hemolysin depends on RNAIII formation (109) (**Fig. 1.10**). Notably, high levels of PSMs were found in pathogenic species (128). Due to their amphipathic properties, the key feature of PSMs is a cytolytic effect that was shown to be directed towards several cell types including endothelial cells, leukocytes, and red blood cells. Along these lines, PSMα3 was found to be the most effective cytolytic PSM (115). Interestingly, in contrast to other staphylococcal exotoxins, α-type PSMs were shown to mediate neutrophil lysis even after phagocytotic ingestion, indicating an important role for bacterial survival during *S. aureus* infections (115). Recent studies revealed a PSM-dependent activation of the formyl peptide receptor 2 (FPR2) in human neutrophils resulting in chemotaxis and Ca^{2+} influx (129). Hence, since this thesis focuses on the activities of PSMs on human neutrophils, the general role of FPRs will be discussed in the following chapter.

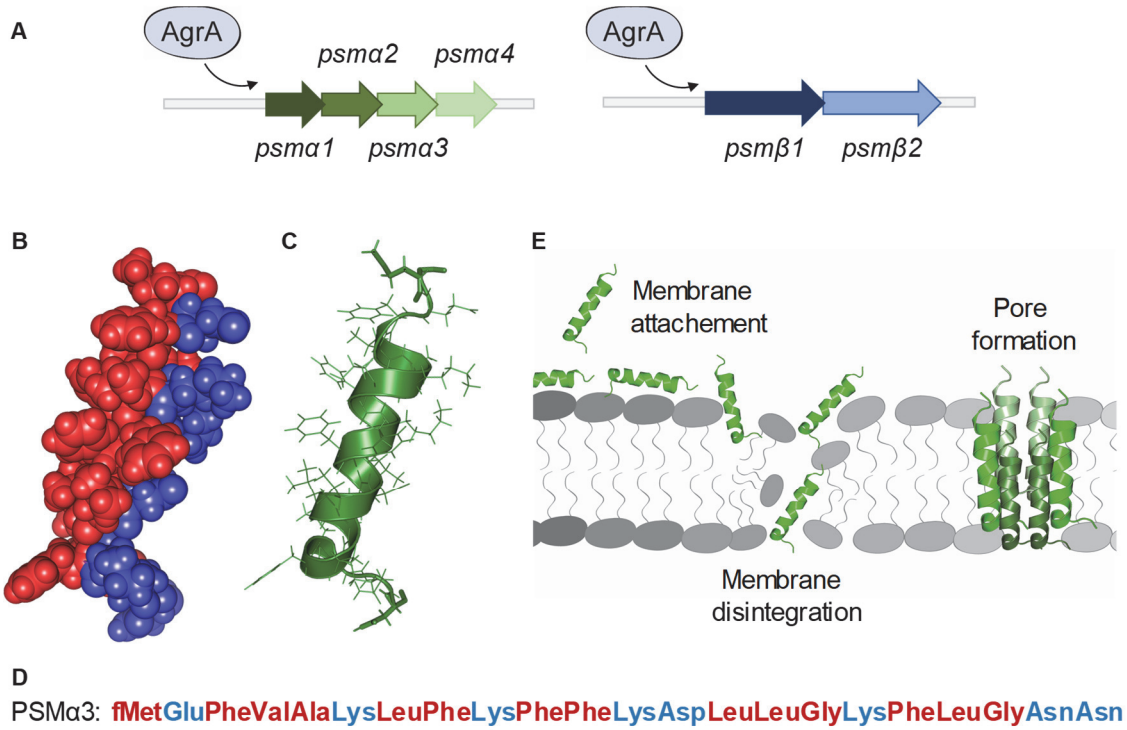

Fig. 1.10 A *psm*-gene control of staphylococci modified from Le et al. 2015 (109). Expression of α- and β-type PSMs is mediated by the promoter AgrA in a RNAIII-independent manner, while γ-type PSMs (equivalent to δ-hemolysin) are directly encoded by RNAIII (see **Fig. 1.9**). **B-C** Crystal structure of amphipathic PSMα3 (PDB accession number: 5kgy) in sphere rendering (**B**, polar residues are highlighted in blue and lipophilic residues in red) or as α-helical cartoon with residues presented as sticks (**C**). N-terminal parts of the peptide are directed to the top. **D** Amino acid sequence of PSMα3 with residues highlighted in the colors as indicated for panel **B**. **E** Recent opinion about receptor-independent PSM cell lysis: amphipathic PSM molecules attach to cellular membranes with subsequent structural disintegration and final pore-formation. Figures **B-E** are modified from Cheung et al. (115).

1.6 Formyl peptide receptors (FPRs)

1.6.1 FPRs in infection and inflammation

As mentioned before, microbial induction of inflammation relies on both, recognition of PAMPs and virulence factors, and the formers require the presence of dedicated pattern recognition receptors (PRRs) (15). Nonetheless, a clear discrimination between activation of PRRs and receptor-independent effects of virulence factors is often difficult, and several co-receptors are involved in toxin activity.

An important class of PRRs are formyl peptide receptors (FPRs), entitled in terms of their ability to recognize bacterial and mitochondrial N-formylated peptides and protein fragments (130,131). Three G-protein-coupled human FPRs have been described so far, FPR1, FPR2 and FPR3, respectively. While FPR1 and FPR2 are predominantly expressed in various myeloid cells including monocytes and neutrophils, FPR3 expression is restricted to monocytes. In addition, FPR1 could be detected in non-myeloid cells such as hepatocytes, astrocytes or microglia cells, and FPR2 transcripts were found in both epithelial and endothelial cells, hepatocytes, or neuroblastoma cells (132). Upon activation, FPRs mediate neutrophil chemotaxis, degranulation and superoxide formation, but also the expression of inflammatory cytokines such as IL-8 or nuclear factor κ-light-chain-enhancer of activated B cells, and finally affect neutrophil apoptosis and the subsequent initiation of resolution (131).

The number and structures of FPR-ligands is rather diverse and will be discussed for FPR1 and FPR2 in more detail within the next sections. In contrast, the *in vivo* role of FPR3 is still under investigation (130).

1.6.2 Formyl peptide receptor 1 (FPR1)

FPR1 displays the archetype of G-protein-coupled FPRs and can be activated by a plethora of N-formylated bacterial and mitochondrial peptides. The most potent agonist for FPR1 is the short peptide fMLP (colloquial, more correctly referred to as fML*F*) derived from *E. coli,* that is widely applied to study FPR1 functions (131). In contrast to initial findings, it has been demonstrated that FPR1 also binds non-formylated peptides, although in a much lesser extent. Agonist binding leads to the subsequent activation of the G_i-type protein and mediates an increase in intracellular Ca^{2+} and stimulation of kinases including phosphoinositide 3-kinase (PI3K), p38 mitogen-activated protein kinase (MAPK), and ERK (133).

Interestingly, bacterial pathogens are able to secrete peptides that antagonize FPR1 ligands (130). For instance, a majority of clinical staphylococcal isolates expresses the chemotaxis inhibitory protein of *Staphylococcus aureus* (CHIPS) that selectively inhibits FPR1 activation at nanomolecular concentrations and might therefore support *S. aureus* to evade from host recognition (130,134).

1.6.3 Formyl peptide receptor 2 (FPR2)

FPR2, also termed as FPR-like 1 (FPRL1) receptor, shares a 69% sequence homology with FPR1 (133). Amongst others, the expression of FPR2 is regulated by TNFα or signaling through glucocorticoid receptors and other PRRs (135). In contrast to FPR1, FPR2 shows lower affinity towards fMLP and other N-formylated peptide agonists, but recognizes longer and more diverse structures (132). In this respect, FPR2 was demonstrated to bind several endogenous proteins, peptides and lipids including serum amyloid A (SAA), the antimicrobial peptide LL-37, LXA_4 (FPR2 is therefore sometimes referred to as FPR2/ALX receptor), or annexin A1, respectively. Interestingly, while SAA and LL-37 binding is related to pro-inflammatory activities, both annexin A1 and LXA_4 were shown to inhibit neutrophil migration and thus mediate anti-inflammatory responses via FPR2 (133). These contradictory ligand-dependent effects are still not fully understood but might be explained by distinct homo- and heterodimeric states of FPR2 and FPR1 upon stimulation (136). Noteworthy, it was recently described that PSMs released from highly pathogenic *S. aureus* USA300 exceed their chemotactic activities by targeting FPR2 at nanomolecular concentrations, thereby underlining the eminent roles of both PSMs and FPR2 during staphylococcal-host-interaction (129).

In contrast, the synthetic peptide Trp-Arg-Trp-Trp-Trp-Trp-$CONH_2$ (WRW4) was shown to be a specific antagonist for FPR2 and is therefore widely used as tool in biochemical studies targeting FPR2 signaling (137). Moreover, *S. aureus* secretes a protein termed FPRL1 inhibitory protein (FLIPr) that shares an overall structural homology of 28% with CHIPS, but specifically inhibits FPR2 activation at low concentrations (138).

2 AIM OF THE THESIS

Acute inflammation and its subsequent resolution are key mechanisms of the human immune system to respond to homeostatic imbalances. Various innate immune cells including neutrophils and tissue-resident cells are involved in inflammatory reactions, and interact and regulate their functions via pro- and anti-inflammatory mediators (15,16,21). Among the group of these mediators, lipid metabolites derived from polyunsaturated FAs are key regulators during inflammatory conditions. Over the past decades, a plethora of LMs have been described to be involved in physiologic and pathophysiologic processes (27). Although intensive research has focused on eicosanoid formation and pharmacological intervention in related diseases, the pathological activation of LM biosynthesis is still not completely understood.

I - Chemical agents such as the Ca^{2+} ionophore A23187 are commonly known as agents to induce the biosynthesis of bioactive LMs, while naturally occurring agents such as fMLP, PAF or C5a were virtually incapable in sufficient FA release and subsequent formation of LMs (5,53,79,139). It was recently described that human macrophages challenged with intact bacteria display distinct LM biosynthesis that was clearly related to their phenotypical subtype and the pathogenicity of the applied microbes (140).

> ***This thesis aims to describe the underlying molecular mechanisms for bacterial stimulation of bioactive lipids in neutrophils and focuses on the activation of 5-LOX that acts as a key enzyme in LT formation (1).***

For that reason, intact pathogenic and non-pathogenic bacteria as well as sterile-filtered bacteria-conditioned medium containing secreted microbial exotoxins were investigated to activate 5-LOX in different human cell types. In order to relate the resulting LT formation with particular bacterial secondary metabolites, genetically modified *S. aureus* strains, deficient in distinct toxin expression and isolated bacterial exotoxins were evaluated for their ability to activate LM formation in human neutrophils. Moreover, the rise of drug-resistant infections strengthens the necessity of alternative therapeutic strategies besides established antimicrobials (3,141). Thus, the involvement of the PRR FPR2 and pharmacological intervention using the receptor antagonist WRW4 were studied to give insights into potential therapy strategies against *S. aureus* infections.

II - Considering the eminent role of LTs in acute phases of inflammation, various compounds have been described to modulate LM formation (10,142). Besides nonsteroidal anti-inflammatory drugs (NSAIDs) that inhibit COX-mediated prostanoid formation, only the direct 5-LOX inhibitor zileuton and the cysLT receptor antagonist montelukast could reach therapeutic application (37,142,143). Targeting 5-LOX-mediated LT formation seems to be reasonable since both LTB_4 and cysLTs were shown to drive inflammatory processes (1,64). On the other hand, 5-LOX may contribute to beneficial LX and Rv formation via transcellular pathways involving several leukocytes, tissue associated cells and corresponding biosynthetic pathways (22). Considering the obvious overall structural similarities of mammalian LOXs, selective inhibition of a certain isoform seems to be challenging (40). In this respect, direct inhibition of 5-LOX might be an inappropriate strategy to manipulate inflammatory processes. Accordingly, recent studies claimed an increase in anti-inflammatory SPM biosynthesis and

beneficial 12-/15-LOX activity in human macrophages and whole blood preparations pre-treated with the FLAP inhibitors MK886 or MK-0591 (99,144). In addition, previous publications described the importance of a 5-LOX/FLAP *in situ* interaction for sufficient LT formation, and that the assembly of this protein complex can be prevented by inhibition of FLAP (12,60). Unfortunately, FLAP inhibitors could not reach the pharmaceutical market to date, mainly due to inappropriate pharmacokinetic properties of highly lipophilic compounds and the *in vivo* loss of potency (8,10).

The present thesis aims to elucidate possible interaction sites of FLAP with 5-LOX in order to understand the in situ assembly of a LT-biosynthetic protein complex and thereby might optimize the development of novel FLAP inhibitors.

For this reason, site-directed mutagenesis of amino acid residues (Ala^{27}, Ser^{41}, Thr^{66}, Ser^{108}, Tyr^{112}, Ile^{119}) located in distinct parts of the homotrimeric FLAP protein (91) was performed and 5-LOX/FLAP interaction as well as LT formation of these mutants were investigated using a HEK293 (human embryonic kidney) cell model stably transfected with human 5-LOX and FLAP isoforms as reported previously (98). Furthermore, putative phosphorylation sites within the FLAP structure (Ser^{41}, Ser^{108}) were examined, as a recent study revealed the presence of such residues within the structurally related LTC_4S (13).

Taken together, this thesis aims to enhance the knowledge of LT biosynthesis in infection-induced inflammation and the concurrent participation of 5-LOX and its helper protein FLAP. Additionally, mutagenesis and activity studies addressing FLAP might support prospective drug development approaches.

3 MATERIALS AND METHODS

3.1 Materials

Unless depicted specifically, reagents were obtained from the following providers:

Acetic acid	VWR (Darmstadt, Germany)
Acetonitrile	GE Healthcare Life Science (Freiburg, Germany)
Acrylamide	VWR (Darmstadt, Germany)
Alexa Fluor 488 goat anti-rabbit	Invitrogen (Darmstadt, Germany)
Alexa Fluor 555 goat anti-mouse	Invitrogen (Darmstadt, Germany)
AA	Cayman Chemical (Biomol, Hamburg, Germany)
Bovine serum albumin (BSA)	AppliChem (Darmstadt, Germany)
Brain heart infusion broth (BHI)	Sigma-Aldrich (Taufkirchen, Germany)
Bromophenol blue	Merck (Darmstadt, Germany)
Ca^{2+} ionophore A23187	Cayman Chemical (Biomol, Hamburg, Germany)
$CaCl_2$	AppliChem (Darmstadt, Germany)
CellTiter-Glo®	Promega GmbH (Mannheim, Germany)
ChemoTxSystem ChemoTx Nr 101-5	Neuro Probe, Inc. (Gaithersburg, MD, USA)
CHIPS	HycultBiotech (Uden, Netherlands)
d4-LTB_4	Cayman Chemical (Biomol, Hamburg, Germany)
d4-PGE_2	Cayman Chemical (Biomol, Hamburg, Germany)
d5-LXA_4	Cayman Chemical (Biomol, Hamburg, Germany)
d5-RvD2	Cayman Chemical (Biomol, Hamburg, Germany)
d8-5*S*-HETE	Cayman Chemical (Biomol, Hamburg, Germany)
d8-AA	Cayman Chemical (Biomol, Hamburg, Germany)
Dextrane	Sigma-Aldrich (Taufkirchen, Germany)
DMEM with glutamine	GE Healthcare Life Science (Freiburg, Germany)
DMSO	Merck (Darmstadt, Germany)
Dulbecco's Buffer Substance (PBS)	SERVA Electrophoresis (Heidelberg, Germany)
Duolink® detection reagents FarRed	Sigma-Aldrich (Taufkirchen, Germany)
Duolink® PLA probe anti-mouse MINUS	Sigma-Aldrich (Taufkirchen, Germany)
Duolink® PLA probe anti-rabbit PLUS	Sigma-Aldrich (Taufkirchen, Germany)
EDTA	AppliChem (Darmstadt, Germany)
Ethanol	Fisher Scientific (Schwerte, Germany)
FA free BSA	Sigma-Aldrich (Taufkirchen, Germany)
Fetal calf serum (FCS)	Sigma-Aldrich (Taufkirchen, Germany)
fMLP	Sigma-Aldrich (Taufkirchen, Germany)
Fura-2AM	Fisher Scientific (Schwerte, Germany)
Geneticin G418	GE Healthcare Life Science (Freiburg, Germany)
Glucose	AppliChem (Darmstadt, Germany)
Glutathione	AppliChem (Darmstadt, Germany)
Glycerol	Caesar & Loretz GmbH (Hilden, Germany)
HEPES	Merck (Darmstadt, Germany)

HPLC/UPLC solvents	VWR (Darmstadt, Germany)
HCl	VWR (Darmstadt, Germany)
Hygromycin B	Invitrogen (Darmstadt, Germany)
Leupeptin	Sigma-Aldrich (Taufkirchen, Germany)
L-Glutamine	BioChem GmbH (Karlsruhe, Germany)
Lipofectamine™ LTX Plus Reagent	Invitrogen (Darmstadt, Germany)
LY293111	Cayman Chemical (Biomol, Hamburg, Germany)
LY294002	Cayman Chemical (Biomol, Hamburg, Germany)
$MgCl_2$	VWR (Darmstadt, Germany)
$MgSO_4$	AppliChem (Darmstadt, Germany)
Methanol	Fisher Scientific (Schwerte, Germany)
Methyl formate	VWR (Darmstadt, Germany)
MK886	Cayman Chemical (Biomol, Hamburg, Germany)
n-Hexane	VWR (Darmstadt, Germany)
Non-essential amino acids	Sigma-Aldrich (Taufkirchen, Germany)
Non-immune goat serum	Invitrogen (Darmstadt, Germany)
Nutrient broth no 1 medium (NB)	Sigma-Aldrich (Taufkirchen, Germany)
Penicillin/Streptomycin-solution	GE Healthcare Life Science (Freiburg, Germany)
PGB_1	Cayman Chemical (Biomol, Hamburg, Germany)
Phenylmethylsulfonyl fluoride	Sigma-Aldrich (Taufkirchen, Germany)
Pierce™ 16% Formaldehyde	Fisher Scientific (Schwerte, Germany)
KCl	VWR (Darmstadt, Germany)
KH_2PO_4	AppliChem (Darmstadt, Germany)
PSMα1 and PSMα3	synthesized at Genosphere Biotechnology (Stuttgart, Germany)
RO-31-8220	Tocris Bioscience (Ellisville, MI, USA)
RPMI 1640 Medium	Sigma-Aldrich (Taufkirchen, Germany)
RSC-3388	VWR (Darmstadt, Germany)
Saccharose	AppliChem (Darmstadt, Germany)
SB203580	Cayman Chemical (Biomol, Hamburg, Germany)
SDS	Roth GmbH (Karlsruhe, Germany)
Skepinone-L	Cayman Chemical (Biomol, Hamburg, Germany)
NaCl	Roth GmbH (Karlsruhe, Germany)
Soybean trypsin inhibitor	Sigma-Aldrich (Taufkirchen, Germany)
Trifluoroacetic acid (TFA)	Merck (Darmstadt, Germany)
Tris-HCl	Roth GmbH (Karlsruhe, Germany)
Tritium-labeled ^{3}H-AA	Biotrend Chemicals GmbH (Köln, Germany)
Triton X-100	Roth GmbH (Karlsruhe, Germany)
Trypan blue	Sigma-Aldrich (Taufkirchen, Germany)
Trypsin-EDTA	GE Healthcare Life Science (Freiburg, Germany)
Tween® 20	Roth GmbH (Karlsruhe, Germany)
UO126	Sigma-Aldrich (Taufkirchen, Germany)
WKYMVm	Tocris Bioscience (Ellisville, MI, USA)
WRW4	VWR (Darmstadt, Germany)

Zileuton	Sequoia Research Products (Oxford, UK)
α-Hemolysin	Sigma-Aldrich (Taufkirchen, Germany)
β-Mercaptoethanol	Roth GmbH (Karlsruhe, Germany)

3.2 Buffers and media

Acidified water	8 mL PBS-HCl 912 mL MilliQ water
BHI medium	37 g BHI 1 L MilliQ water
KREPS-HEPES	20 mM HEPES 135 mM NaCl 5 mM KCl 1 mM $MgSO_4$ 0.4 mM KH_2PO_4 5.5 mM glucose in MilliQ water, pH 7.4
Laemmli buffer	50 mM Tris-HCl pH 6.8 2% SDS 10% glycerol 2% β-mercaptoethanol 12.5 mM EDTA 0.02% bromophenol blue in MilliQ water
NB medium	25 g NB 1 L MilliQ water
PBS	9.55 g Dulbecco's Buffer Substance 1 L MilliQ water
$PBS^{+/+}$	1 mM $CaCl_2$ 0.5 mM $MgCl_2$ in PBS
PBS-HCl	60 mL HCl 1 M 1 L PBS
PGC	0.1% glucose 1 mM $CaCl_2$ in PBS
Stripping buffer	15 g glycine 1 g SDS 10 mL Tween® 20 in 1 L MilliQ, adjust pH 2.2
TBS	151.5 g Tris-HCl 146 g NaCl in 2.5 L MilliQ water, pH 7.4

TBS-tween	0.1% Tween® 20 in TBS buffer
Triton lysis buffer	20 mM Tris-HCl pH 7.4 150 mM NaCl 2 mM EDTA 1% Triton-X-100 *Add freshly:* 1 mM phenylmethylsulfonyl fluoride 10 µg/mL soybean trypsin inhibitor 10 µg/mL leupeptin

3.3 Methods

3.3.1 Leukocyte isolation from human blood preparations

Peripheral human blood was collected from healthy fasted donors at the university hospital Jena, Germany. Leukocytes were freshly isolated from concentrated heparinized blood preparations as published previously (145). In brief, dextran-sedimentation of erythrocytes was followed by density gradient centrifugation on lymphocyte separation medium (Histopaque® - 1077, Sigma-Aldrich, Taufkirchen, Germany). Pelleted polymorphonuclear leukocytes (PMNL, neutrophils) were resuspended in ice-cold PBS prior to hypoosmotic lysis of remaining erythrocytes. Subsequently, neutrophils were washed twice with ice-cold PBS and diluted to a final cell density in buffer solution as indicated for each assay.

All experiments with human blood preparations were performed in accordance with relevant guidelines and were approved by the ethical review committee of the university hospital Jena, Germany (license number: 4968-11/16). The donors further excluded any inflammatory diseases and the taking of drugs prior to blood donation.

3.3.2 HEK293 cell cultivation

HEK293 cells were cultivated as adherent monolayers using DMEM (Dulbecco's Modified Eagle's Medium with glutamine) containing 10% heat-inactivated FCS, 100 U/mL penicillin and 100 µg/mL streptomycin. In order to study the subcellular translocation of 5-LOX and the *in situ* assembly of a LT-biosynthetic complex with FLAP at the nuclear envelope, HEK293 were stably transfected with pcDNA3.1 plasmids encoding for 5-LOX and FLAP, respectively, using a Lipofectamine™ LTX Plus Reagent according to the manufacturer's instructions. 400 µg/mL geneticin G418 (for 5-LOX) and 200 µg/mL hygromycin B (for FLAP) were supplemented to the cultivation medium to allow polyclonal selection. Western blot analysis (see *Preparation of Western blot samples*) and IF microscopy (*Immunofluorescence Microscopy (IF)*) were performed in to evaluate proper expression of transfected proteins.

To investigate the effect of mutated amino acid residues within the structure of FLAP, a Q5™ Site-Directed Mutagenesis Kit (New England Biolabs GmbH, Frankfurt a. M., Germany) was used according to the vendor's protocol to construct pcDNA3.1 plasmids for the transfection of HEK293 cells. pcDNA3.1_FLAP(hygromycin) was utilized as template for mutation (98). Primers were designed with NEBaseChanger software (New England Biolabs GmbH, Frankfurt a. M., Germany) as follows:

Table 3.1 Primer-sequences for mutation using Q5™ Site-Directed Mutagenesis Kit, T_a - annealing temperature.

Mutation	Primer – forward (5'-3')	Primer – reverse (5'-3')	T_a (°C)
I119A	GAAACGCATCGCACTCTTCCTGTTC	CCAAATATGTAGCCAGGG	60
Y112A	CACCCCTGGCGCCATATTTGGGAAAC	CTCTGCGTTCTCTCTCCTAG	63
T66A	TGCGTACCCCGCTTTCCTCGC	TCTACACAGTTCTGGTTGGCAG	68
A27L	TGGATTCTTTCTCCATAAAGTGGAGC	TTCTGGACCACGCTGATG	63
S41A	GAATGGGAGGGCCTTCCAGAGGACC	TGGGTCCTGCTTTCGTGC	68
S41D	GAATGGGAGGGACTTCCAGAGGACC	TGGGTCCTGCTTTCGTGC	68
S108A	GAGAACGCAGGCCACCCCTGGC	TCTCCTAGGTAACCGACAAAG	65
S108D	GAGAACGCAGGACACCCCTGGC	TCTCCTAGGTAACCGACAAAG	68
S108Δ	ACCCCTGGCTACATATTTG	CTGCGTTCTCTCTCCTAG	62

pcDNA3.1_5-LOX-S271A(G418) and pcDNA3.1_5-LOX-S663A(G418) were prepared as described (6,69). Plasmids were amplified overnight in NB medium at 37 °C after transformation in One Shot™ TOP10 Chemically Competent *E. coli* (Invitrogen, Darmstadt, Germany), and DNA was extracted using a GeneJET™ Plasmid Midiprep Kit (Fisher Scientific, Schwerte, Germany) according to the provider's protocol. Efficient mutagenesis was verified by external plasmid sequencing by Eurofins Umwelt Ost GmbH (Jena, Germany).

3.3.3 Determination of cell density

Automatic cell counting of leukocytes and HEK293 cells was performed with Vi-CELL™ XR Beckmann Coulter (Beckmann Coulter GmbH, Krefeld, Germany) including trypan blue staining and viability determination.

3.3.4 Cultivation of bacteria

In order to investigate the effect of bacterial virulence factors on 5-LOX activity and LM formation, the following bacterial strains were utilized:

Table 3.2 Bacterial strains applied in this study. Transductants of *S. aureus* strains were all obtained from L. Tuchscherr from the Institute of Medical Microbiology (University Hospital Jena, Germany).

Strain	Description/Reference
LS1	*S. aureus*, isolated from swollen joint of arthritic mice (107,146)
LS1Δ*agr/sarA*	*S. aureus*, LS1 derivative carrying *agr*::tet and *sarA*::Tn917LTV1 mutations (147)
LS1Δ*hla*	*S. aureus*, LS1 *hla* knockout derivative (148)
LS1Δ*psm*αβ	*S. aureus*, generated by transduction using lysates of RN4220-307 (Δ*psm*α1-4:tetM) and RN4220-308 (Δ*psm*β1-2:tetM) (149)
USA300	*S. aureus*, CA-MRSA (150)
USA300Δ*pvl*	S. aureus, *lukF/S*-PV knockout derivative of USA300 (150)
USA300Δ*psm*αβ	*S. aureus*, *psm*αβ knockout derivative of USA300 (151)
USA300Δ*agr*	*S. aureus*, *agr*::tet derivative of USA300 (152)
TM300	*S. carnosus* (153)
O6:K2:H1	*E. coli*, ATCC19138 from Castellani and Chalmers ATCC®
BL21	*E. coli*, (DE3) competent *E. coli*, obtained from New England Biolabs GmbH (Frankfurt a. M., Germany)

E. coli were grown in NB medium overnight under continuous shaking at 37 °C. On the next day, 50 mL of fresh NB medium were inoculated with 10 µL of overnight cultures and cultivated at 37 °C till an OD_{600} of 1 was reached. *S. aureus* and *S. carnosus* were grown in BHI medium overnight and diluted to an OD_{600} of 0.05 with fresh BHI medium on the next day. Subsequently, staphylococci were cultivated at 37 °C under shaking for another 4 – 5 h. Bacteria cultures were finally centrifuged (3,000 g, 5 min, RT) and resuspended in stimulation buffer as depicted for each experiment. OD_{600} was determined prior to infection of the indicated human cells. An OD_{600} of 1 was thereby assumed to represent 1 x 10^9 bacteria/mL for each strain. In order to gain cell-free bacteria-conditioned medium (BCM) for stimulation, centrifugation-supernatants from overnight cultures of staphylococci or *E. coli* were sterile-filtered using 0.22 µm PVDF syringe filters (Roth GmbH, Karlsruhe, Germany). Bacterial absence within the BCMs was verified by overnight cultivation at 37 °C and subsequent visual control.

3.3.5 Immunofluorescence Microscopy (IF)

In order to investigate the subcellular localization of 5-LOX and FLAP, immunofluorescence (IF) microscopy was performed. Freshly isolated human neutrophils were diluted in PBS containing 1 mM $CaCl_2$ and 0.5 mM $MgCl_2$ ($PBS^{+/+}$) to a cell density of 2 x 10^6 cells/sample,

seeded onto glass coverslips and incubated for 15 min at 37 °C and 5% CO_2. Cells were subsequently stimulated in $PBS^{+/+}$ at 37 °C and 5% CO_2 as indicated. Trypsinized HEK293 cells stably co-expressing 5-LOX and FLAP, wildtype or mutant, respectively, were seeded onto poly-D-lysine coated coverslips (Kleinfeld Labortechnik GmbH, Gehrden, Germany) at a cell density of 0.35 x 10^6 cells/sample in appropriate medium 2 days prior the experiment. Subsequently, HEK293 cells were stimulated in either DMEM without additives or $PBS^{+/+}$ at 37 °C and 5% CO_2 as indicated.

Incubations were terminated by adding 4% formaldehyde solution (diluted from Pierce™ 16% Formaldehyde) in PBS for 15 min at RT. Samples were washed with PBS prior to cell permeabilization with 100% ice-cold acetone for 5 min and 0.25% Triton X-100 in PBS for 10 min at RT. PBS-washed samples were incubated overnight at 4 °C with primary antibodies using a mouse-anti-5-LOX monoclonal antibody (6A12, dilution 1:100, kindly provided from Prof. D. Steinhilber, Goethe University Frankfurt, Germany) or mouse-anti-5-LOX (1:1,000, BD Biosciences, Heidelberg, Germany), and rabbit-anti-FLAP polyclonal antibody (Abcam, Cambridge, UK), each diluted in 10% non-immune goat-serum. Samples were then incubated with Alexa Fluor 488 goat-anti-rabbit (1:1,000) and Alexa Fluor 555 goat-anti-mouse (1:1,000) secondary antibodies at RT for 1 h and finally fixated on microscope slides using ProLong Diamond Antifade Mountant (Invitrogen, Darmstadt, Germany) containing DAPI to stain cell nuclei. IF images were collected with a Zeiss Axiovert 200M microscope, and a Plan-APOCHROMAT 40x/1.3 Oil DIC (UV)VIS-IR 0.17/∞ objective using AxioCam MR camera (Carl Zeiss, Jena, Germany) for image acquisition. Pictures, given with a size of 15 µm (neutrophils) or 20 µm (HEK293), are representative for at least three independent experiments.

3.3.6 Proximity Ligation Assay (PLA)

In order to visualize *in situ* protein-protein interactions, PLA was performed according to the provider's instructions (Duolink® PLA Technology, Sigma-Aldrich, Taufkirchen, Germany). HEK293 cells stably expressing 5-LOX and FLAP, wildtype or mutant, respectively, were seeded, incubated and permeabilized as described for IF microscopy. An additional blocking procedure for 1 h at 37 °C using Duolink® blocking solution was performed prior to overnight incubation at 4 °C with primary antibodies as mentioned. Subsequently, samples were incubated with Duolink® In Situ PLA Probes for 1 h at 37 °C. PLA probes (anti-mouse MINUS and anti-rabbit PLUS) thereby represent specific secondary antibodies carrying oligonucleotides that can be linked in case the investigated proteins are in closer proximity than 40 nm (12). Samples were thereto incubated with a ligase and appropriate nucleotides at 37 °C for 30 min. Newly generated, circled DNA fragments were subsequently amplified by rolling circle amplification (RCA) by incubation with polymerase for 100 min at 37 °C. Protein-protein interactions are visualized by fluorescently labeled oligonucleotides that were used for RCA. PLA images were acquired as described for IF microscopy after fixation of samples with DAPI-containing ProLong Diamond Antifade Mountant (Invitrogen, Darmstadt, Germany) on glass slides. Pictures are given as overview of 100 µm or single-cell image of 20 µm size and are representative for at least 3 independent experiments.

3.3.7 Analysis of intracellular Ca^{2+}

Intracellular Ca^{2+} influx upon stimulation with various virulence factors was assayed by continuous fluorescence reading. In brief, 5 x 10^7 neutrophils were stained with 2 µM Fura-2AM after resuspension in KREPS-HEPES buffer for 45 min at 37 °C and 5% CO_2 in the dark. Cells were centrifuged (300 g, 5 min) and subsequently resuspended to a density of 5 x 10^6 neutrophils/mL in KREBS-HEPES buffer containing 0.1% BSA and 1 mM $CaCl_2$. 100 µL of this suspension were pipetted onto black 96-well microplates PS F-bottom (Greiner bio-one, Frickenhausen, Germany) prior to the depicted stimulation. Fluorescence emission λ_{em} at 510 nm was continuously measured following excitation λ_{ex} at 340 nm and 380 nm, respectively. In order to normalize ratios of emissions at both excitation wavelengths (340 nm / 380 nm), cells were treated with 1% Triton X-100 representing maximal Ca^{2+} influx that was set to 1.

Adherent HEK293 cells stably expressing 5-LOX and FLAP were stained in KREBS-HEPES buffer supplemented with 2 µM Fura-2AM for 30 min at 37 °C and 5% CO_2 (dark). Detached HEK293 cells were pelleted (300 g, 5 min) and resuspended in KREBS-HEPES buffer containing 0.1% BSA and 1 mM $CaCl_2$. 0.1 x 10^6 cells/well were seeded and assayed for Ca^{2+} influx as described for neutrophils.

3.3.8 Cytotoxicity assays

In order to evaluate the cytotoxic effect of various stimulatory agents, lactate dehydrogenase (LDH) release was assayed in freshly isolated human neutrophils. In brief, 5 x 10^6 cells/mL PGC buffer were treated with the indicated stimuli or 1% Triton X-100 (as total cell lysis control) for 10 min at 37 °C and subsequently pelleted at 350 g (4 °C, 5 min). Supernatants were diluted 1:20 with PBS containing 0.1% glucose and LDH release was detected by CytoTox-ONE™ Homogenous Membrane Integrity assay kit (Promega GmbH, Mannheim, Germany) according to the provided protocol, followed by fluorometric detection (λ_{ex} 560 nm, λ_{em} 590 nm).

Cell viability was additionally measured with Vi-CELL™ XR Beckmann Coulter GmbH (Krefeld, Germany). Briefly, 5 x 10^6 neutrophils in PGC buffer were treated as indicated and subsequently stained with trypan blue prior to automatic cell counting (see *Determination of cell density*). Viability is given as percentage of viable compared to the total number of cells.

3.3.9 Determination of 5-LOX product formation in HEK293 cells

5-LOX product formation of HEK293 cells stably expressing 5-LOX and FLAP, wildtype or mutant, respectively, was assayed after trypsinization of adherent cells, centrifugation (300 g, 10 min, RT) and resuspension to a final cell density of 1 x 10^6 cells/mL in PGC buffer. Cells were preincubated with 0.1% DMSO (vehicle control) or 300 nM MK866 for 10 min at 37 °C prior to stimulation with 2.5 µM Ca^{2+} ionophore A23187 and 2 µM AA for another 10 min at 37 °C. Incubations were terminated by adding one volume of ice-cold methanol. Solid-phase

extraction (*SPE I*) was performed as described (see *Solid-phase extraction*) after addition of 200 ng PGB_1 (internal standard) and sample acidification using PBS-HCl. 5-LOX products include 5-HpETE, the corresponding alcohol 5-HETE, and all-*trans*-isomers of LTB_4 and were analyzed by RP-HPLC (see *RP-HPLC-UV analysis*).

3.3.10 Determination of LM formation in human neutrophils

Freshly isolated human neutrophils were diluted in PGC buffer to a final density of 5 x 10^6 cells/mL. As indicated, cells were preincubated for 15 min with vehicle or compounds, respectively, prior to stimulation with the indicated agents for 10 min at 37 °C. Incubations were stopped with two volumes of ice-cold methanol and 0.99 ng d8-5*S*-HETE, 46.8 ng d8-AA, 1.07 ng d4-PGE_2, 1.08 ng d5-LXA_4, 1.14 ng d5-RvD_2 and 1.02 ng d4-LTB_4 (Cayman Chemical, Biomol, Hamburg, Germany) were added as diagnostic ions for internal standardization. Samples were kept on ice for at least 3 h in order to precipitate remaining proteins and were finally subjected to solid-phase extraction (*SPE II*) as stated below (see *Solid-phase extraction*), followed by UPLC-MS/MS analysis of LMs (see *UPLC-MS/MS analysis*).

3.3.11 Determination of LMs from in vivo experiments

In order to investigate the effect of bacterial exotoxins on LM formation *in vivo*, a murine footpad infection model was performed by A. Siegmund and L. Tuchscherr at the Institute of Medical Microbiology (University Hospital Jena). In brief, C57BL/6 mice were kept under pathogen-free conditions prior to subcutaneous footpad infection (right hind) with 2 × 10^7 CFU (colony-forming units) of *S. aureus*, wildtype or mutant strain, in 50 µL PBS, respectively. The left hind footpad was simultaneously inoculated with 50 µL of vehicle control. USA300 infected mice were sacrificed 2, 6, 9, 24, and 48 h after infection, whereas USA300Δ*psm*αβ infected animals were sacrificed 48 h post-infection. Samples from 4 randomly selected mice were utilized per group/experiment. Homogenized foot pad tissues were stored at -80 °C and finally subjected to solid-phase extraction (*SPE II*) in order to isolate LMs prior to analysis by UPLC-MS/MS. Total LM formation was normalized to 1 µg total protein within the homogenates.

All animal experiments were performed in accordance with the guidelines of the German Society for Laboratory Animal Science 22-2684-04-02-003/15 (Thüringen, Jena) as published previously (154).

3.3.12 Chromatographic analysis of LMs

Solid-phase extraction

Depending on the further chromatographic analysis, LMs were isolated and concentrated using the following SPE methods:

***SPE I*:** In order to prepare samples for RP-HPLC-UV analysis, incubations were centrifuged at 800 g for 10 min at 4 °C and subsequently subjected to MilliQ water conditioned Clean up C18 RP-columns (100 mg, UCT, Bristol, PA, USA). Flushing with 1 mL MilliQ water and 1 mL 0.25% methanol was followed by elution with 300 µL 100% methanol.

***SPE II*:** Samples for UPLC-MS/MS analysis were centrifuged at 1,200 g, 10 min, 4 °C and supernatants were diluted with 8 mL acidified water prior to application to MilliQ water conditioned Waters Sep-Pak® Vac 6cc extraction columns (Waters, Milford, MA, USA). Samples were washed with 6 mL MilliQ water and *n*-hexane, respectively, and eluted with 6 mL methyl formate. Subsequently, samples were dried under nitrogen stream with TurboVap LV (Biotage, Uppsala, Sweden) and resuspended in 100 – 200 µL ice-cold 50% methanol. Analysis of LMs was performed as described below, and as published recently (99).

RP-HPLC-UV analysis

5-LOX products were analyzed by RP-HPLC using a Nova-Pak C18 Radial-Pak Cartridge, 60 Å, 4 µm, 5 mm X 100 mm, 1/pkg (Waters, Eschborn, Germany). 50 - 100 µL sample preparation from SPE I were injected and separated with an isocratic mixture of methanol/ water/trifluoroacetic acid (73:27:0.007) and constant flow of 1.2 mL/min followed by UV-detection at 280 nm (for *trans*-LTB_4-isomers) or 235 nm (for 5-H(p)ETE), respectively. Quantification was performed using PGB_1 as internal standard.

UPLC-MS/MS analysis

In order to detect LMs formed in neutrophils or *in vivo*, sample preparations from SPE II were analyzed by UPLC-MS/MS (Acquity™ UPLC system, Waters, Milford, MA, USA; QTRAP 5500 Mass Spectrometer, ABSciex, Darmstadt, Germany; Turbo V™ Source and electrospray ionization) as reported recently (99). In brief, LMs were separated on an ACQUITY UPLC® BEH C18 column (1.7 µm, 2.1 × 100 mm; Waters, Eschborn, Germany) with a flow rate of 0.3 mL/min at 50 °C. MilliQ water (A) and methanol (B) both acidified with 0.01% acetic acid were used as mobile phase starting with 42% methanol (v/v), increasing up to 86% (v/v) over 12.5 min and ending isocraticly with 98% till 15.5 min. Negative ion mode (ion spray voltage 4000 V, heater temperature 500 °C) was used to detect the following lipids with their corresponding transitions:

Table 3.3 UPLC-MS/MS analysis of LMs determined in this study. DP - Declustering Potential, EP - Entrance Potential, CE - Collision Energy, CXP - Collision Cell Exit Potential, RT - Retention Time, Q1 - first quadrupole; Q3 - third quadrupole.

Lipid mediator	Q1 (m/z)	Q3 (m/z)	RT (min)	DP (V)	EP (V)	CE (eV)	CXP (V)
d5-RvD2	380.3	141.2	6.4	-80	-10	-23	-14
RvD1	375.2	215.1	6.8	-80	-10	-26	-13
RvD2	375.2	175.1	6.4	-80	-10	-30	-13
RvD3	375.2	147.1	6.4	-80	-10	-25	-13
RvD4	375.2	101.1	7.8	-80	-10	-22	-10

Lipid mediator	Q1 (m/z)	Q3 (m/z)	RT (min)	DP (V)	EP (V)	CE (eV)	CXP (V)
d5-LXA$_4$	356.3	115.2	6.8	-80	-10	-19	-14
LXA$_4$	351.2	115.1	6.9	-80	-10	-20	-13
LXA$_5$	349.2	115.1	5.8	-80	-10	-20	-13
LXB$_4$	351.2	221.1	6.3	-80	-10	-20	-13
d4-PGE$_2$	355.3	193.2	6.1	-80	-10	-25	-16
PGE$_2$	351.2	271.0	6.1	-120	-10	-20	-13
PGD$_2$	351.3	233.1	6.3	-80	-10	-16	-15
PGF$_{2\alpha}$	353.3	193.1	6.5	-80	-10	-34	-11
TXB$_2$	369.3	169.1	5.8	-80	-10	-22	-15
d4-LTB$_4$	339.3	197.2	9.2	-80	-10	-22	-13
20-OH-LTB$_4$	351.3	195.1	4.8	-80	-10	-24	-15
PD1/PDX	359.2	153.1	8.8	-80	-10	-21	-9
RvD5	359.2	199.1	8.9	-80	-10	-21	-13
Mar1	359.2	250.1	9.1	-80	-10	-20	-16
t-LTB$_4$	335.2	195.1	8.7	-80	-10	-22	-13
LTB$_4$	335.2	195.1	9.2	-80	-10	-22	-13
5*S*,6*R*-diHETE	335.2	115.1	10.6	-80	-10	-20	-13
5,15-diHETE	335.2	201.0	8.8	-50	-10	-30	-13
d8-5*S*-HETE	327.3	116.1	12	-80	-10	-17	-10
17-HDHA	343.2	245.1	11.5	-80	-10	-17	-14
14-HDHA	343.2	205.1	11.7	-80	-10	-17	-14
13-HDHA	343.2	193.1	11.6	-80	-10	-17	-14
7-HDHA	343.2	141.1	11.9	-80	-10	-18	-15
4-HDHA	343.2	101.1	12.4	-80	-10	-17	-15
18-HEPE	317.2	259.1	10.5	-80	-10	-16	-23
15-HEPE	317.2	219.1	10.7	-80	-10	-18	-12
12-HEPE	317.2	179.1	10.8	-80	-10	-19	-12
11-HEPE	317.2	167.1	10.7	-80	-10	-19	-12
5-HEPE	317.2	115.1	11.2	-80	-10	-18	-12
15-HETE	319.2	219.1	11.4	-80	-10	-19	-12
12-HETE	319.2	179.1	11.7	-80	-10	-21	-12
11-HETE	319.2	167.1	11.6	-80	-10	-21	-12
8-HETE	319.2	155.0	11.7	-50	-10	-18	-13
5-HETE	319.2	115.1	12.1	-80	-10	-21	-12
d8-AA	311.3	267.1	13.8	-100	-10	-16	-18
AA	303.3	259.1	13.8	-100	-10	-16	-18
EPA	301.3	257.1	13.6	-100	-10	-16	-18
DHA	327.3	283.1	13.8	-100	-10	-16	-18

Quantification was performed using standard calibration curves for each LM and subsequent correction of variations within the set of samples with the help of the corresponding deuterated diagnostic ion (indicated in bold letters). All LM standards were obtained from Cayman Chemical (Biomol, Hamburg, Germany).

3.3.13 Western blot analysis

Preparation of Western blot samples

Neutrophils were diluted in PBS containing 0.1% glucose and 1 mM $CaCl_2$ to a final cell density of 2 x 10^7 cells/mL. 500 µL of the cell suspension were treated as indicated for each experiment and reactions were terminated by centrifugation (500 g, 30 s, 4 °C) followed by lysis of pelleted cells with 100 µL triton lysis buffer for 20 min on ice. If necessary, remaining cell fragments were degraded by sonication (output control 1, const. duty cycle, 3 x 10 s) with Branson Ultrasonics™ Sonifier S-250A (Fisher Scientific, Schwerte, Germany).

Trypsinized HEK293 cells were centrifuged (300 g, 5 min) and resuspended in fresh DMEM medium. 1 x 10^7 cells were subsequently pelleted and lysed using 100 µL of triton lysis buffer for 15 min on ice and repeated vortexing.

Finally, cell lysates were centrifuged for 10 min (20,000 g, 4 °C) prior to collection of resulting supernatants. In order to determine protein concentrations of Western blot samples, a DC™ protein assay (Bio-Rad Laboratories, Munich, Germany) was performed. In brief, 5 µL of cell lysates were incubated with 25 µL of reagent A' (freshly prepared mixture of Biorad Reagent A and Biorad reagent S, 50:1) and 200 µL of Biorad Reagent B for 15 min at RT prior to absorbance detection at 750 nm. Protein concentrations were calculated using a BSA standard curve ranging from 0 to 2,000 µg/mL. 60 µL of cell lysates were finally diluted with 20 µL of 4-fold Laemmli buffer and boiled at 96 °C for 5 min.

SDS-PAGE and Western blot

SDS-Polyacrylamide gel electrophoresis (SDS-PAGE) was performed in order to separate proteins prior to wet-tank blotting on nitrocellulose membranes. 10% polyacrylamide gels were utilized for investigations of 5-LOX, ERK1/2, p38 MAPK and β-actin, 12% polyacrylamide gels for human FPR2 and 16% polyacrylamide gels for 5-LOX, β-actin, and FLAP, respectively. Blocking with 5% BSA in TBS for 1 h was performed in order to exclude unspecific antibody-binding, followed by overnight incubation at 4 °C with primary antibodies at an antibody-specific dilution in 5% BSA in TBS-tween solution (**Table 3.4**). On the next day, fluorescence-labeled antibodies diluted in 5% BSA in TBS were used for visualization of blotted proteins after incubation for 1 h at RT (**Table 3.5**).

Table 3.4 Antibodies and corresponding dilutions for Western blot analysis. (m) - monoclonal, (p) – polyclonal.

Antibody	Dilution	Provider
rabbit-anti-ERK1/2 (m)	1:1,000	Cell Signaling Technology Inc. (Danvers, MA, USA)
mouse-anti-$^{Thr202/Tyr204}$phospho-ERK1/2 (m)	1:2,000	Cell Signaling Technology Inc. (Danvers, MA, USA)
rabbit-anti-p38 MAPK(m)	1:1,000	Cell Signaling Technology Inc. (Danvers, MA, USA)
rabbit-anti-$^{Thr180/Tyr182}$phospho-p38 MAPK (p)	1:1,000	Cell Signaling Technology Inc. (Danvers, MA, USA)
mouse-anti-β-actin (m)	1:1,000	Cell Signaling Technology Inc. (Danvers, MA, USA)
rabbit-anti-β-actin (m)	1:1,000	Cell Signaling Technology Inc. (Danvers, MA, USA)
mouse-anti-5-LOX (m)	1:1,000	BD Biosciences, (Heidelberg, Germany)
rabbit-anti-FLAP (p)	1:1,000	Abcam (Cambridge, UK)
rabbit-anti-FPR2 (p)	1:1,000	Novus Biologicals (Abingdon, UK)

Secondary antibodies were selected as follows: Proteins of interest were stained in green (IRDye® 800 CW) and housekeeping proteins were stained in red (IRDye® 680 LT). Images were obtained using an Odyssey infrared imager (Li-Cor Biosciences, Lincoln, NE, USA) with subsequent densitometric analysis with the corresponding Odyssey scan software. Immunoblotting of phosphorylated proteins was followed by overnight incubations of nitrocellulose membranes in stripping buffer at RT and detection of the corresponding native protein in order to normalize phosphorylation events to equal protein amounts.

Table 3.5 Fluorescence-labeled secondary antibodies and corresponding dilutions for Western blot analysis.

Secondary antibody	Dilution	Provider
IRDye® 680 LT goat-anti-mouse	1:40,000	Li-Cor Biosciences GmbH (Bad Homburg, Germany)
IRDye® 680 LT goat-anti-rabbit	1:80,000	Li-Cor Biosciences GmbH (Bad Homburg, Germany)
IRDye® 800 CW goat-anti-mouse	1:10,000	Li-Cor Biosciences GmbH (Bad Homburg, Germany)
IRDye® 800 CW goat-anti-rabbit	1:15,000	Li-Cor Biosciences GmbH (Bad Homburg, Germany)

3.3.14 Neutrophil chemotaxis assay

Neutrophil migration through a 5 µm ChemoTx® 101-5 membrane was assayed using a Promega CellTiter-Glo® Luminescent Cell Viability Assay. In brief, freshly isolated human neutrophils were diluted in RPMI containing 10% heat-inactivated FCS, 100 U/mL penicillin, and 100 µg/mL streptomycin to a final density of 3.2 x 10^6 cells/mL and preincubated with inhibitors for 10 min on ice, as indicated. Subsequently, chemotactic stimuli including 30 nM LTB_4 and 10 µg/mL PSMα3 were added to a 96-well-plate prior to covering the plate with a ChemoTx® 101-5 membrane. 80,000 neutrophils were pipetted on top of the membrane and infiltration into the lower chamber containing chemotactic agents or vehicle control, respectively, was determined after 1 h at 37 °C (5% CO_2). Infiltrated cells were thereby stained with CellTiter-Glo® on a 384-well-plate according to the manufacturer's protocol followed by luminescence measurement. Calculation of migrated cells was performed with the help of a neutrophil standard curve directly added to the migration chamber without chemotactic agent.

3.3.15 ^{3}H-Arachidonic acid release

Release of [5,6,8,9,11,12,14,15-^{3}H(N)]-AA (^{3}H-AA) was assayed in freshly isolated human neutrophils. In brief, neutrophils, resuspended in RPMI medium to a density of 1 x 10^7 cells/mL, were incubated with 0.5 µCi/mL of ^{3}H-AA for 2 h at 37 °C and 5% CO_2. Cells were subsequently washed with PBS containing 2 mg/mL of FA-free BSA in order to remove unbound ^{3}H-AA and finally resuspended in PGC buffer prior to preincubation with test compounds or 0.1% DMSO vehicle, respectively (on ice). Stimulation with the indicated agents was performed for 10 min at 37 °C and reactions were stopped on ice, followed by centrifugation at 300 g (4 °C). 500 µL of supernatants were collected, diluted with 2 mL of liquid scintillation counting solution Rotiszint® eco plus (Roth GmbH, Karlsruhe, Germany) and radioactivity was measured by scintillation counting (Micro Beta Trilux, Perkin Elmer, Waltham, MA).

3.3.16 Statistics and graphical presentation

Graphs were generated using a GraphPad Prism software (GraphPad Software Inc., San Diego, CA). Data are given as mean ± standard error of the mean (SEM) of N independent experiments or N different donors. Statistical analysis was performed using GraphPad InStat 3 (GraphPad Software Inc., San Diego, CA) or SigmaPlot 13.0 software (Systat Software Inc., San Jose, CA) by applying an appropriate statistical test as indicated in each figure. In case data lacked a gaussian normal distribution, tested by Shapiro-Wilk test, raw data was logarithmized to 10 (log_{10}) for analysis. p-values < 0.05 were considered as significant and labeled with * or #, respectively, while concrete values are denoted for $0.05 \leq p \leq 0.20$. Principle component analysis (PCA) was performed using OriginPro 2015G software (OriginLab Corporation, Northampton, MA).

Microsoft PowerPoint was used to reassemble microscopic images. PyMOL Tcl-Tk GUI (Schrödinger, Mannheim, Germany) was utilized for graphical visualization of crystal structures with PDB accession numbers given for every presented protein/enzyme, and ChemSketch Software (ACD/Labs, Toronto, Canada) was used to create structural formula.

4 RESULTS

Please note that the following figures are partly adopted from our recent publication *Exotoxins from Staphylococcus aureus activate 5-lipoxygenase and induce leukotriene biosynthesis* (Romp et al.), that is currently in press at Cellular and Molecular Life Sciences, see Appendix) (155).

4.1 Bacterial exotoxins stimulate 5-LOX activity *in cellulo*

4.1.1 Pathogenic bacteria and their secreted exotoxins induce 5-LOX translocation in HEK_5-LOX/FLAP cells

It was recently reported by our group that macrophages challenged with intact bacteria release a distinct pattern of LMs depending on the macrophage phenotype (140). Since LT formation was strikingly induced upon bacterial stimulation, we aimed at investigating the underlying molecular mechanism that activate the 5-LOX pathway. Hence, a HEK293 cell-system stably co-expressing 5-LOX with its helper protein FLAP (HEK_5-LOX/FLAP) was used as experimental model and stimulated with intact bacteria in order to assess a possible bacterial induction of LM formation besides immunospecific effects such as receptor activation and phagocytosis, respectively (98).

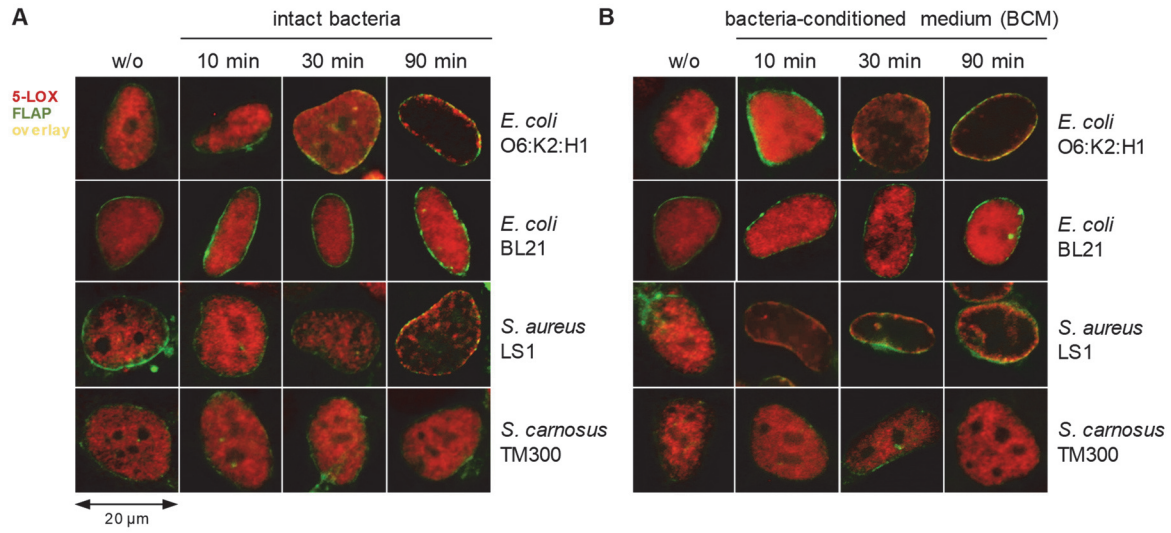

Fig. 4.1 Pathogenic bacteria and their corresponding bacteria-conditioned medium activate 5-LOX-translocation in HEK_5-LOX/FLAP cells. Subcellular distribution of 5-LOX was investigated in non-immunocompetent HEK293 cells stably expressing 5-LOX and FLAP. **A** HEK_5-LOX/FLAP cells were stimulated by intact pathogenic *E. coli* (O6:K2:H1) or *S. aureus* (LS1) and non-pathogenic *E. coli* (BL21) or *S. carnosus* (TM300) at 37 °C for the indicated timepoints using a MOI ratio of 1:50 (HEK293 cells versus bacteria) in $PBS^{+/+}$. **B** HEK_5-LOX/FLAP cells were incubated in $PBS^{+/+}$ in presence of 10% bacteria-conditioned medium (BCM) collected by sterile-filtration of cultures from *E. coli* (O6:K2:H1), *S. aureus* (LS1), *E. coli* (BL21) or *S. carnosus* (TM300). Incubations were performed at 37 °C for the indicated periods of BCM-exposure. Images of 20 µm size are shown as overlay of 5-LOX (Alexa Fluor 555, red) and FLAP (Alexa Fluor 488, green) staining and represent three independent experiments. Unstimulated samples were kept in $PBS^{+/+}$ for either the longest or shortest incubation time in order to exclude unspecific side effects on 5-LOX activation.

In resting HEK_5-LOX/FLAP cells, 5-LOX is located within soluble parts of the nucleus, while it co-localizes with FLAP at the nucleus upon activation (98). Both pathogenic bacteria, the Gram-negative *E. coli* strain O6:K2:H1 (156) and the Gram-positive *S. aureus* LS1 (146), stimulated 5-LOX translocation, starting at approximately 30 min (*E. coli*) or 90 min (*S. aureus*) after bacterial exposure. By contrast, HEK_5-LOX/FLAP challenged with non-pathogenic *E. coli* BL21 (157) or *S. carnosus* TM300 (158,159) did not show 5-LOX redistribution even after 90 min of stimulation (**Fig. 4.1A**). Since secretion of exotoxins is discussed to be a key determinant for bacterial pathogenicity (160), we performed the stimulation with sterile-filtered medium of bacterial cultures (BCM) that lacks intact bacteria or cell debris. In fact, BCMs derived from pathogenic bacteria induced 5-LOX/FLAP co-localization at the nucleus. Noteworthy, for BCM of *S. aureus* LS1 activation of 5-LOX appeared to be faster compared to the stimulation with corresponding intact bacteria and was observable already 10 min after BCM addition. Again, BCMs of non-pathogenic bacteria failed to induce 5-LOX translocation (**Fig. 4.1B**).

The exotoxin α-hemolysin from *S. aureus* is described to be a crucial virulence factor in staphylococcal-related diseases (116-118,161). We therefore investigated time- and dose-dependent effects of this PFT on HEK_5-LOX/FLAP cells. 5-LOX translocation occurred after 30 min of exposure to toxin-concentrations of 1 and 10 µg/mL, while 0.1 µg/mL α-hemolysin were insufficient to induce 5-LOX/FLAP co-localization, even after 90 min of stimulation. By contrast, Ca^{2+} ionophore A23187, which is commonly applied to study 5-LOX activity, induced subcellular translocation of 5-LOX already within 10 min after addition (98) (**Fig. 4.2A**).

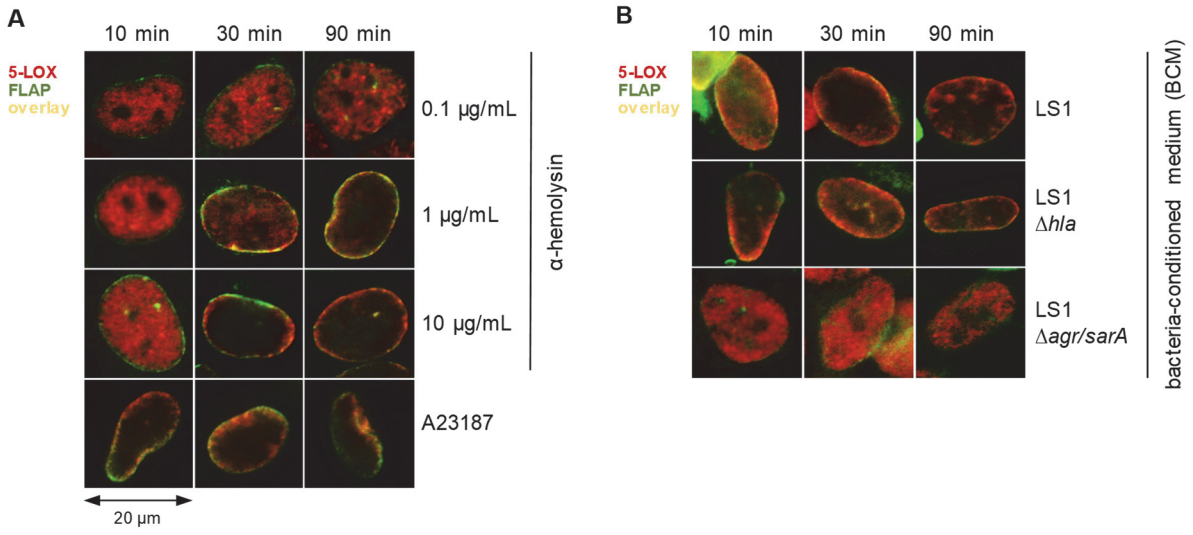

Fig. 4.2 Staphylococcal exotoxins mediate 5-LOX translocation in HEK293 cells. Subcellular localization of 5-LOX was evaluated by IF microscopy. **A** HEK_5-LOX/FLAP cells were stimulated by recombinant α-hemolysin at the indicated concentrations (0.1 to 10 µg/mL) or 0.5 µM A23187 at 37 °C for the indicated exposure times. **B** HEK_5-LOX/FLAP cells were exposed to 10% BCM of *S. aureus* LS1 (wildtype, LS1Δ*hla*, LS1Δ*agr/sarA*) in $PBS^{+/+}$ at 37 °C and for the indicated time periods. Unconditioned medium was applied for the longest and shortest incubation time in order to exclude an influence of the vehicle (not shown). Images of 20 µm size are shown as overlay of 5-LOX (Alexa Fluor 555, red) and FLAP (Alexa Fluor 488, green) staining and are representative for three independent experiments.

Next, HEK_5-LOX/FLAP cells were stimulated with BCMs from *S. aureus* LS1 wildtype and from two genetically modified strains lacking either α-hemolysin (Δ*hla*) or complete *agr*- and *sarA*-mediated exotoxin expression (Δ*agr/sarA)* (147,148). While both, BCMs from wildtype and LS1Δ*hla* induced 5-LOX translocation already 10 min after BCM exposure, only a complete knockout of exotoxins in LS1Δ*agr/sarA* could prevent the activation of 5-LOX in this respect (**Fig. 4.2B**). Taken together, these data suggest a key participation but not an exclusive role of α-hemolysin in bacterial stimulation, at least in the HEK293 cell-model.

4.1.2 Bacterial activation of 5-LOX in HEK293 cells is mediated by increased intracellular Ca^{2+} levels but independent of phosphorylation

α-Hemolysin is described to activate cellular kinases (162), and enzymatic activity of 5-LOX is strongly upregulated by phosphorylation by p38 MAPK-dependent MK-2/3 (163). Therefore, we aimed at investigating the role of p38 MAPK during bacterial stimulation in HEK_5-LOX/FLAP cells. Interestingly, pretreatment with the selective p38 MAPK inhibitors skepinone-L or SB203580 (164) did not prevent 5-LOX translocation upon stimulation with BCM from *S. aureus* LS1 (**Fig. 4.3A**). Additionally, the 5-LOX mutant *S271A*, that cannot be phosphorylated by p38 MAPK-dependent MK-2/3 (69), co-localized with FLAP upon BCM exposure (**Fig. 4.3B**). Equal co-expression of 5-LOX wildtype or 5-LOX(*S271A)* together with FLAP was confirmed by Western blot analysis (**Fig. 4.3C**). Accordingly, these results indicate an alternative mechanism of 5-LOX activation by bacterial toxins in HEK_5-LOX/FLAP cells, independent of kinase-mediated events.

Besides phosphorylation, intracellular Ca^{2+} levels and Ca^{2+} binding to the N-terminal domain of 5-LOX are key determinants for enzyme activity (7). Thus, stimulation of HEK_5-LOX/FLAP cells by either recombinant α-hemolysin or *S. aureus* LS1 wildtype BCM were performed in presence of 10 mM EDTA. In fact, 5-LOX translocation was prevented by Ca^{2+} complexation for both stimuli, substantiating an eminent role of Ca^{2+} influx for bacterial 5-LOX activation (**Fig. 4.3D**). Moreover, examination of intracellular Ca^{2+} levels in HEK293 cells by fluorescence-based analysis revealed a significant, time-dependent increase of Ca^{2+} concentrations upon stimulation with either isolated α-hemolysin or BCM of LS1 wildtype compared to vehicle incubations (**Fig. 4.3E/F**). Interestingly, BCM from LS1 wildtype caused a minor but obviously faster reply then α-hemolysin and showed comparable kinetics as found for ionomycin-induced Ca^{2+} influx. Additionally, while the complete depletion of exotoxins in BCM from LS1Δ*agr/sarA* could be related to insufficient Ca^{2+} mobilization, BCM from LS1 solely lacking α-hemolysin (LS1Δ*hla*) still induced comparable Ca^{2+} influx as the wildtype control (**Fig. 4.3F**). Together, the bacterial activation of 5-LOX translocation in HEK_5-LOX/FLAP cells strongly correlates with the increase of intracellular Ca^{2+}. However, efficient stimulation apparently requires further staphylococcal exotoxins distinct from α-hemolysin, although this archetype of PFTs appears to be involved in this process.

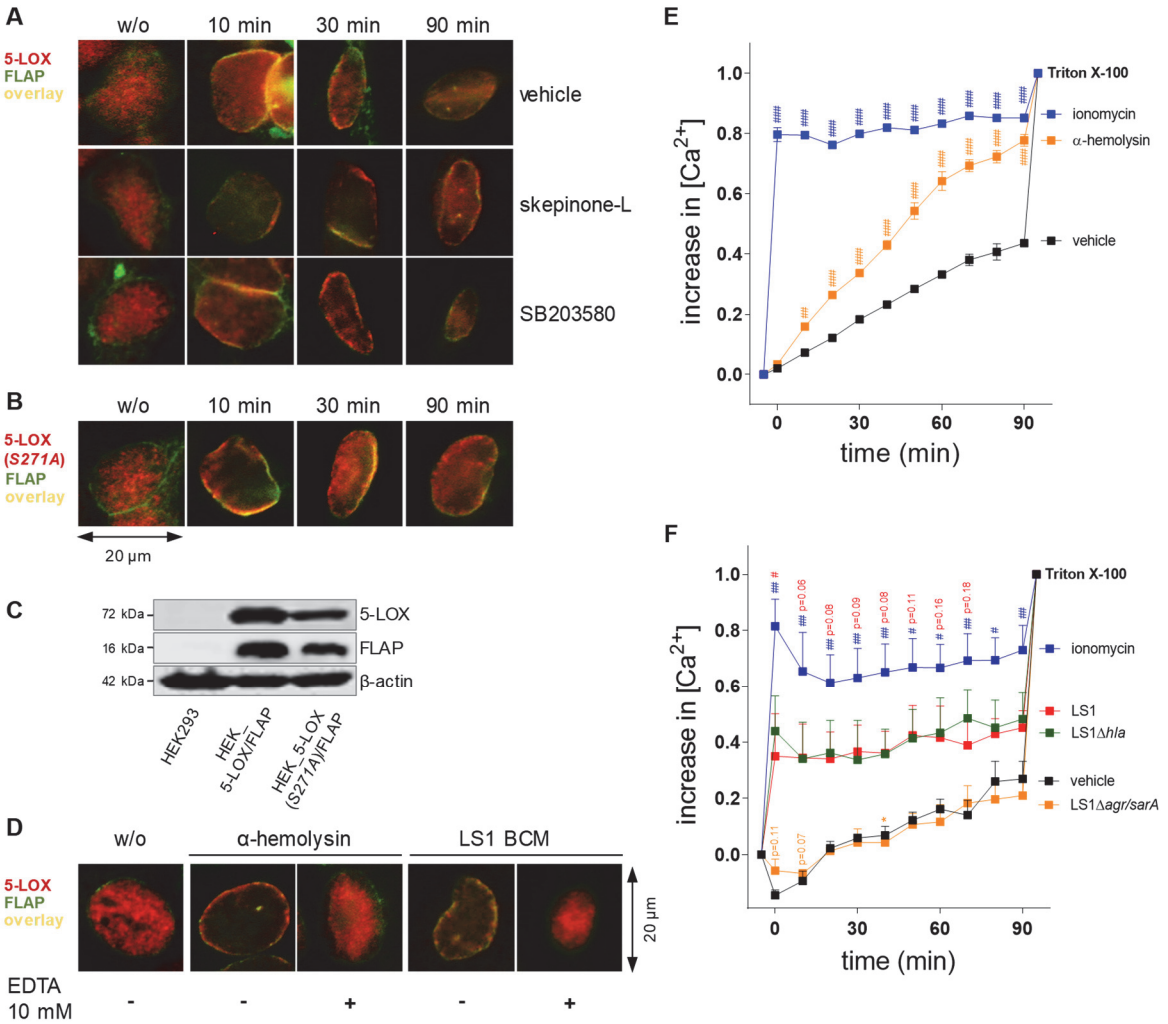

Fig. 4.3 Bacteria-induced 5-LOX translocation in HEK293 cells is affected from intracellular Ca^{2+} influx but independent of p38 MAPK activation. Subcellular distribution of 5-LOX was examined by IF microscopy. **A** HEK_5-LOX/FLAP cells were preincubated with 0.1% DMSO (vehicle control), 0.3 µM skepinone-L, or 1 µM SB203580 prior to stimulation by 10% BCM of *S. aureus* LS1 in $PBS^{+/+}$ at 37 °C for the indicated timepoints. **B** HEK293 cells stably expressing FLAP and the mutant 5-LOX(*S271A*) were incubated in presence of 10% BCM of *S. aureus* LS1 for the indicated exposure times at 37 °C in $PBS^{+/+}$. Microscopic images of 20 µm size are given as overlay of 5-LOX or 5-LOX(*S271A*) (Alexa Fluor 555, red) and FLAP (Alexa Fluor 488, green) staining and are representative for three independent experiments. **C** Stable expression of 5-LOX, wildtype or mutant, and FLAP in HEK293 cells was verified by immunoblotting. Western blot images are representative for three independently collected HEK293 cell lysates. **D** Subcellular 5-LOX localization of HEK_5-LOX/FLAP cells was examined by microscopic analysis upon stimulation by 10% LS1 BCM or 10 µg/mL α-hemolysin in presence of 10 mM EDTA or vehicle control. Images of 20 µm size are given as overlay of 5-LOX (Alexa Fluor 555, red) and FLAP (Alexa Fluor 488, green) staining and represent three independent experiments. **E-F** Intracellular Ca^{2+} levels were continuously detected in Fura-2AM-labeled HEK293 cells upon stimulation with 10 µg/mL α-hemolysin (E) or 10% BCM of *S. aureus* LS1 (wildtype, Δ*hla* or Δ*agr/sarA*) (F), 2 µM ionomycin or vehicle control (water or unconditioned medium) at 37 °C. Data are normalized to subsequent Triton X-100 cell lysis and are presented as mean ± SEM of three experiments. $^{\#}p < 0.05$, $^{\#\#}p < 0.01$ and $^{\#\#\#}p < 0.001$ LS1, α-hemolysin or ionomycin vs. vehicle control, $^{*}p < 0.05$, $^{**}p < 0.01$ and $^{***}p < 0.001$ *S. aureus* LS1 mutant strain vs. the corresponding LS1 wildtype applying one-way ANOVA with Tukey multiple comparison post-hoc test.

4.1.3 Staphylococcal exotoxins mediate LM formation in human neutrophils

Since staphylococcal exotoxins mediate 5-LOX redistribution in HEK_5-LOX/FLAP cells, we asked whether stimulation by bacterial toxins cause LT formation also in neutrophils. Noteworthy, the HEK293 cell model was shown to lack LT biosynthesis from endogenous AA even after treatment with A23187 and is therefore inappropriate to study LM biosynthesis in general (98). For that reason, we utilized freshly isolated human neutrophils that are prominent leukocytes participating in LT formation (64). LM formation of neutrophils induced by *S. aureus* BCMs or isolated exotoxins was assayed by UPLC-MS/MS and biosynthesis of 5-HETE, LTB_4, t-LTB_4 and the LTB_4-degradation product 20-OH-LTB_4 were chosen as representative 5-LOX products. Notably, neutrophils appeared to be much more sensitive for bacterial toxins than HEK_5-LOX/FLAP cells since concentrations of 1% BCM were sufficient to examine 5-LOX activity in this respect. Exposure time was evaluated in advance and revealed 10 min as optimum for LT formation (data not shown).

As indicated in **Fig. 4.4A**, neutrophil stimulation with BCMs from *S. aureus* LS1 wildtype significantly induced the formation of bioactive lipids. By contrast, exposure to BCM from LS1Δ*agr/sarA* did not cause 5-LOX product formation. Interestingly, strains deficient in α-hemolysin expression induced equal amounts of 5-LOX products compared to wildtype. In line with these findings, only minor activation of 5-LOX was observed after treatment with isolated α-hemolysin, even at a high concentration of 100 µg/mL (**Fig. 4.4A**). Analysis of additional LMs revealed a slight decrease in 12- and 15-LOX activity (represented by 14-HDHA, 12-HEPE and 12-HETE biosynthesis) and PG formation upon stimulation with LS1Δ*hla* BCMs, while the global knockout of exotoxins in LS1Δ*agr/sarA* prevented the formation of LMs independently from their biosynthetic origin (**Fig. 4.4B**). In addition, both BCMs from LS1 wildtype and LS1Δ*hla* significantly increased intracellular Ca^{2+} concentrations up to 10 min of exposure and in a comparable manner as the ionomycin control. By contrast, BCM from LS1Δ*agr/sarA* was not capable to induce Ca^{2+} influx. As expected from the results on LT formation, isolated α-hemolysin that was able to induce Ca^{2+} mobilization in the HEK293 cell-model failed to stimulate neutrophils even at higher concentrations (**Fig. 4.4C**), explaining the absent release of LMs from neutrophils discussed above.

Subcellular localization of 5-LOX and FLAP was analyzed upon stimulation with staphylococcal BCMs, and both BCMs from LS1 wildtype and LS1Δ*hla* induced 5-LOX/FLAP co-localization in neutrophils, while 5-LOX remained in soluble parts of the nucleus upon exposure to BCM that completely lacks *agr*- and *sarA*-mediated exotoxin expression (LS1Δ*agr/sarA*) (**Fig. 4.4D**). Intriguingly, isolated α-hemolysin appeared to be incapable to induce 5-LOX translocation indicating an involvement of other toxins in the activation of LM formation in human neutrophils. Thus, these data also underline cell-specific effects that have to be considered for terminating conclusions.

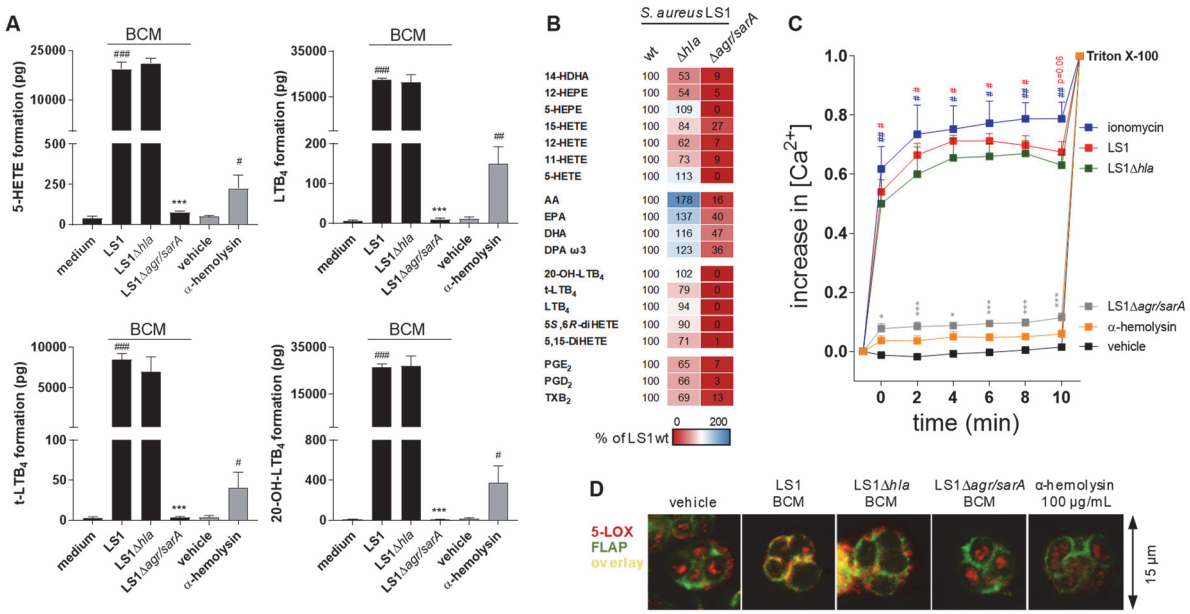

Fig. 4.4 5-LOX activation and concurrent LM formation in neutrophils by staphylococcal exotoxins is mediated by an elevation of intracellular Ca^{2+} levels. A-B 5 x 10^6 neutrophils/mL were stimulated by 1% BCM of *S. aureus* (LS1 wildtype, LS1Δ*hla* or LS1Δ*agr/sarA*), 100 µg/mL recombinant α-hemolysin or vehicle control (unconditioned medium or water) for 10 min at 37 °C. Data are presented as mean ± SEM (A) or as heat map in % of LS1 wildtype (B) of N=3 different blood donors. $^{\#}p < 0.05$, $^{\#\#}p < 0.01$ and $^{\#\#\#}p < 0.001$ LS1 or α-hemolysin vs. vehicle control or $^{*}p < 0.05$, $^{**}p < 0.01$ and $^{***}p < 0.001$ vs. the corresponding LS1 wildtype strain using one-way ANOVA with Tukey multiple comparison post-hoc test. **C** Fura-2AM-labeled neutrophils were stimulated by 2 µM ionomycin, 100 µg/mL α-hemolysin, 1% unconditioned medium or 1% BCM of *S. aureus* (LS1, LS1Δ*hla* or LS1Δ*agr/sarA*) under continuous fluorescence reading at 37 °C followed by Triton X-100 cell lysis. Intracellular Ca^{2+} concentrations normalized to Triton X-100 lysis are given as mean ± SEM of N=4 different donors. $^{\#}p < 0.05$, $^{\#\#}p < 0.01$ and $^{\#\#\#}p < 0.001$ LS1 or ionomycin vs. vehicle control or $^{*}p < 0.05$, $^{**}p < 0.01$ and $^{***}p < 0.001$ LS1 deletion mutant vs. the corresponding LS1 wildtype strain using one-way ANOVA with Tukey multiple comparison post-hoc test. **D** 5-LOX translocation in neutrophils challenged with 1% BCM of *S. aureus* LS1 (wildtype, LS1Δ*hla*, LS1Δ*agr/sarA*), 1% unconditioned medium or 100 µg/mL α-hemolysin was evaluated by IF microscopy. Microscopic images of 20 µm size are given as overlay of 5-LOX (Alexa Fluor 555, red) and FLAP (Alexa Fluor 488, green) staining and are representative for three independent experiments.

4.1.4 Effects of staphylococcal PSMs on LM biosynthesis in human neutrophils

In contrast to α-hemolysin-stimulated HEK_5-LOX/FLAP cells, neutrophils appeared to be resistant against the archetype of staphylococcal exotoxins, implying the contribution of other released bacterial inducers for 5-LOX activation. In order to reveal the staphylococcal exotoxins that are involved in LM formation of neutrophils, cells were stimulated with BCM of LS1Δ*psm*αβ that lacks the expression of α- and β-type PSMs. LT formation was significantly decreased upon exposure to LS1Δ*psm*αβ BCM compared to the wildtype control (**Fig. 4.5A**). Interestingly, while knockout of PSMs resulted in impaired LT levels, LMs derived from other enzymes (*i.e.* 12- and 15-LOX, COX) remained less affected (**Fig. 4.5B**). Additionally, neutrophils were stimulated with BCMs from the methicillin-resistant *S. aureus* strain USA300 and its corresponding strain USA300Δ*pvl*, insufficient in PVL expression, to investigate the effects of these cytolytic exotoxins on LM biosynthesis. Intriguingly, knockout of PVLs did not alter LT formation compared with USA300 wildtype BCM (**Fig. 4.5A**, grey bars), indicating a superior role of PSMs on 5-LOX activation compared to other staphylococcal exotoxins. In line

with this, isolated PSMα1 and PSMα3, both considered to be the most potent PSMs, dose-dependently induced LT formation at concentrations of 1 and 10 µg/mL, that generally correspond to PSM amounts detected in *S. aureus* strains before (165) (**Fig. 4.5C**).

In order to summarize the findings from neutrophil stimulations with either BCMs of LS1 wildtype or genetically modified derivatives (Δ*hla*, Δ*psm*αβ, Δ*agr/sarA*) as well as corresponding recombinant exotoxins, a principle component analysis (PCA) was performed as shown in **Fig. 4.5D**. While 5-LOX product formation clearly correlated with the presence of PSMs within BCMs of LS1 wildtype and LS1Δ*hla* or stimulation by isolated PSMα3, a tendency towards 12-LOX- and COX-mediated LMs was found for stimuli lacking PSM expression (*i.e.* vehicle (unconditioned medium), LS1Δ*psm*αβ, LS1Δ*agr/sarA* or recombinant α-hemolysin (alpha-toxin)).

Knockout of PSMα and PSMβ significantly decreased BCM-mediated Ca^{2+} influx in neutrophils compared to wildtype and ionomycin treatment, whereas isolated PSMα3 induced a fast but less intense intracellular Ca^{2+} mobilization that declined up to 10 min of exposure time (**Fig. 4.5E**). Accordingly, LM mediator formation was completely abolished in presence of 10 mM EDTA (**Fig. 4.5F**). Moreover, 5-LOX subcellular localization was affected by both LS1 wildtype BCM and isolated PSMs, respectively, leading to co-localization with FLAP at the nuclear membrane. By contrast, stimulation with BCM of LS1Δ*psm*αβ failed to induce 5-LOX translocation (**Fig. 4.5G**), underlining the importance of PSMs for *S. aureus*-induced LT formation in human neutrophils. However, both BCM of LS1Δ*psm*αβ and recombinant PSMs induced 5-LOX redistribution in HEK_5-LOX/FLAP cells which might further indicate cell-specific effects of staphylococcal exotoxins (**Fig. 4.5G**). Moreover, these findings are in line with our results for HEK_5-LOX/FLAP stimulations.

Staphylococcal toxins mainly cause pore-formation and subsequent cell death (114). We therefore asked whether LM formation of neutrophils might be related to cell lysis instead of specific molecular mechanisms. 5-LOX activity *in cellulo* was shown to be dependent on 5-LOX/FLAP co-localization and interaction, and FLAP inhibitors such as MK886 are ineffective in incubations with isolated 5-LOX or under cell-free conditions (86,98). Pretreatment of neutrophils with the FLAP inhibitor MK886 and stimulation with LS1 wildtype BCM significantly reduced LT formation, indicating a functional cellular environment during LM formation. Presence of the direct 5-LOX inhibitor zileuton was less effective but likewise decreased 5-LOX related products to approximately 50% of the vehicle control (**Fig. 4.6A**). In line with recent findings by our group that investigated the pharmacological profile of inhibitors targeting distinct branches of LM biosynthesis in human macrophages (99), FLAP inhibition selectively decreased the formation of 5-LOX-mediated products in neutrophils compared to other enzymatic pathways (*i.e.* COX, 12- or 15-LOX) (**Fig. 4.6B**). Moreover, inhibition of the 5-LOX pathway increased the formation of mediators derived from other biosynthetic branches, presumably due to a substrate shunt, and this effect was less pronounced for the direct inhibition of 5-LOX by zileuton compared to MK886.

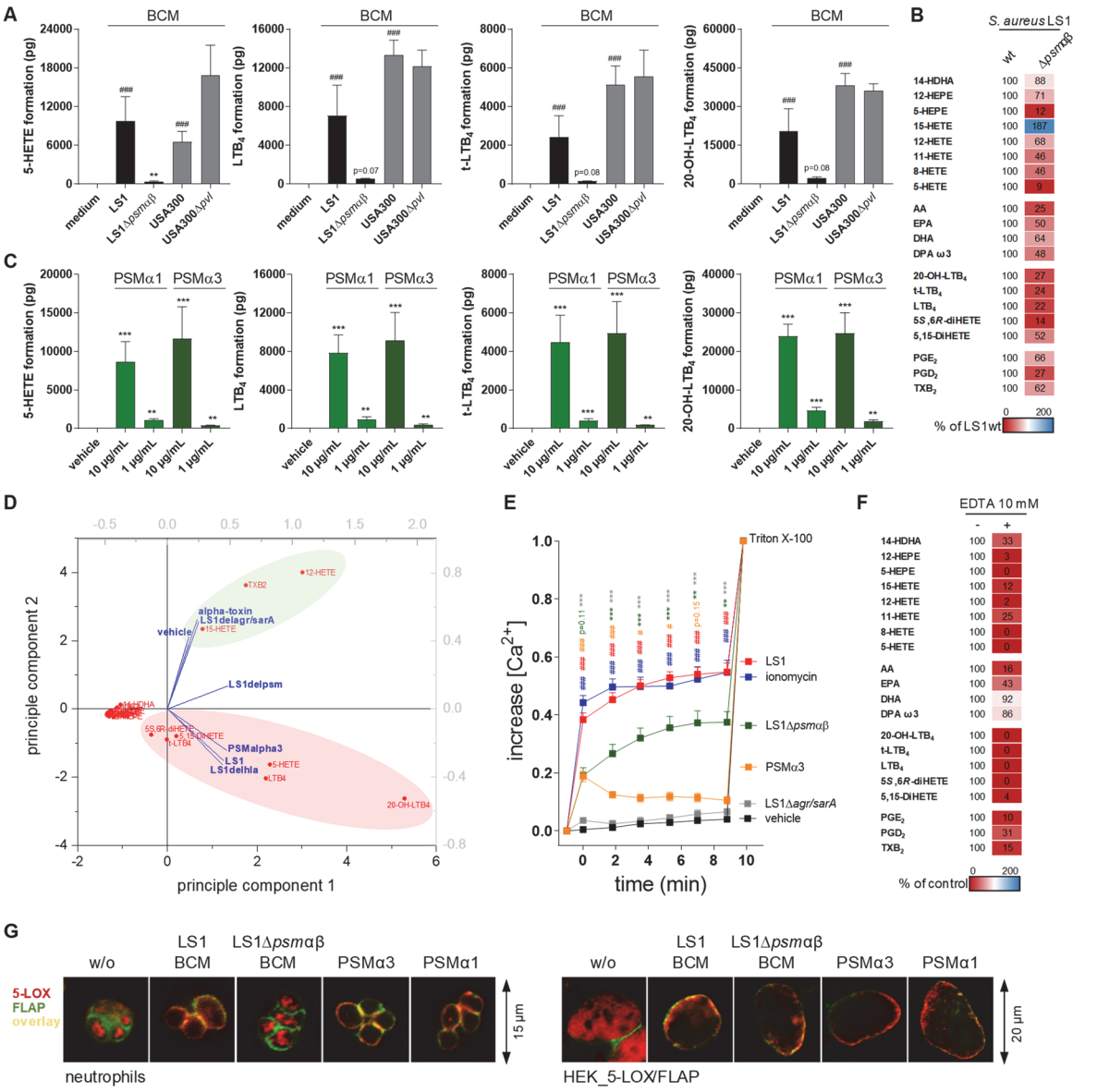

Fig. 4.5 PSMs of *S. aureus* mediate 5-LOX activation in neutrophils. A-B 5 x 10^6 neutrophils/mL were stimulated by 1% BCM of *S. aureus* LS1 wildtype, LS1Δ*psm*αβ, USA300 wildtype or USA300Δ*pvl* for 10 min at 37 °C and LM formation was determined by UPLC-MS/MS. Data are given as pg (A) or % of the corresponding wildtype *S. aureus* strain (B) and as mean ± SEM for N=3 independent donors. $^{\#}p < 0.05$, $^{\#\#}p < 0.01$ and $^{\#\#\#}p < 0.001$ wildtype strains vs. vehicle control (unconditioned medium) or $^{*}p < 0.05$, $^{**}p < 0.01$ and $^{***}p < 0.001$ knockout vs. the corresponding *S. aureus* wildtype strain using one-way ANOVA with Tukey multiple comparison post-hoc test. **C** LM formation of neutrophils upon stimulation with 1 or 10 µg/mL PSMα1 and PSMα3 for 10 min at 37 °C was assessed by UPLC-MS/MS. Data are expressed in pg of 5 x 10^6 neutrophils as mean ± SEM of N=3 donors. $^{*}p < 0.05$, $^{**}p < 0.01$, $^{***}p < 0.001$ vs. vehicle using one-way ANOVA with Tukey multiple comparison post-hoc test. **D** Principal component analysis (PCA) of LMs (red) detected by UPLC-MS/MS upon treatment of neutrophils with isolated bacterial toxins (α-toxin = α-hemolysin, PSMα3), LS1 BCM (del = Δ) or unconditioned medium (vehicle) (blue). Free FA were excluded for analysis to focus on biosynthesized mediators. **E** Intracellular Ca^{2+} levels of Fura-2AM-labeled neutrophils were assessed upon stimulation with 2 µM ionomycin, 10 µg/mL PSMα3, 1% unconditioned medium or 1% BCM of *S. aureus* (LS1, LS1Δ*psm*αβ or LS1Δ*agr/sarA*) under continuous fluorescence reading for 10 min at 37 °C. Data are presented as mean ± SEM of Triton X-100 normalized values, N=7 donors. $^{\#}p < 0.05$, $^{\#\#}p < 0.01$ and $^{\#\#\#}p < 0.001$ LS1 or ionomycin vs. vehicle control or $^{*}p < 0.05$, $^{**}p < 0.01$ and $^{***}p < 0.001$ mutant vs. the corresponding LS1 wildtype strain using one-way ANOVA with Tukey multiple comparison post-hoc test. **F** LM formation of 5 x 10^6 neutrophils stimulated by 10 µg/mL PSMα3 for 10 min at 37 °C in presence of 10 mM EDTA was evaluated by UPLC-MS/MS. Data are given as % of the vehicle control and as mean of N=3 independent donors. **G** Subcellular localization of 5-LOX (Alexa Fluor 555, red) and FLAP (Alexa Fluor 488, green) in HEK_5-LOX/FLAP cells or human neutrophils was examined by IF microscopy upon treatment with 10% (HEK) or 1% (neutrophils) BCM of LS1 wildtype, LS1Δ*psm*αβ, or 10 µg/mL PSMα1 or PSMα3 for 10 min at 37 °C. Images are representative for three different experiments (HEK) or donors (neutrophils), respectively.

In addition, estimation of cell viability by either trypan blue staining or analysis of LDH release revealed only minor cytotoxic effects upon BCM treatment. BCM of LS1Δ*agr/sarA* did not affect cell viability and thus confirm the less-virulent state of the strain (**Fig. 4.6C/D**). Finally, in order to exclude cell lysis as crucial factor for LM biosynthesis, neutrophils were treated with lytic concentrations of Triton X-100. Interestingly, triton-induced cell lysis could not be related to LT formation compared to PSMα3 stimulation, underlining a distinct mechanism of LOX activation far from ordinary cell disruption (**Fig. 4.6E**).

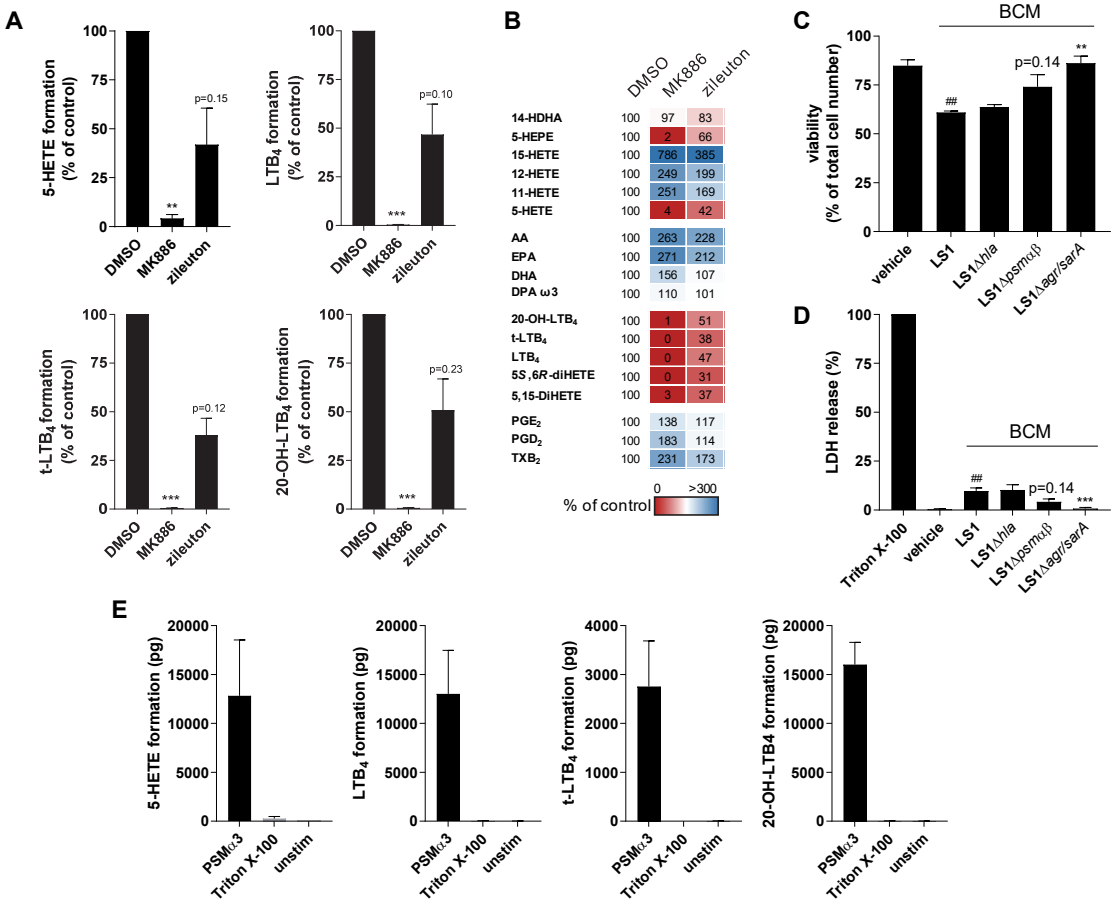

Fig. 4.6 Exotoxin-induced LT formation requires an intact cellular context and is independent of cell lysis. A-B 5 x 10^6 neutrophils/mL were preincubated with 300 nM MK886 or 3 µM zileuton for 10 min at 37 °C and subsequently stimulated by 1% LS1 BCM for another 10 min at 37 °C. LM formation was determined by UPLC-MS/MS. Data are expressed in % of the vehicle control (0.1% DMSO) as bars for 5-LOX products (A) or heat map including additional LMs (B) and as mean ± SEM of N=3 different donors. *p < 0.05, **p < 0.01 and ***p < 0.001 vs. vehicle control using two-tailed Student's t-test. **C** Neutrophils were challenged with 1% BCM of LS1 wildtype, LS1Δ*hla*, LS1Δ*psm*αβ, and LS1Δ*agr/sarA* followed by assessment of cell viability by trypan blue staining and automatic cell counting. Data are given as % of viable cells vs. total cell number. **D** LDH release of neutrophils was assayed upon treatment with 1% BCM of *S. aureus* LS1 wildtype, LS1Δ*hla*, LS1Δ*psm*αβ, and LS1Δ*agr/sarA* for 10 min at 37 °C. Values are presented as % of Triton X-100 total cell lysis and as mean ± SEM of N=3 independent donors. #p < 0.05, ##p < 0.01 and ###p < 0.001 LS1 vs. vehicle control or *p < 0.05, **p < 0.01 and ***p < 0.001 knockout vs. the corresponding LS1 wildtype strain using one-way ANOVA with Tukey multiple comparison post-hoc test. **E** LM formation of 5 x 10^6 neutrophils stimulated by 10 µg/mL PSMα3, 0.1% Triton X-100 or vehicle control (unstim) for 10 min at 37 °C. Data are presented in pg and as mean ± SEM of N=3 independent donors.

4.1.5 Analysis of staphylococcal-induced LM formation in vivo

In vivo LM formation was examined by UPLC-MS/MS in tissue homogenates of mice hind paws that were subcutaneously infected with *S. aureus* USA300. Formation of 5-LOX products including 5-HETE, LTB_4, and t-LTB_4 were found to be induced compared to vehicle control and showed increased levels up to 48 h with a temporal decline at 24 h post-infection. By contrast, the COX-mediated metabolites PGE_2 and TXB_2 lacked an analogue time course and were constantly increased in infected tissues up to 48 h after infection. Interestingly, while 5-LOX products and TXB_2 remained at basal levels within uninfected tissues, PGE_2 was increased in a comparable manner within corresponding vehicle controls, indicating a formation independent of bacterial presence and apparently resulting from tissue damage by the buffer injection (**Fig. 4.7A**).

Additionally, mice paws infected with USA300Δ*psm*αβ showed a significant decrease in LTB_4 formation compared to wildtype preparations at 48 h post-infection. While 5-HETE and t-LTB_4 showed an equal tendency to be decreased by PSM knockout, PGE_2 and TXB_2 derived from COX-enzymes appeared to be unaltered in this respect (**Fig. 4.7B**). These findings indicate the involvement of PSMs in LM formation following bacterial infection *in vivo* and underline the dependency of staphylococcal infections from exotoxin secretion.

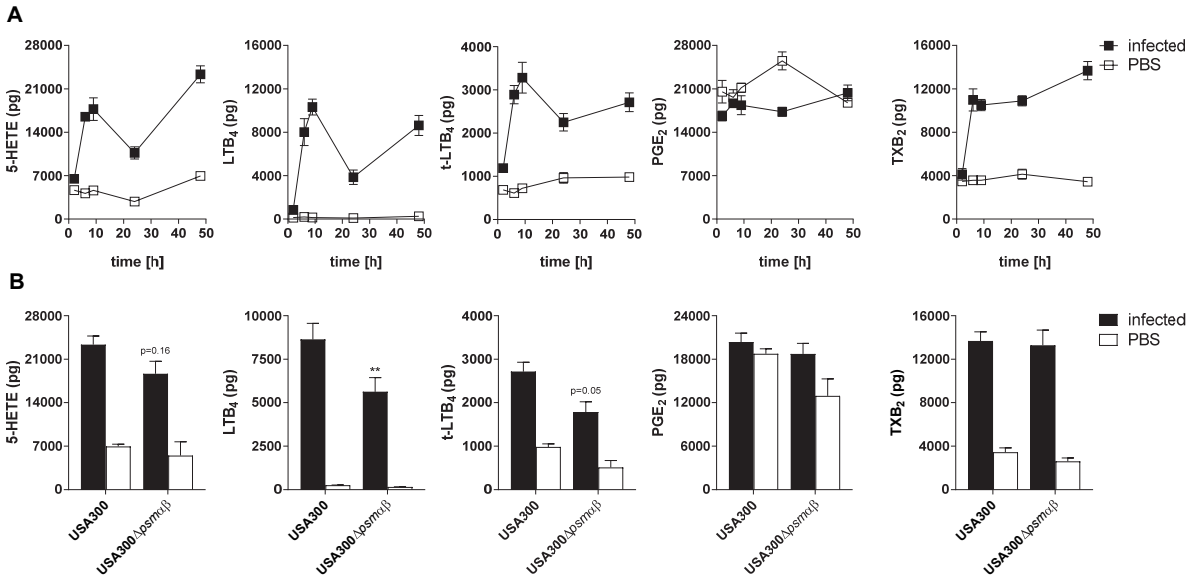

Fig. 4.7 LM formation upon staphylococcal infection *in vivo* is affected from PSM expression. C57BL/6 mice were subcutaneously infected by injection of 2 x 10^7 CFU of *S. aureus* USA300, wildtype or PSM deletion mutant, into the right hind paw of each mouse. **A** LM formation of mice infected with USA300 wildtype for the indicated timepoints. **B** LMs detected in murine paws 48 h post-infection with either USA300 wildtype or USA300Δ*psm*αβ, respectively. LM formation within paw homogenates was evaluated by UPLC-MS/MS and normalized to 1 µg total protein. Data are given as mean ± SEM of 4 mice per group and are compared to the vehicle control, represented by simultaneous injection of 50 µL PBS buffer into the opposite (left) hind paw. *p < 0.05, **p < 0.01 and ***p < 0.001 vs. the corresponding USA300 wildtype strain using one-way ANOVA with Tukey multiple comparison post-hoc test.

4.2 The FPR2 receptor mediates PSM-induced 5-LOX activation in human neutrophils

4.2.1 The FPR2 receptor antagonist WRW4 antagonizes PSM-induced LM formation

As it was reported before that PSMs mediate their chemotactic abilities by targeting the FPR2 (also referred to as FPR2/ALX or FPRL1) receptor (129,131,166), we aimed at investigating the role of this receptor for PSM-induced LM biosynthesis. Western blot analysis revealed the highest FPR2 expression in neutrophils compared to lysates from monocytes and monocyte-derived macrophages (M1 and M2 phenotype, respectively) (**Fig. 4.8A**).

As mentioned earlier, FPRs are characterized by recognition of bacterial and mitochondrial N-formylated peptides (130,131), and the synthetic peptide fMLP induced LT formation in neutrophils after LPS priming (80,167). In line, fMLP was characterized as a highly specific FPR1 receptor agonist with low FPR2 affinity (131). In order to prove FPR2 over FPR1 as cellular target for PSMs and to evaluate a simultaneous activation of FPR1 by formylated staphylococcal peptides within the applied BCMs, we examined the LM profile of human neutrophils challenged with either BCM from *S. aureus* LS1 or fMLP (**Fig. 4.8B**).

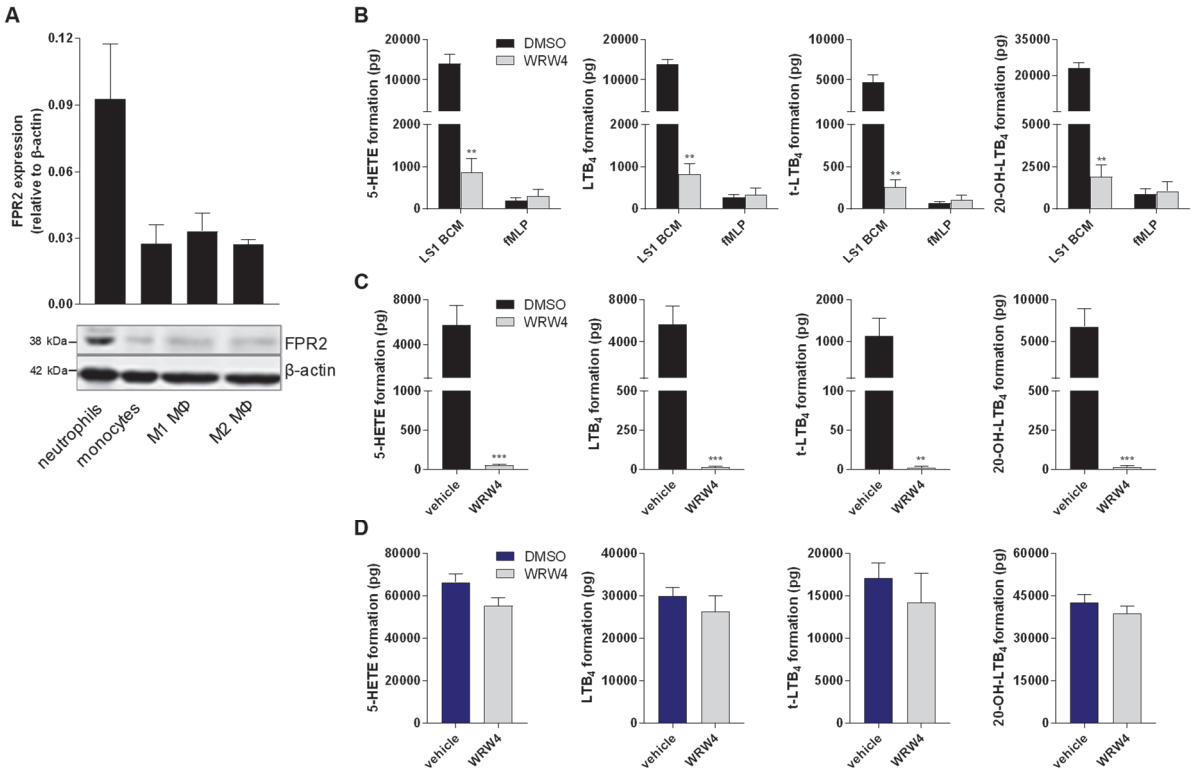

Fig. 4.8 PSM-induced LT formation is prevented by FPR2 receptor antagonism. A FPR2 expression of human leukocytes was verified by immunoblotting and subsequent densitometric evaluation and normalization to β-actin. Western blot images are representative for lysates from three independent cell donors. **B-D** 5 x 10^6 neutrophils/mL were pretreated for 10 min at 37 °C with 10 µM WRW4 or vehicle control (0.1% DMSO) prior to stimulation with 1% LS1 BCM or 1 µM fMLP (B), 10 µg/mL PSMα3 (C), or 2.5 µM A23187 (D) for another 10 min at 37 °C. LM formation was determined by UPLC-MS/MS. Data are presented in pg as mean ± SEM of N=3 independent blood donors. Statistical analysis was performed using paired, two-tailed Student's t-test. ***p < 0.001, **p < 0.01, *p < 0.05 WRW4 vs. the corresponding vehicle control.

fMLP appeared to be much inferior to activate LT biosynthesis compared to LS1 BCM (more than 20-fold). Moreover, when cells were pretreated with the selective FPR**2** peptide antagonist WRW4 (137), LM formation was significantly reduced in neutrophils stimulated with LS1 BCM, while fMLP activation remained unaffected in this respect (**Fig. 4.8B**). However, when neutrophils were challenged with recombinant staphylococcal PSMα3, LT formation could be inhibited significantly and almost completely by WRW4 (**Fig. 4.8C**). Noteworthy, antagonism of FPR2 by WRW4 did not affect Ca^{2+} ionophore A23187-induced 5-LOX product formation (**Fig. 4.8D**), indicating that WRW4 selectively decreases bacteria-induced LM biosynthesis independent of a direct 5-LOX inhibition.

4.2.2 Modulation of FPR2 but not FPR1 affects PSM-induced 5-LOX activation

In order to substantiate the PSM-mediated activation of FPR**2**, we investigated LM formation of neutrophils in presence of the chemotaxis inhibitory protein of *S. aureus* (CHIPS), which was shown to selectively antagonize the FPR1 ligand fMLP at nanomolecular concentrations (134). Stimulation by either fMLP or PSMα3 both induced LM formation in neutrophils, although PSM-mediated activation appeared to be superior compared to fMLP. In addition, while fMLP-induced LT biosynthesis could be inhibited by CHIPS to approximately 50%, PSM-activation remained unaffected in presence of the inhibitory protein (**Fig. 4.9A**).

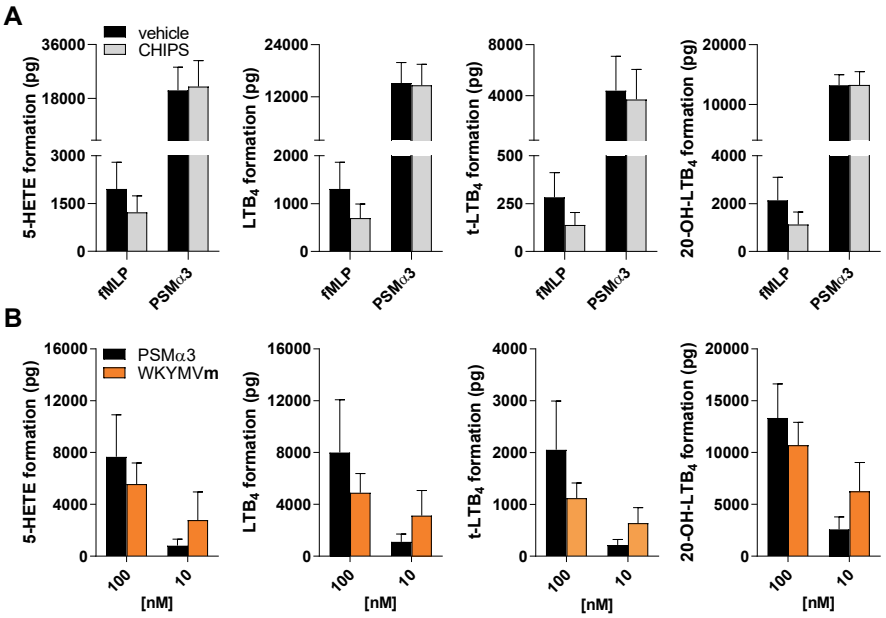

Fig. 4.9 Activation of FPR2 but not FPR1 is crucial for PSM-mediated LT formation. A 5 x 10^6 neutrophils/mL were pretreated with 1 µg/mL CHIPS (chemotaxis inhibitory protein of *Staphylococcus aureus*) or vehicle control (0.1% DMSO) prior to stimulation with 10 µg/mL PSMα3 or 1 µM fMLP for 10 min at 37 °C. Statistical analysis was performed using paired, two-tailed Student's t-test. ***p < 0.001, **p < 0.01, *p < 0.05 CHIPS vs. the corresponding vehicle control. **B** Neutrophils were challenged by PSMα3 or WKYMVm at the indicated concentrations for 10 min at 37 °C. 5-LOX product formation was detected by UPLC-MS/MS and is presented in pg as mean ± SEM of N=2-3 independent donors.

Moreover, LT formation of neutrophils was examined upon treatment with the synthetic hexapeptide WKYMVm (methionine-D-conformer) that was shown to activate the FPR2 receptor. Interestingly, conformational variations within the N-terminal amino acid residue of WKYMV**m** was related to a 25-fold increased FPR2 activation compared to WKYMV**M** (168,169). Accordingly, WKYMVm dose-dependently induced 5-LOX product formation of neutrophils to a comparable extent as PSMα3 at concentrations of 10 and 100 nM (**Fig. 4.9B**). Taken together, our data indicate a similar activation and LM biosynthesis for PSMs compared to agents predominantly modulating FPR2 instead of FPR1.

4.2.3 Activation of ERK1/2 by S. aureus BCM and isolated PSMα3 modulates LM biosynthesis

Binding to FPR2 and subsequent G_i-protein-coupled activation of cellular kinases such as ERK and the p38 MAPK was discussed for a plethora of natural and synthetic peptides and lipids (170). Moreover, 5-LOX product formation was found to be increased by p38 MAPK-dependent phosphorylation at Ser^{271} and ERK-mediated phosphorylation at Ser^{663} (6,69,171). In order to investigate the effects of staphylococcal peptides on 5-LOX-affecting kinases in neutrophils, cells were stimulated with BCM from *S. aureus*, isolated PSMα3, or A23187 for the indicated time points followed by subsequent determination of p38 MAPK and ERK1/2-phosphorylation by Western blot analysis. All stimuli induced phosphorylation of p38 MAPK at Thr^{180}/Tyr^{182} (172) to a similar extent and with a maximum between 3 and 5 min of exposure (**Fig. 4.10A**). Comparable activation patterns could be observed for ERK1/2 phosphorylation at Thr^{202}/Tyr^{204} (for ERK1, and Thr^{185}/Tyr^{187} for ERK2) (173), reaching highest levels between 3 to 5 min and decreasing up to 10 min of stimulation. Noteworthy, PSMα3 appeared to be the most effective activator of ERK1/2 in this respect (**Fig. 4.10A**).

Additionally, neutrophils were pretreated with the FPR2 receptor antagonist WRW4 and kinase activation was evaluated after 5 min of exposure to the indicated stimuli. Interestingly, while p38 MAPK phosphorylation appeared to be widely unaffected from WRW4, both BCM- and PSM-induced ERK1/2 activation could be decreased by FPR2 antagonism, although not statistically significant ($p=0.06$ and 0.13) (**Fig. 4.10B**). Again, PSMα3 was found to be superior over BCM or A23187 in activating ERK1/2 signaling. Noteworthy, preincubation at 37 °C apparently reduced overall kinase activation compared neutrophils that were directly stimulated without any pretreatment (compare **Fig. 4.10A** and **4.10B**).

Besides p38 MAPK and ERK1/2 activation, FPR2 signaling was also related to the activation of protein kinase C (PKC) and PI3K (170). Therefore, neutrophils were pretreated with WRW4, skepinone-L (a selective inhibitor for p38 MAPK), UO126 (ERK1/2 activation inhibitor), LY294002 (PI3K inhibitor) or RO-31-8220 (PKC inhibitor) (164,174-176), respectively, and stimulated with A23187, LS1 BCM or isolated PSMα3 for 10 min at 37 °C. As shown before, WRW4 markedly reduced BCM- and PSM-induced LM formation, while A23187 activation remained widely unaffected from FPR2 antagonism.

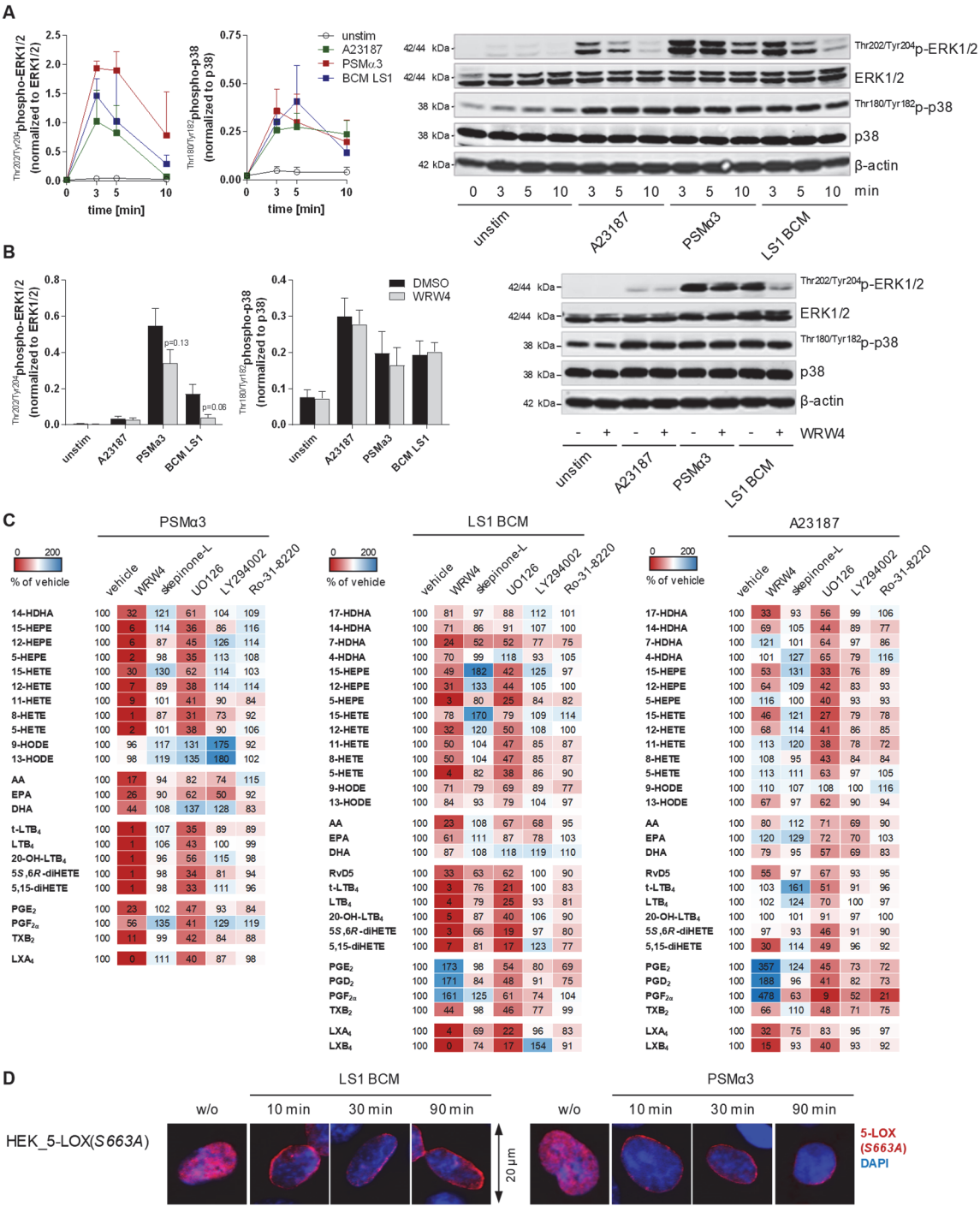

Fig. 4.10 PSM-induced LM formation is mediated by ERK1/2 activation. A 1 x 10^7 neutrophils/mL were stimulated by 1% LS1 BCM, 10 µg/mL PSMα3, or 2.5 µM A23187 for the indicated timepoints at 37 °C. **B** Neutrophils were preincubated with 10 µM WRW4 or vehicle control (0.1% DMSO) for 5 min at 37 °C prior to stimulation with 1% LS1 BCM, 10 µg/mL PSMα3, or 2.5 µM A23187 for 5 min at 37 °C. Cells were lysed and phosphorylation of p38 MAPK and ERK1/2 was verified by immunoblotting. Data are given as phosphorylated normalized to native protein and as mean ± SEM. Images are representative for N=4 lysates of independent cell donors. ***p < 0.001, **p < 0.01, *p < 0.05 WRW4 vs. vehicle control performing paired, two-tailed Student's t-test. **C** LM formation of 5 x 10^6 neutrophils/mL after pretreatment with 10 µM WRW4, 1 µM skepinone-L, 1 µM UO126, 10 µM LY294002, 1 µM RO-31-8220 or vehicle control on ice for 15 min prior to stimulation with 10 µg/mL PSMα3, 1% LS1 BCM or 2.5 µM A23187 for 10 min at 37 °C. Data shown in heat maps are given as % of vehicle control and as mean of N=4 independent donors. **D** HEK293 cells expressing 5-LOX(*S663A*) were treated with 10% LS1 BCM or 10 µg/mL PSMα3 for the indicated timepoints. Images are representative for three independent experiments and show an overlay of 5-LOX(*S663A*) (Alexa Fluor 555, red) and DAPI-stained nuclei. W/o samples were kept in buffer for the shortest or longest incubation time to exclude unspecific effects.

Noteworthy, WRW4 inhibition appeared to be insufficient upon BCM stimulation for mediators that were formed independently from the 5-LOX pathway (*i.e.* COX, 12- and 15-LOX products), while PSM-induced LM formation was almost completely inhibited by WRW4. By contrast, inhibition of either PI3K, PKC or p38 MAPK did not affect LM biosynthesis, regardless of the applied stimulus. Intriguingly, the ERK1/2-inhibitor UO126 showed a comparable reduction of LMs as WRW4 when neutrophils were stimulated with either BCM or PSMα, but appeared to be less active upon A23187 treatment, especially in respect of reducing 5-LOX products (**Fig. 4.10C**).

Since PSM-mediated ERK-activation might play an eminent role in LM formation, we aimed to investigate the effect of phosphorylation at 5-LOX-Ser^{663} upon stimulation with *S. aureus*-derived stimuli. In HEK293 cells stably transfected with the 5-LOX(*S663A*), both BCM of LS1 and recombinant PSMα3 induced 5-LOX translocation to the nuclear envelope after 10 min of stimulation (**Fig. 4.10D**), indicating that FPR2-mediated and ERK1/2 dependent phosphorylation of 5-LOX might be subordinated for sufficient translocation in HEK293 cells.

4.2.4 PSMs mediate LM biosynthesis by affecting cPLA$_{2\alpha}$ activity and FA release

Besides activation of biosynthetic enzymes, LM formation strongly depends on sufficient FA release. Among different PLs, cPLA$_{2\alpha}$ is eminent for AA liberation and depends on Ca^{2+} and on phosphorylation by ERK (27,32,177). Therefore, the role of PSMs and staphylococcal exotoxins on FA release was investigated in neutrophils challenged by recombinant PSMα3, LS1 BCM or A23187 in presence of the selective cPLA$_{2\alpha}$ inhibitor RSC-3388 (178,179), and UPLC-MS/MS analysis was performed to evaluate LM biosynthesis. While all A23187-induced LMs were found to be reduced by RSC-3388, the inhibitory effect was less pronounced in neutrophils stimulated by PSMα3 or LS1 BCM, respectively. Interestingly, although the overall inhibitory potency was less, RSC-3388 showed a comparable pattern as the FPR2 antagonist WRW4 upon PSM and BCM treatment (**Fig. 4.11A** and compare **Fig. 4.10C**). This observation supports the involvement of cPLA$_{2\alpha}$-dependent FA release in PSM-induced FPR2 activation and LM formation.

Furthermore, release of ^{3}H-AA in neutrophils stimulated with BCM of *S. aureus* LS1 wildtype or mutants and recombinant exotoxins was evaluated. While BCM of LS1 wildtype and LS1Δ*hla* as well as isolated PSMα3 markedly induced ^{3}H-AA release, both LS1Δ*agr/sarA* and α-hemolysin were apparently insufficient to mediate AA liberation (**Fig. 4.11B**). LS1Δ*psm*αβ-induced effects could be related to a clear but not complete reduction of ^{3}H-AA release, indicating the participation of additional staphylococcal toxins in releasing FA from membrane phospholipids.

Interestingly, when neutrophils were pretreated with WRW4, RSC-3388 or UO126, the ^{3}H-AA release upon stimulation with PSMα3, LS1 BCM and A23187 was found to be decreased depending on the applied stimulus. On the one hand, WRW4 was most effective in inhibiting AA release upon treatment with PSMα3, whereas RSC-3388 and UO126, that both reduced LM biosynthesis upon PSM-challenge (**Fig. 4.10C**), barely affected the liberation of ^{3}H-AA in this respect. However, no differences were found in the inhibitory potency of the applied

compounds when BCM of LS1 was utilized for stimulation. On the other hand, RSC-3388 was most effective for A23187-treated neutrophils, underlining the eminent role of $cPLA_{2\alpha}$ for AA release under challenge with this Ca^{2+} mobilizing agent (180). In line with the results from above, both WRW4 and UO126 did not significantly affect the release of ^{3}H-AA upon A23187 stimulation (**Fig. 4.11C**). Moreover, the overall AA release was found to be superior for A23187 treatment, which correlates with the overall LM biosynthesis in this respect. Intriguingly, PSMα3 showed increased FA liberation compared to LS1 BCM challenge, which is in a sharp contrast to the total amount of detected LMs that were markedly higher for BCM stimulations (compare **Fig. 4.8B**). Together, our findings suppose a complex interplay of FA release and phospholipase A_2 activation that seems to be strikingly stimulus dependent.

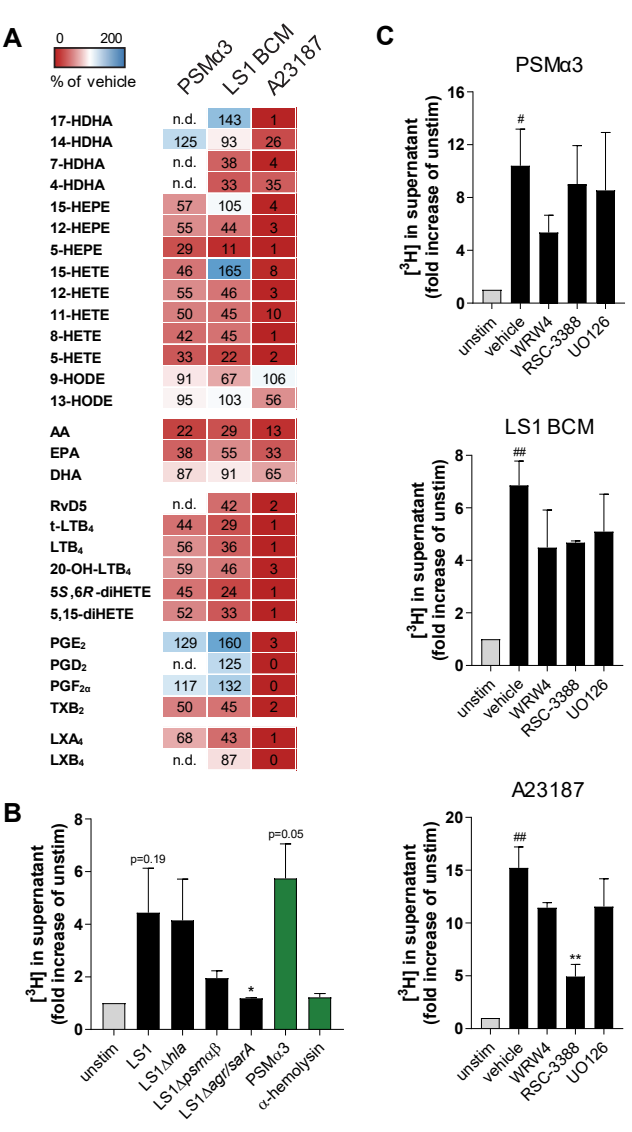

Fig. 4.11 PSMs regulate LM biosynthesis by induction of FA release in neutrophils. **A** 5 x 10^6 neutrophils were preincubated on ice for 15 min with 10 µM RSC-3388 prior to stimulation with 10 µg/mL PSMα3, 1% LS1 BCM or 2.5 µM A23187 for 10 min at 37 °C. LM formation was determined by UPLC-MS/MS. Data shown in heat maps are given as % of the vehicle control and as mean of N=4 independent donors. **B** ^{3}H-AA-labeled neutrophils were stimulated with 1% BCM of LS1 (wildtype, LS1Δ*hla*, LS1Δ*psm*αβ, LS1Δ*agr/sarA*), 10 µg/mL PSMα3 or 10 µg/mL α-hemolysin for 10 min at 37 °C. Radioactivity in the supernatant was subsequently detected by scintillation counting. Data are given as fold-increase of unstimulated samples and as mean ± SEM of N=4 (N=3 for α-hemolysin) independent donors. $^{\#}p < 0.05$, $^{\#\#}p < 0.01$ and $^{\#\#\#}p < 0.001$ LS1, PSMα3 or α-hemolysin vs. unstimulated or $^{*}p < 0.05$, $^{**}p < 0.01$ and $^{***}p < 0.001$ LS1 mutant vs. the corresponding wildtype strain using one-way ANOVA with Tukey multiple comparison post-hoc test. **C** ^{3}H-AA-labeled neutrophils were pretreated with 10 µM WRW4, 10 µM RSC-3388, 1 µM UO126 or 0.1% DMSO (vehicle) for 5 min on ice prior to stimulation by 1% BCM of LS1 wildtype, 10 µg/mL PSMα3 or 2.5 µM A23187, followed by scintillation counting. Data are given as fold-increase of ^{3}H-related radio-activity of unstimulated samples and as mean ± SEM of N=3 independent donors. $^{\#}p < 0.05$, $^{\#\#}p < 0.01$ and $^{\#\#\#}p < 0.001$ PSMα3, LS1 BCM or A23187 vs. unstimulated control using paired, two-tailed Student's t-test or $^{*}p < 0.05$, $^{**}p < 0.01$ and $^{***}p < 0.001$ inhibitors vs. the vehicle using one-way ANOVA with Tukey multiple comparison post-hoc test.

4.2.5 Role of PSM-induced LT formation during inflammation

Besides their cytolytic activity, PSMs and the related activation of FPR2 have been recently shown to play pivotal roles in inducing neutrophil infiltration upon staphylococcal infections (129,166). Thus, we asked whether PSM-induced LT formation could be involved in neutrophil recruitment by mediating the release of chemotactic LTB_4 and the subsequent activation of the high-affinity LTB_4 receptor BLT1 (181). A chemotaxis assay was performed and neutrophil infiltration through a 5 µm ChemoTx® 101-5 membrane was assayed upon treatment with LTB_4 or PSMα3, respectively. As expected, LTB_4 induced neutrophil recruitment that in turn was blocked by the BLT1-receptor antagonist LY293111 (182). By contrast, PSMα3 apparently mediated a direct neutrophil infiltration by targeting the FPR2 receptor, since WRW4 was found to reduce leukocyte recruitment. Notably, preliminary determination of sufficient PSM-concentrations to induce chemotaxis was in contrast to recent findings that described a bell-shaped effect with highest magnitude at 1 µg/mL PSMα3 (129). However, 10 µg/mL PSMα3 appeared to be superior for chemotaxis in our experimental setting (data not shown), although differences within cell number determination and incubation conditions might be an explanation for this discrepancy. Interestingly, inhibition of LT formation by the FLAP inhibitor MK886 (86) or LTB_4 binding to BLT1 by LY293111 failed to prevent neutrophil infiltration upon PSM-stimulation (**Fig. 4.12A**). Although considerable amounts of LTs are released by neutrophils challenged with PSMα3, these data indicate that neutrophil recruitment primarily depends on the direct binding of PSMs to FPR2 without involving the chemotactic abilities of LTB_4, at least in our experimental setup.

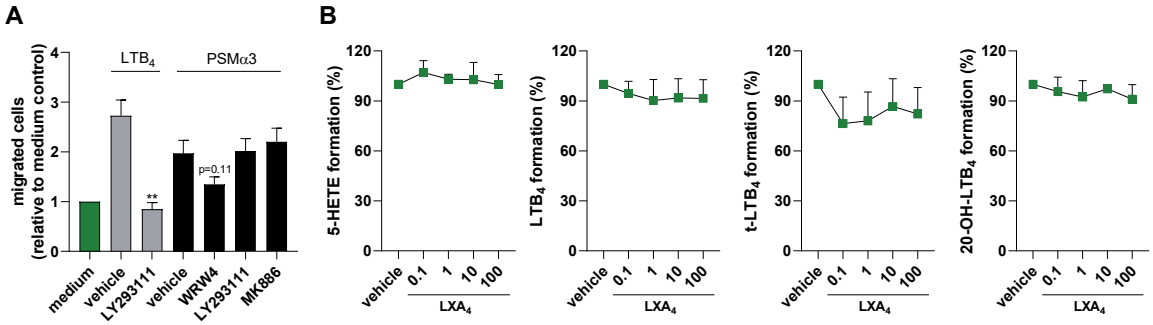

Fig. 4.12 A PSM-mediated chemotaxis is independent of LT formation. Migration of neutrophils through a 5 µm ChemoTx® 101-5 membrane was assayed after pretreatment with 30 µM LY293111, 10 µM WRW4, 300 nM MK866 or vehicle control for 10 min on ice prior to applying 30 nM LTB_4 or 10 µg/mL isolated PSMα3 as chemotactic agents. Infiltrated cells were detected by CellTiter-Glo® according to the manufacturer's protocol. Data are given as migrated cells relative to the corresponding unstimulated samples and as mean ± SEM of N=4 independent donors. Statistical analysis was performed using paired, two-tailed Student's t-test. *p < 0.05, **p < 0.01 and ***p < 0.001 inhibitor vs. vehicle control. **B LXA_4 does not affect PSM-induced LM formation.** 5-LOX product formation of 5 x 10^6 neutrophils/mL was determined by UPLC-MS/MS. Cells were simultaneously stimulated by 10 µg/mL PSMα3 and the indicated concentrations of LXA_4 (0.1 to 100 nM), respectively, for 10 min at 37 °C. Data are given as % of the vehicle control and as mean ± SEM of N=3 independent donors.

Finally, FPR2 is discussed to mediate the anti-inflammatory, pro-resolving effects of LXA_4 (183,184). Thus, PSMα3-induced 5-LOX product formation was determined in presence of this well-established SPM. As presented in **Fig. 4.12B**, LM formation remained unaffected from simultaneous stimulation by increasing concentrations of LXA_4 (0.1 to 100 nM). This data supports previous findings showing that distinct ligand-specific conformations of FPR2 and subsequent signaling cascades might be different for LXA_4 and PSMs, respectively (136).

4.3 Mutagenesis of FLAP affects the interaction with 5-LOX and the inhibition by MK886

4.3.1 Sequence analysis of mutated pcDNA3.1_FLAP(hygromycin)

When Ferguson and co-workers first revealed an inhibitor-bound crystal structure of FLAP in 2007, they described distinct characteristic subunits including four transmembrane helices, two cytosolic and one lumenal loop as well as the N- and C-terminal segments facing the inner side of phospholipid membranes (91). Moreover, the authors reported on inhibitor binding deduced from directed mutagenesis studies (91). Here we performed a site-directed mutagenesis study in order to identify a possible binding site for 5-LOX at FLAP (**Fig. 4.13A**).

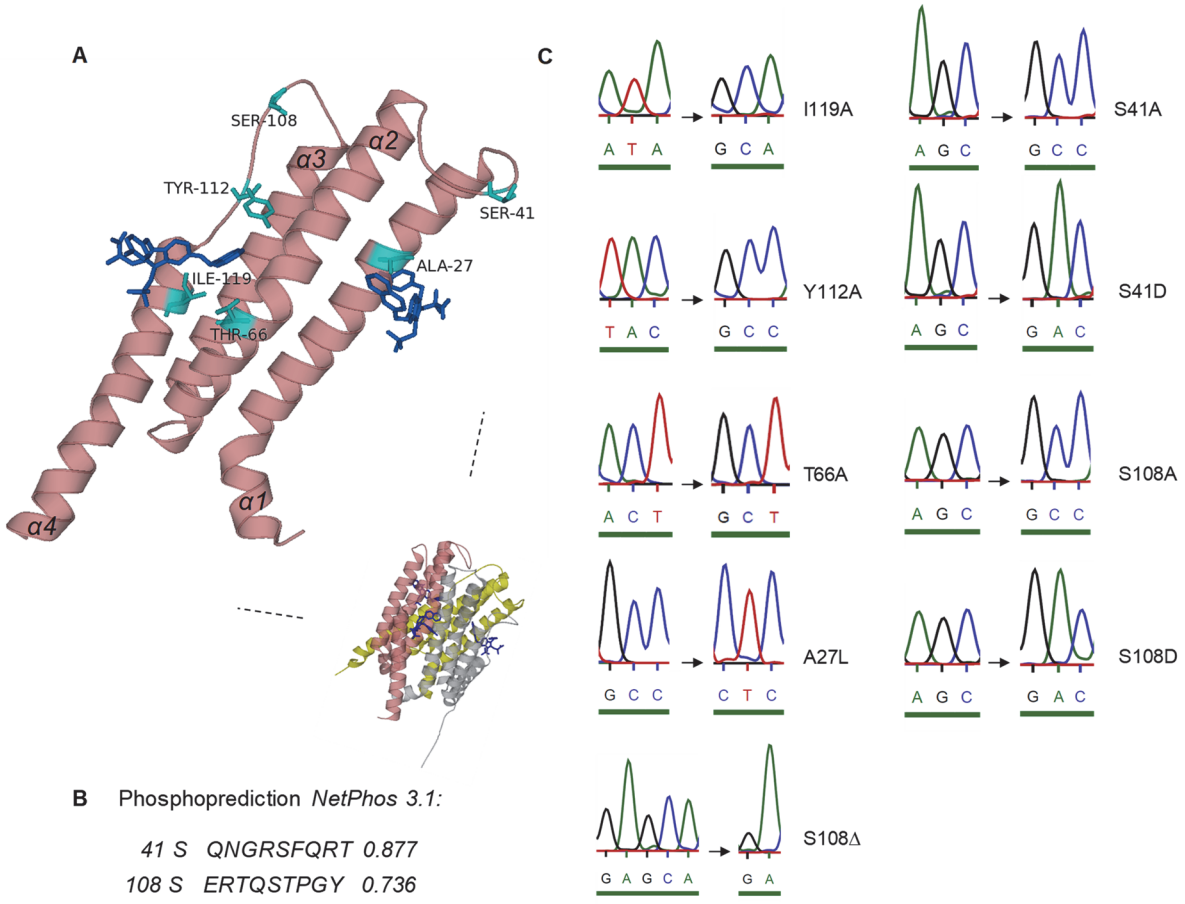

Fig. 4.13 Site-directed mutagenesis of putative residues involved in 5-LOX/FLAP interaction. A Three-dimensional structure of FLAP (PDB accession number 2q7m) as trimer (minor). Locations of mutated amino acid residues (light blue) are shown for one selected monomer (red) in presence of the FLAP inhibitor MK-591 (blue). **B** Phosphoprediction by *NetPhos3.1* using the FLAP amino acid sequence including the corresponding probability scores. **C** Sufficient mutations within the plasmid pcDNA3.1_FLAP(hygromycin) encoding for each FLAP isoform were verified by Eurofins Umwelt Ost GmbH (Jena, Germany).

Ile^{119} located at the intersection of C2 to helix α4, Tyr^{112} positioned at the second cytosolic loop C2, and polar Thr^{66} of transmembrane helix α2 in FLAP were replaced by alanine residues (*I119A*, *Y112A*, *T66A*), thereby changing the bulky amino acid side chains into small lipophilic moieties. Additionally, lipophilic Ala^{27} from helix α1 was mutated into leucine in order to achieve a steric hindrance at this position (*A27L*). Recently, it was published that serine phosphorylation affects LTC_4S activity mediated by p70S6 kinase *in vitro* (13). Since FLAP is sharing an overall sequence homology of 31% with LTC_4S and likewise belongs to the MAPEG protein family (88), we asked whether FLAP might be a target for phosphorylation-dependent regulation. Amongst others, the phosphoprediction software *NETPhos3.1* revealed two putative phosphorylation sites at Ser^{41} and Ser^{108} with corresponding phosphorylation probability scores of 0.877 and 0.736, respectively (**Fig. 4.13B**). Thus, Ser^{41} and Ser^{108} were additionally investigated as possible phosphorylation sites of FLAP in this part of the thesis. Both residues were mutated to either phosphomimetic aspartate or to alanine (*S41A*, *S108A*, *S41D*, and *S108D*) (185). Moreover, a deletion mutant of FLAP that lacks Ser^{108} was created (*S108*Δ). Mutation was performed using a Q5™ Site-Directed Mutagenesis Kit. Mutagenesis was verified by DNA sequencing and is presented in **Fig. 4.13C**.

4.3.2 Expression of 5-LOX and FLAP wildtype or mutants in HEK293 cells

HEK293 cells were stably transfected with 5-LOX and FLAP wildtype or mutants, respectively, using a Lipofectamine™ LTX with Plus Reagent kit as described, and subsequent polyclonal selection by geneticin (5-LOX) or hygromycin (FLAP) was performed. Sufficient transfection after antibiotic selection was verified by IF analysis. Representative overview images of each cell line are shown in **Fig. 4.14A**, with 5-LOX stained in red and FLAP in green color and indicate an equal expression of both 5-LOX and FLAP wildtype or mutated isoforms. Moreover, Western blot analysis and densitometric evaluation confirmed protein expression (**Fig. 4.14B**).

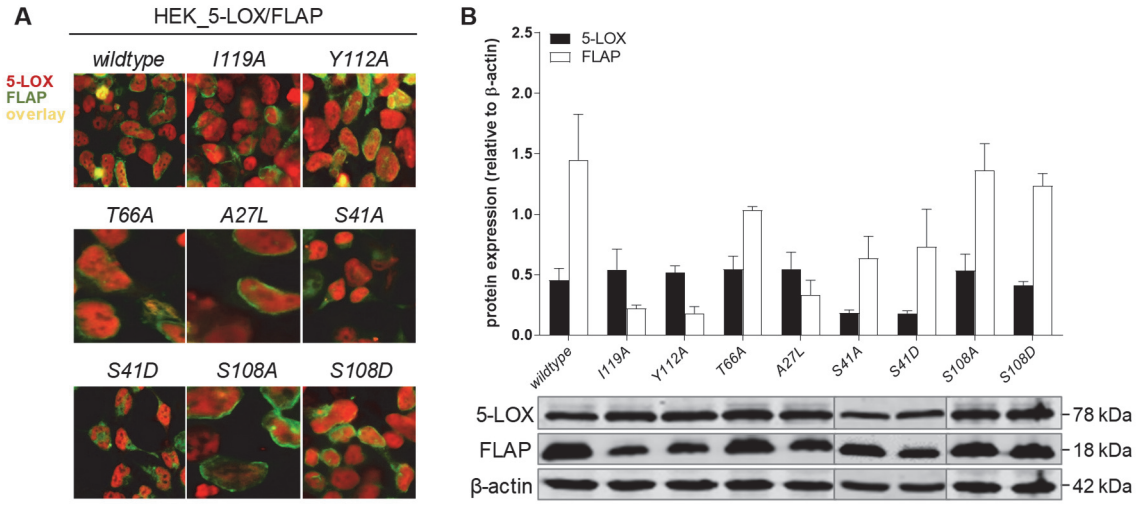

Fig. 4.14 HEK293 cells stably co-express 5-LOX and FLAP. A IF microscopy was performed to evaluate equal co-expression of 5-LOX (Alexa Fluor 555, red) and FLAP- (Alexa Fluor 488, green) wildtype or mutant, respectively. **B** Western blot analysis with subsequent densitometric analysis relative to β-actin was applied to evaluate expression of 5-LOX and FLAP.

5-LOX appeared to be equal for each cell line, except of HEK_5-LOX/FLAP(*S41A*) and HEK_5-LOX/FLAP(*S41D*) cells that showed minor but still adequate expression of the enzyme. On the other hand, FLAP expression was found to be more diverse, but satisfactory for each cell line, although HEK_5-LOX/FLAP(*I119A*) and HEK_5-LOX/FLAP(*Y112A*) showed a lower expression of FLAP compared to HEK_5-LOX/FLAP(*wildtype*) cells (**Fig. 4.14B**). Noteworthy, variations within the antibody recognition that may have resulted from the structural modifications of FLAP have not been considered in our experimental setting but might further impact the binding intensities. The results for HEK_5-LOX/FLAP(*S108*Δ) are presented in **Fig. 4.18**.

4.3.3 Influence of FLAP mutagenesis on 5-LOX product formation

In the respective HEK293 cell lines, 5-LOX product formation was examined in presence of the FLAP inhibitor MK886 upon stimulation with 2.5 µM Ca^{2+} ionophore A23187 and 2 µM exogenous AA. Total cellular LT formation including 5-H(p)ETE (alcohol and peroxide) and *trans*-isomers of LTB_4 appeared to be comparable and independent of FLAP mutations, although barely lower amounts were detected within HEK_5-LOX/FLAP(*S41A*) and HEK_5-LOX/FLAP(*S41D*), apparently resulting from lower expression of 5-LOX within these cells (**Fig. 4.15A/B)**. Pretreatment with MK886 significantly decreased product formation in cells expressing wildtype FLAP to approximately 60% of vehicle control. In case of mutated FLAP isoforms, only *A27L* and *S41A* could be inhibited to the same extent, while a minor but still significant inhibition to 70 – 80% was observed for *I119A*, *T66A*, *S41D* and *S108A*, respectively (**Fig. 4.15A/B/C**). Surprisingly, the inhibitory effect of MK886 was completely abolished in both HEK_5-LOX/FLAP(*Y112A*) and HEK_5-LOX/FLAP(*S108D*), indicating either FLAP-independent 5-LOX product formation or insufficient MK886 binding to the FLAP mutant in these cells (**Fig. 4.15A/B/C**).

5-LOX is catalyzing a two-step conversion of AA into 5-HpETE and subsequently into the instable intermediate LTA_4 (1). *In cellulo*, FLAP may enhance the second reaction step to form LTs (53,98), while exogenous addition of AA somehow limits its participation in this respect (98). Since FLAP seemingly lacks any enzymatic activity (88), we examined the ratio of 5-H(p)ETE versus LTB_4-isomers in order to evaluate the influence of FLAP and respective mutations on 5-LOX product formation in the HEK293 cell model; *i.e.* insufficient FLAP action is indicated by higher values of the metabolic ratio of 5-H(p)ETE/LTB_4-isomers. HEK_5-LOX/FLAP(*wildtype*) cells stimulated by A23187 plus AA displayed a ratio of roughly 1.2 of 5-H(p)ETE compared to LTB_4-isomers and almost equal values were found when 5-LOX was co-expressed with the FLAP mutants *I119A* (1.4), *Y112A* (1.5), *A27L* (1.2), *S41A* (1.7), and *S108A* (1.0). However, cells expressing *S41D* (2.3) and *S108D* (2.0) showed increased ratios implying a subordinate role of FLAP compared to the wildtype protein. On the other hand, FLAP appeared to enhance the second reaction step of 5-LOX in HEK_5-LOX/FLAP(*T66A*) (0.7) cells (**Fig. 4.15D**).

Although decreasing the overall 5-LOX product formation, MK886 was reported to increase the ratio of 5-H(p)ETE versus LTB_4-isomers by augmented inhibition of the pseudo-

lipoxygenation of 5-LOX compared to the peroxide formation within the first reaction step (98). Notably, pretreatment with MK886 significantly increased this ratio in HEK_5-LOX/FLAP(*wildtype*) cells as well as in the FLAP mutant strains *T66A*, *A27L*, *S41A*, *S41D* and *S108A*. However, cells expressing the FLAP mutants *I119A*, *Y112A* and *S108D* showed unaltered ratios of 5-H(p)ETE versus LTB_4-isomers in presence of MK886. These results are in line with the inhibitory potency of MK886 for these mutants and show a direct correlation between the ability of MK886 to reduce 5-LOX product formation and the simultaneous increase of the metabolic ratio (**Fig. 4.15D**). (Note that LTA_4H expression within HEK293 cells appears to be insufficient to form detectable amounts of LTB_4 from LTA_4. Thus, non-enzymatically produced *trans*-LTB_4-isomers were evaluated and included in the overall 5-LOX product formation.)

A

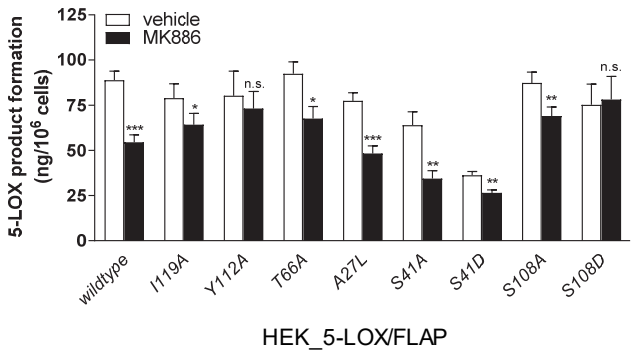

B

HEK_5-LOX/FLAP (ng/10^6 cells)	vehicle	MK886
wildtype	88.9 ± 4.5	54.6 ± 3.6
I119A	79.0 ± 7.0	64.3 ± 5.6
Y112A	80.2 ± 12.2	73.2 ± 8.5
T66A	92.5 ± 5.8	67.7 ± 5.9
A27L	77.4 ± 4.0	48.3 ± 3.8
S41A	64.0 ± 6.6	34.4 ± 4.0
S41D	31.6 ± 4.4	23.2 ± 3.2
S108A	87.3 ± 5.4	69.0 ± 4.4
S108D	75.3 ± 10.2	78.2 ± 11.4

C

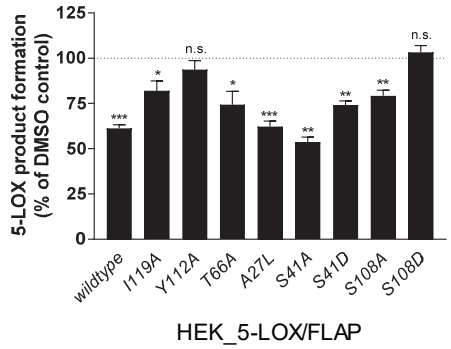

D

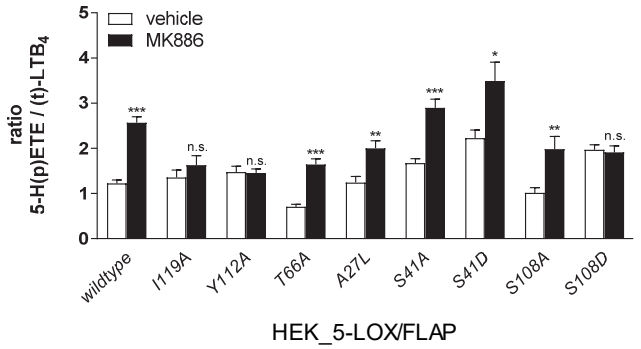

Fig. 4.15 Mutagenesis of FLAP affects 5-LOX product formation and inhibition by MK886. HEK_5-LOX/FLAP cells stably co-expressing 5-LOX with the indicated mutant of FLAP were stimulated with 2.5 µM A23187 and 2 µM AA in presence of 300 nM MK886 or vehicle control (0.1% DMSO) for 10 min at 37 °C. 5-LOX product formation including 5-H(p)ETE and *trans*-isomers of LTB_4 was determined using RP-HPLC. **A-B** Product formation of 1 x 10^6 HEK293 cells in ng. **C** Inhibition by MK886 presented as 5-LOX product formation in % of the corresponding vehicle control. **D** Ratio of 5-H(p)ETE to *trans*-isomers of LTB_4 in presence of 300 nM MK886 or vehicle control. All data are given as mean ± SEM, N=5. Statistical analysis was performed using paired, two-tailed Student's t-test. N.s. - not significant. ***$p < 0.001$, **$p < 0.01$, *$p < 0.05$ MK886 vs. the corresponding vehicle control.

4.3.4 Subcellular distribution of 5-LOX is independent of FLAP mutagenesis

Subcellular distribution of 5-LOX under stimulatory conditions has been connected to 5-LOX activity in the cellular context (53,71). In addition, mutations of 5-LOX affecting the ability to associate with FLAP at the nuclear envelope have been related to altered 5-LOX product formation before (60). We therefore asked whether structural modifications of FLAP influence the co-localization with 5-LOX at the nuclear envelope, estimated by IF microscopy upon stimulation with A23187 for either 10 or 30 min. 5-LOX, located within the nucleus under resting conditions, translocated to the nuclear membrane in all cell lines, independent of mutations within FLAP. Moreover, the co-localization of 5-LOX and FLAP was apparent at the nuclear envelope already after 10 min of stimulation and did not vary at 30 min A23187 exposure (**Fig. 4.16**).

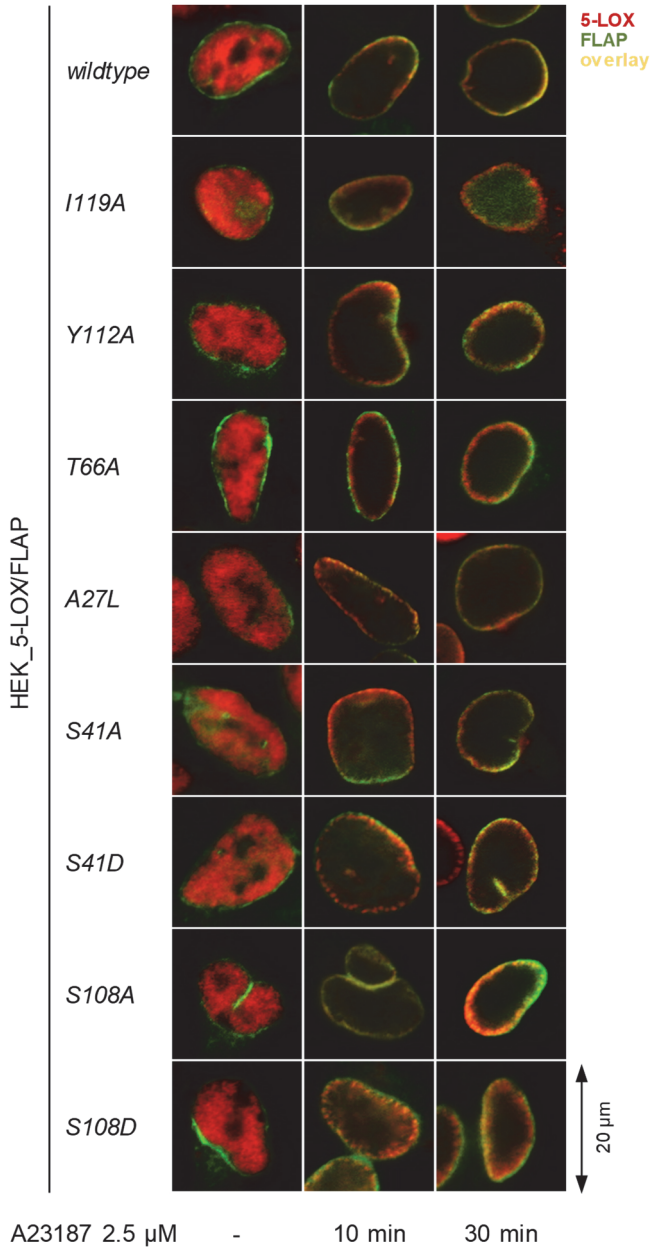

Fig. 4.16 Subcellular localization of 5-LOX is independent of mutagenesis of FLAP. Subcellular localization of 5-LOX was determined by IF microscopy in HEK293 cells stably expressing 5-LOX (Alexa Fluor 555, red) and FLAP wildtype or mutant (Alexa Fluor 488, green), upon stimulation with 2.5 µM A23187 at 37 °C for the indicated time points. Images of 20 µm size are representative for three independent experiments.

4.3.5 In situ interaction of mutated FLAP isoforms with 5-LOX

Besides co-localization at the nuclear membrane, an *in situ* interaction of 5-LOX and FLAP resulting in a LT-synthetic protein complex was shown more recently to affect 5-LOX product formation (12,60). Hence, a proximity-ligation approach (PLA) was applied in order to study 5-LOX/FLAP interactions at closer proximity than 40 nm.

As expected, direct interactions of 5-LOX and FLAP remained absent under unstimulated conditions in all investigated cell lines, whereas stimulation by A23187 resulted in a time- and FLAP-dependent assembly of protein complexes at the nuclear envelope (**Fig. 4.17**). 5-LOX/FLAP interactions appeared to be unaffected from the mutagenesis of FLAP at Thr^{66}, Ala^{27}, Ser^{41}, and Ser^{108} (only *S108A*), as fluorescent proximity signals could be observed similarly to the wildtype control after both 10 and 30 min of A23187 activation. By contrast, despite evident co-localization, HEK293 cells co-expressing 5-LOX and either *I119A* or *Y112A* showed noticeably reduced interactions at 10 min of ionophore exposure, although the signal appeared to be enhanced after prolonged A23187 challenge of 30 min. Intriguingly, a 5-LOX/FLAP interaction remained absent within HEK_5-LOX/FLAP(*S108D*) cells, even at long time stimulations with A23187 (**Fig. 4.17**). These findings suggest that structural variations of FLAP due to selected mutations affect the ability to interact with 5-LOX to form a synthetic complex, which was found to be a key feature for sufficient AA transfer and LT formation (12). In particular, mutation of Ser^{108} towards a phosphomimetic aspartate moiety abolishes the interaction of FLAP with 5-LOX upon stimulation with A23187.

4.3.6 Deletion of Ser^{108} results in insufficient 5-LOX/FLAP interaction

Besides tyrosine and threonine, serine residues serve as crucial phosphorylation sites for eukaryotic cellular kinases, and replacement of these amino acids by phosphomimetic aspartate or non-phosphorylatable alanine are common strategies to study phosphorylation events *in cellulo* (185,186). However, although our previous data might indicate Ser^{108} as potential kinase target within FLAP to regulate 5-LOX product formation, all efforts to prove an existing phosphorylation by phospho-proteomics in either HEK_5-LOX/FLAP cells or human neutrophils failed due to insufficient detection of FLAP (data not shown). We therefore asked whether Ser^{108}, located on the second cytosol-facing loop (C2) of FLAP, might act as essential residue for 5-LOX/FLAP interaction and activity, independent of the possibility of being affected by phosphorylation. Thus, stable co-expression of 5-LOX with a mutant of FLAP that lacks Ser^{108} (*S108*Δ) was performed and equal protein amounts could be verified by both, immunofluorescent staining and Western blot analysis followed by densitometric evaluation, respectively (**Fig. 4.18A/B**). Upon stimulation with A23187 and AA for 10 min, a total 5-LOX product formation of approximately 65 ng per 1 x 10^6 cells could be detected, which is comparable to the FLAP wildtype (88.9 ng, **Fig. 4.18C** and **Fig. 4.15B**).

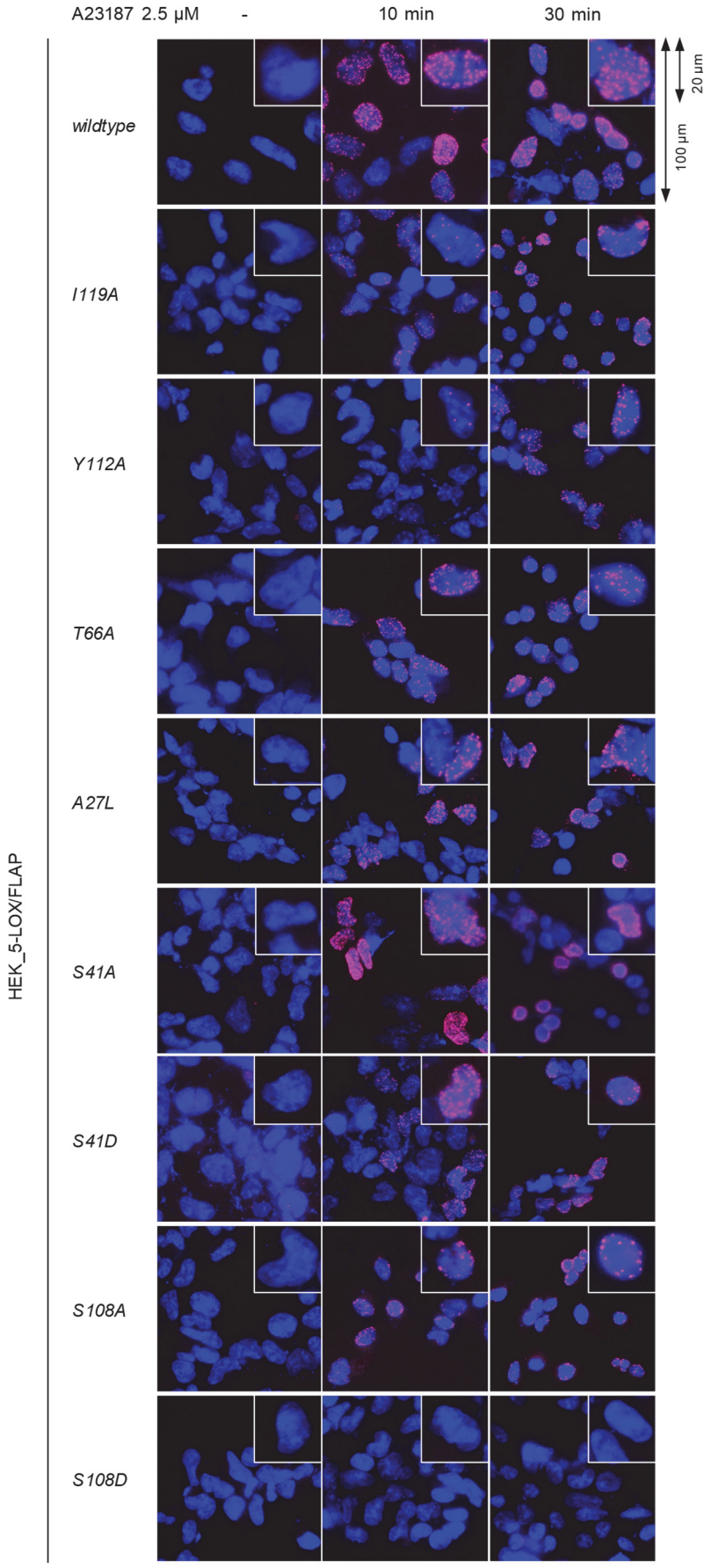

Fig. 4.17 Mutagenesis of FLAP affects the interaction of 5-LOX and FLAP at the nuclear envelope. *In situ* 5-LOX/FLAP-interaction in HEK293 cells stably ex-pressing 5-LOX and FLAP-wildtype or mutant, respectively, was determined by PLA upon stimulation with 2.5 µM A23187 at 37 °C for the indicated time points. Overview images (100 µm) and selected cells (20 µM) are representative for at least three independent experiments. Protein-protein interactions are represented as magenta spots within an overlay image with DAPI-stained nuclei (blue).

Noteworthy, 5-LOX product formation remained unaffected from pretreatment with 300 nM MK886, indicating an inferior role of the structurally modified FLAP mutant in LM biosynthesis. Accordingly, the metabolic ratio of 5-H(p)ETE versus all-*trans* LTB_4-isomers was found to be 3-fold higher than in wildtype cells and appeared unaltered in presence of MK886 (**Fig. 4.18D**). Although 5-LOX translocated to the nucleus upon A23187 stimulation (**Fig. 4.18E** and **Fig. 4.16**), an *in situ* assembly of the LT-synthetic complex could not be observed in HEK_5-LOX/FLAP(*S108*Δ) cells (**Fig. 4.18F** and **Fig. 4.17**). Taken together, our data indicate a crucial role of Ser^{108} and the corresponding steric arrangement of loop C2 of the FLAP trimer in supporting 5-LOX activity and LT formation.

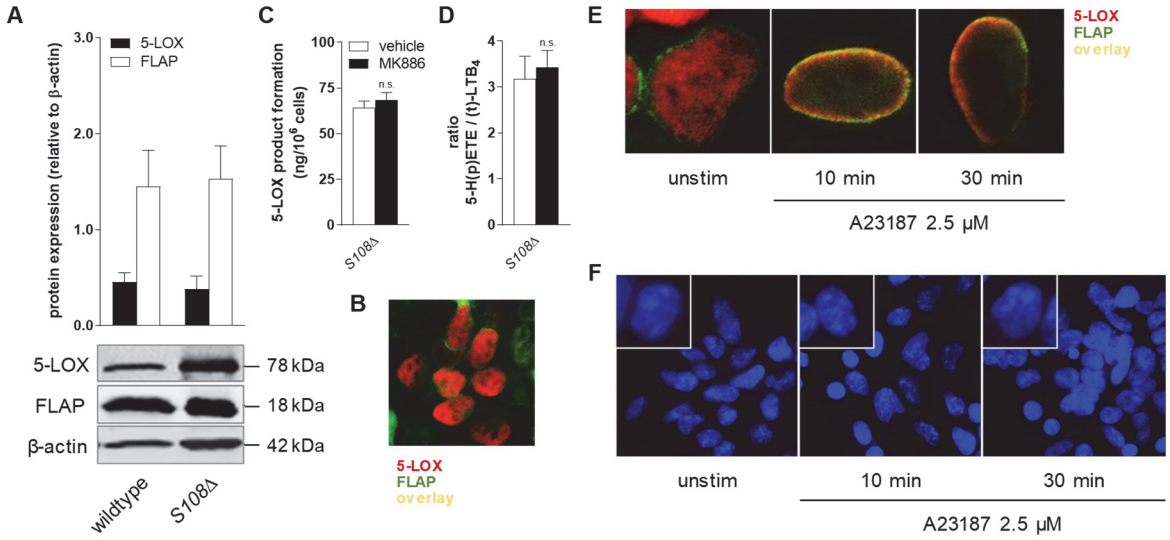

Fig. 4.18 Deletion of Ser^{108} prevents 5-LOX/FLAP interaction and inhibition by MK886. A Western blot analysis was performed in order to determine stable expression of 5-LOX and FLAP wildtype or *S108*Δ, respectively, in HEK293 cells followed by densitometric evaluation relative to β-actin. **B** Stable co-expression of 5-LOX and FLAP(*S108*Δ) in HEK293 cells was determined by IF microscopy (5-LOX - Alexa Fluor 555, red; FLAP - Alexa Fluor 488, green). **C/D** 1 x 10^6 HEK_5-LOX/FLAP(*S108*Δ) cells/mL were preincubated with 300 nM MK886 or vehicle (0.1% DMSO) for 10 min at 37 °C prior to stimulation with 2.5 A23187 and 2 µM AA for another 10 min at 37 °C. 5-LOX products including 5-H(p)ETE and all-*trans*-isomers of LTB_4 were detected by RP-HPLC. Data are given as mean ± SEM in ng (C) or as ratio of 5-H(p)ETE vs. *trans* LTB_4-isomers (D), N=5. Statistical analysis was performed using paired, two-tailed Student's t-test. N.s. - not significant. **E** Subcellular localization of 5-LOX was determined by IF microscopy in HEK293 cells stably expressing 5-LOX (Alexa Fluor 555, red) and FLAP(*S108*Δ) (Alexa Fluor 488, green) upon stimulation with 2.5 µM A23187 at 37 °C for the indicated time points. **F** PLA was performed to detect an *in situ* interaction of 5-LOX and FLAP(*S108*Δ) in HEK293 cells upon stimulation with 2.5 µM A23187 at 37 °C. Protein-protein interactions are represented as magenta spots within an overlay image with DAPI-stained nuclei (blue).

5 DISCUSSION

5-LOX activation and the subsequent formation of LTs are associated with inflammatory processes and disorders (1). Although intensive research efforts have focused on LM formation during the last century, only few and widely artificial chemical compounds have been applied to study 5-LOX regulation *in vitro* (5). By contrast, it has been reported recently by our group that human macrophages release a subset of pro- and anti-inflammatory LMs, including LTs, upon challenge with intact bacteria (140). Here we describe bacterial exotoxins as crucial determinants to induce LM formation upon bacterial infections and unveil staphylococcal PSMs as potent 5-LOX activators in human neutrophils. Besides, the rise of multiresistent microorganism and their increasing impact on inflammatory diseases underline the demand for novel antimicrobial and anti-inflammatory compounds (3,141). Thus, this thesis presents the FPR2 receptor as well as the 5-LOX helper protein FLAP as potential pharmacological targets to modulate LM biosynthesis upon exotoxin exposure. Moreover, mutational studies of FLAP revealed the cytosolic loop C2 as crucial structural domain for the formation of a LT-synthetic protein complex with 5-LOX, which will be important for ongoing drug development.

5.1 Bacterial exotoxins stimulate LM formation and 5-LOX activity *in cellulo*

Distinct mechanism might be responsible for *in cellulo* LM formation upon bacterial stimulation. On the one hand, phagocytosis of microorganism is a key feature of neutrophils and macrophages during infection (187). LTs were shown to stimulate phagocytosis and it has been discussed whether the internalization process simultaneously induces LM biosynthesis (188-190). On the other hand, microbial pattern recognition by surface receptors such as FPRs and toll-like receptors (TLRs) are crucial functions of the innate immune system (130,191). In order to evaluate whether bacteria elicit LT formation apart from immunospecific mechanisms resulting from a direct bacteria-host interaction, a non-immunocompetent HEK293 cell model stably co-expressing 5-LOX and FLAP was used in this study. Here, we show that HEK_5-LOX/FLAP cells could be activated by both intact bacteria and sterile-filtered BCM, indicating an eminent role of secreted bacterial factors in mediating 5-LOX translocation. Intriguingly, 5-LOX activation exclusively appeared for pathogenic bacteria strains, namely the Gram-positive *S. aureus* (LS1) and the Gram-negative *E. coli* (O6:K2:H1), while non-pathogenic *S. carnosus* (TM300) and *E. coli* (BL21) could not induce 5-LOX distribution upon stimulation. Since phagocytosis and expression of TLRs or FPRs were found to be absent in HEK293 cells (192-194), our data indicate a more general mechanism for bacterial activation independent of direct bacteria-host cell interactions, but dependent on secreted soluble factors within the bacteria culture medium.

Although a comparable mechanism might be conceivable for the stimulatory effect of different bacteria strains, we focused on the Gram-positive *S. aureus* for further investigations. *S. aureus* is considered as common human commensal but can cause health care- and community-associated infections of diverse severity (4,105). Staphylococcal exotoxins including α-hemolysin and α-type PSMs have been related to the virulence of community-

associated *S. aureus* infections before (116-118,195). Moreover, among the genus of staphylococci, *S. aureus* and *S. epidermidis* are debated as main pathogens in humans, apparently due to the pronounced presence of virulence factors within these strains (110). The expression of staphylococcal toxins is regulated by the *agr* quorum-sensing system and *sarA* (109,113) and genetic knockout of these regulatory genes could be related to extenuated virulence (110). Accordingly, in our study, BCM of LS1Δ*agr/sarA* lacking the overall set of exotoxins (147) failed to induce 5-LOX translocation in HEK_5-LOX/FLAP cells. Recombinant α-hemolysin, the archetype of staphylococcal toxins (119), induced 5-LOX redistribution in a dose- and time-dependent manner, while BCM from LS1Δ*hla* insufficient in α-hemolysin expression (148) was still operative.

Although HEK293 cells are an appropriate model to study 5-LOX/FLAP co-localization, HEK293 cells lack LT formation from endogenously released AA (98). By contrast, human neutrophils were shown to produce sufficient amounts of LMs, and 5-H(p)ETE, LTB_4 (including all *trans*-isomers) as well as the ω-oxidized degradation product 20-OH-LTB_4 are considered as predominant LMs released upon neutrophil stimulation (196,197). Host neutrophils act as first opponent as soon as bacteria overcome epithelial barriers and recognize, ingest, and kill invading microorganism (198). Moreover, leukocytes are supposed to be the primary defense against *S. aureus* (105,107). Apart from a direct physical host-bacteria-interaction, our data indicate that neutrophils can likewise be stimulated by *S. aureus* exotoxins. Accordingly, neutrophils showed remarkable LT release upon treatment with *S. aureus* wildtype BCMs (LS1 and USA300, respectively). Incubations with LS1Δ*hla*, LS1Δ*psm*αβ, LS1Δ*agr/sarA* or USA300Δ*pvl*, revealed PSMs as key regulators for LM biosynthesis. In line with these findings, only recombinant PSMs (*i.e.* PSMα1 and PSMα3), but not α-hemolysin-induced 5-LOX translocation and LM formation. A summarizing principle component analysis additionally uncovered the striking correlation between 5-LOX activation and PSM presence in neutrophil stimulations, whereas α-hemolysin showed a similar pattern as vehicle incubations. Noteworthy, this is in sharp contrast to HEK_5-LOX/FLAP cells, were α-hemolysin efficiently activated 5-LOX translocation. Knockout of α- and β-type PSMs resulted in a clear but incomplete reduction of LM biosynthesis in neutrophils. The lack of PSMs apparently blocked the formation of 5-LOX products, but barely affected LMs derived from other enzymatic branches. On the other hand, knockout of α-hemolysin could not affect 5-LOX product biosynthesis but remarkably decreased 12-LOX products (*e.g.* 14-HDHA, 12-HEPE, 12-HETE) and PGs. These LMs might result from impurities with other immune cells (predominantly platelets) within the incubation as consequence of insufficient blood cell separation. Also, our results are in accordance with studies showing that human neutrophils are resistant towards α-hemolysin even at higher concentrations (199), apparently due to the lower expression of ADAM-10, the co-receptor that enhances pore-formation (200). By contrast, it was reported earlier that rabbit neutrophils release LTs (201) and that alveolar epithelial A549 produce PGs upon stimulation with α-hemolysin (202). Besides, cytolytic PVLs were insufficient in activating LM biosynthesis of neutrophils here, since knockout within USA300Δ*pvl* could not affect overall product formation. These findings are in accordance with recent opinions that describe a limited role of PVLs in staphylococcal infections (203). However, although PSMs obviously operated as main 5-LOX activators in neutrophils, additional exotoxins and bacteria secreted factors might be involved in LM formation. Noteworthy, we here did not focus on other *agr*-

mediated staphylococcal toxins including β-hemolysin or δ-hemolysin (equivalent to PSMγ) (114), which might contribute to 5-LOX activation and could explain remaining but minor LM biosynthesis even after stimulation by LS1Δ*psm*αβ BCM. Further studies should likewise focus on other leukocytes in order to provide more knowledge about exotoxin-induced LM formation. It might be conceivable that monocytes, macrophages, or dendritic cells, all expressing additional FA-metabolizing enzymes, could differentially react on exotoxin exposure and release a distinct spectrum of LMs. In fact, recent investigations of our group found increased SPM formation of human macrophages upon stimulation with isolated α-hemolysin, underlining the previously discussed cell-specificity of staphylococcal exotoxins (unpublished data). In addition, distinct neutrophil subpopulations have been associated to varied susceptibilities to *S. aureus* infections and subsequent macrophage activation in mice (204). It might be of interest whether these neutrophils can be activated by staphylococcal exotoxins to the same extent and if LMs are involved in this process. However, it has to be mentioned that bacterial exotoxins have already been discussed as inducers of LTs in human granulocytes, although thiol-activated instead of native toxins have been applied (205). These studies have been published by the end of the last century, when genetic knockout approaches were not commonly applied and the complete set of staphylococcal toxins was still elusive (115). *E.g.*, it was shown that leukocidins (PVLs) induce LTB_4 formation in neutrophils (206). However, lower amounts of LTs were detected compared to our study and purification of leukocidins from bacteria cultures might have been related to impurities with other exotoxins (PSMs have not been discovered yet at that time) (206,207).

According to the PSM effect in neutrophils, knockout of PSMα and PSMβ markedly altered LT formation in an *in vivo* model when mice paws were infected with the methicillin-resistant *S. aureus* USA300 strain. By contrast, the absence of PSMs barely affected PG and TX formation, indicating an alternative mechanism of their formation upon *S. aureus* infection. Noteworthy, we did not identify infiltrating leukocytes in this *in vivo* model, although neutrophils have been discussed to be critical for staphylococcal infections (107,154). However, it is assumable that additional immune cells other than neutrophils participate in the defense of *S. aureus*, which should be considered in view of cell-specific effects of exotoxins. Moreover, it has to be noted that the overall state of infection after *S. aureus* inoculation was evaluated within a different study and was not in the focus of this work (unpublished data).

Collectively, our data support recent findings that PSM expression is related to the pathogenicity of distinct staphylococci. In detail, PSMs were found to be generally present in pathogenic strains (*e.g.* PSMs constitute about 62% of secreted proteins within USA300 culture filtrates (115)) but could not be detected in most of commensal bacteria (128). Additionally, the evolutionary connection of the *agr* quorum-sensing system and the RNAIII-independent *psm*-gene control with the regulation of further exotoxins underlines PSMs as important part of *S. aureus* virulence (111). Together, our findings add exotoxin-induced LM formation to the list of features contributing to *S. aureus* pathogenicity.

5.2 Staphylococcal PSMs mediate LM biosynthesis in neutrophils by targeting the FPR2 receptor and Ca^{2+} influx

Bacterial toxins were found before to induce LT formation (205). However, although published almost 30 years ago, a potential mechanism elucidating the related 5-LOX activation remained elusive. Here we show that PSMs released from *S. aureus* are crucial for LM biosynthesis, and we identified the FPR2 receptor to be involved in this activation in neutrophils (see **Fig. 5.1**).

It was published recently that PSMs mediate neutrophil chemotaxis and Ca^{2+} influx by targeting the FPR2 receptor (129,208). Accordingly, in our experiments the FPR2 selective receptor antagonist WRW4 significantly inhibited LT formation upon stimulation with recombinant PSMα3 or LS1 BCM. Interestingly, in line with our findings for BCM of LS1Δ*psm*αβ, WRW4 inhibition appeared to be restricted to 5-LOX products and barely affected other LMs compared to wildtype BCM treatment. By contrast, LM formation was globally decreased by WRW4 upon PSM-stimulation. Thus, we assume that additional exotoxins in the BCM might be operative to activate LM biosynthesis, while 5-LOX product formation strongly depends on PSM presence and subsequent FPR2 binding. Interestingly, FPR2 activation has been related to LM biosynthesis before. On the one hand, the antimicrobial peptide LL-37 released by neutrophils induced moderate LTB_4 formation by mediating p38 MAPK activation and phosphorylation of $cPLA_{2\alpha}$ (209). On the other hand, the synthetic peptide receptor agonist WKYMVm was shown to mediate AA release and LTB_4 formation in neutrophils, which is in line with our results (210). Intriguingly, in the same study the pro-inflammatory protein SAA preferentially activated COX-related products by acting on FPR2 without affecting LT formation (210). Together, not only receptor activation but predominantly the molecular properties of FPR2 ligands might influence corresponding LM biosynthesis. This might likewise explain that exotoxins apart from PSMs could target enzymatic branches other than 5-LOX/FLAP.

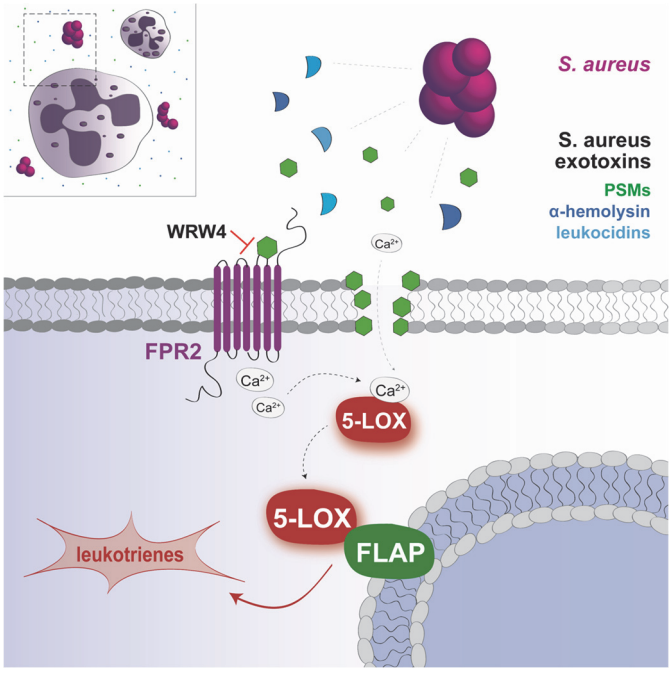

Fig. 5.1 Proposed mechanism for an activation of 5-LOX by PSMs released from *S. aureus*.

FPR2 as G_i-protein-coupled receptor activates distinct cellular kinases (170). Here, PSM-mediated LM formation strongly correlated with ERK1/2 activation and could be inhibited by the ERK1/2-inhibitor UO126 (174). Both, WRW4 and UO126 hampered the LM biosynthesis in a comparable manner, and WRW4 was found to alter BCM and PSM-mediated ERK1/2-phosphorylation at Thr^{202}/Tyr^{204} in neutrophils. Although Ser^{663} of 5-LOX was found to be a direct target of ERK1/2 (6), exotoxin-induced 5-LOX translocation still occurred for the 5-LOX(*S663A*) mutant stably expressed in HEK293 cells. By contrast, inhibition of additional kinases (*i.e.* p38 MAPK, PI3K or PKC) that are discussed to mediate FPR2 signaling (170) failed in decreasing LM biosynthesis, which might underline the superior role of FPR2-ERK-signaling for LT formation in this study. These findings are supported by the fact that inhibition of p38 MAPK by skepinone-L or SB203580, considered as second crucial kinase to mediate 5-LOX activity (69), could not affect 5-LOX translocation or product formation in HEK_5-LOX/FLAP cell or neutrophils, respectively.

Moreover, we found that staphylococcal exotoxins induce LM biosynthesis and 5-LOX translocation by increasing intracellular Ca^{2+} concentrations in HEK293 cells and human neutrophils. Ca^{2+} binding to the N-terminal domain of 5-LOX is a key regulator to induce nuclear translocation and LT formation (7,61,76). Accordingly, Ca^{2+} capturing by EDTA completely prevented LM formation in neutrophils stimulated by *S. aureus* BCM as well as translocalization of 5-LOX in HEK_5-LOX/FLAP cells. Furthermore, Ca^{2+} as determining factor for PSM-mediated 5-LOX product formation might explain the intensified activation of Ca^{2+}-sensitive 5-LOX compared to other lipoxygenase- and COX-enzymes (7). Also, our experiments with EDTA indicate that Ca^{2+} is derived from extracellular instead of intracellular stores, which is in line with previous studies that discuss a sustained Ca^{2+} increase over the plasma membrane as important inducers of 5-LOX products (211). A sufficient Ca^{2+} influx potentially results from either pore-formation, cytolysis, or receptor activation, as discussed for δ-hemolysin (114,212). While FPR2 activation was related to intracellular Ca^{2+} increase before (129,213), cell lysis as unique factors for PSM-mediated LM formation could be repeatedly excluded in our study. On the one hand, LT formation remained absent in presence of lytic concentrations of Triton X-100 and after inhibition by MK866, a FLAP inhibitor that requires cellular integrity for activity (98). In addition, stimulation by LS1 BCM only caused marginal cytotoxicity visualized by LDH release and trypan blue staining. These results are in line with previous reports that indicated diminished cytolytic activities of amphipathic peptides on freshly isolated neutrophils (208,214), and that PSMα3 barely compromised the structural integrity of neutrophil membranes upon short-time incubations (195). Moreover, the phospholipid composition of targeted cells was shown to influence the magnitude of membrane insertion by PSMs and might therefore explain their cell-specific effects (215). However, the fact that HEK293 cells do not express FPR2, while 5-LOX translocation was likewise induced by PSMs, might indicate at least a supportive role of pore-formation by PSMs. Along these lines, Forsman et al. described both receptor-dependent and independent activities of PSMs before (208). It might be of interest whether 5-LOX subcellular localization upon PSM treatment is affected from WRW4 presence and whether AA release (discussed below), but not 5-LOX translocation, possibly acts as critical determinant for LM formation, giving an explanation for the unaltered 5-LOX translocation in HEK_5-LOX(*S663A*) cells. Note that HEK_5-LOX/FLAP cells are insufficient in LT formation from endogenous AA and cannot be utilized for

corresponding investigations. Moreover, since we assume that ERK activation is mediated by FPR2 and HEK293 cells apparently do not express this receptor, the significance of these results is limited. Taken together, while intracellular Ca^{2+} might be increased by both FPR2 activation and minor pore-formation, sufficient LT biosynthesis seems to require receptor activation upon PSM treatment.

In general, LM biosynthesis requires the initial release of FA substrates from phospholipids of cellular membranes by lipases (PLs) (27). Besides $iPLA_2$ and $sPLA_2$, $cPLA_{2\alpha}$ was shown to play a crucial role for LT formation by liberating AA from nuclear membranes in close proximity to the 5-LOX/FLAP complex (27,32). $cPLA_{2\alpha}$ activity is mediated by intracellular Ca^{2+} mobilization resulting in translocation to the nuclear envelope and subsequent FA release (1,32,34). Moreover, activation of ERK and $cPLA_{2\alpha}$-phosphorylation at Ser^{505} are important factors for catalytic activity (177). Here we show that PSM-induced LT formation can be inhibited by RSC-3388, a selective $cPLA_{2\alpha}$ inhibitor (178,179), underlining the eminent role of $cPLA_{2\alpha}$ under our pathophysiological conditions. In line with this, BCM of *S. aureus* strains that lack PSM expression showed diminished release of ^{3}H-AA in neutrophils. Interestingly, RSC-3388 failed to prevent AA release upon stimulation with BCM or PSM, indicating at least an alternative phospholipase that participates in substrate liberation. However, since LM formation was found to be reduced by RSC-3388, we assume that ^{3}H-AA is released without being converted into LMs detected by the applied MS/MS lipidomic approach. Although LM formation was found to be partially decreased in presence of WRW4 and UO126, we still observed ^{3}H-AA release in neutrophils, independent of the applied stimulus, suggesting that FPR2- and ERK-activation might be superior for 5-LOX activity but less important for overall substrate liberation. By contrast, the PSM-mediated intracellular Ca^{2+} increase might dictate the localization of FA liberation, since it was reported previously that the kinetics and amplitude of Ca^{2+} influx affect the translocation of $cPLA_{2\alpha}$ to either the Golgi or nuclear envelope, consequently resulting in distinct metabolization by downstream enzymes such as COXs or 5-LOX/FLAP (216).

Besides cytolytic and pore-forming exotoxins, *S. aureus* releases a subset of molecules to evade from human immune responses (198). Among those, two proteins might be of outstanding importance for PSM-induced LM formation. First, CHIPS was shown to significantly antagonize the activation of FPR**1** receptors (134). Intriguingly, in our study, PSM-mediated LM formation remained unaltered in presence of CHIPS, while fMLP-induced LM biosynthesis was inhibited by approximately 50%, supporting the hypothesis of a preferential activation of FPR**2** over FPR**1** upon stimulation with isolated PSMs. However, when LS1 BCM was applied, minor inhibition by CHIPS could be observed (data not shown), which might underline a marginal but additional activation of FPR**1** and subsequent LM biosynthesis by formylated proteins within staphylococcal BCMs. On the other hand, *S. aureus* was found to release FLIPr that shares 28% of overall structural homology with CHIPS, but specifically inhibits FPR**2** and prevents PSM-induced Ca^{2+} influx (129,138). Unfortunately, in contrast to CHIPS, FLIPr is not commercially available and could therefore not be tested in our study. Nevertheless, LM formation of neutrophils should be investigated in presence of FLIPr in order to substantiate the role of FPR2 in *S. aureus*-induced LM biosynthesis. Moreover, both CHIPS and FLIPr might be putative targets for the treatment of staphylococcal infections to modulate

LM formation and in line the overall inflammatory response under these conditions. The activation of either FPR1 or FPR2 depending on the staphylococcal pathogenicity is summarized in **Fig. 5.2**.

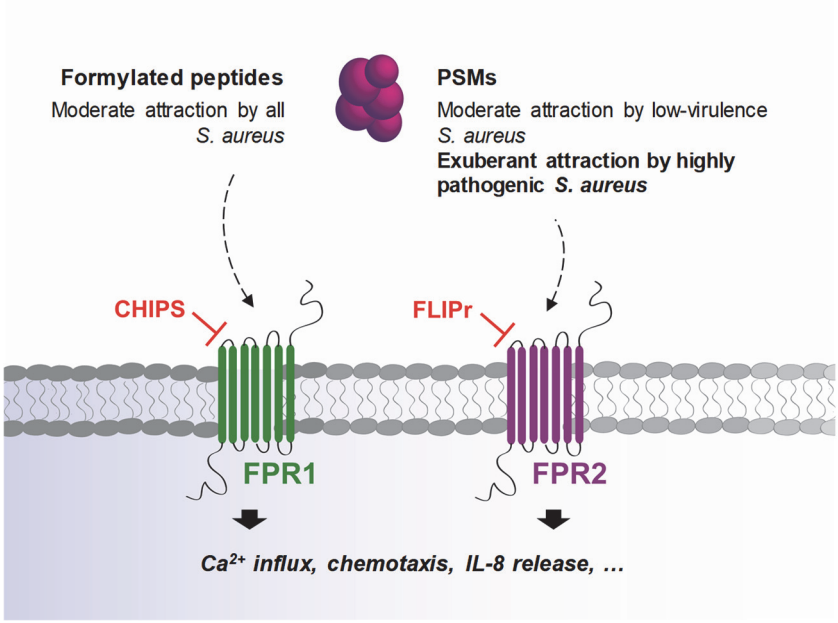

Fig. 5.2 Neutrophil activation by *S. aureus* exotoxins adopted and modified from Kretschmer et al. 2010 (129). Distinct activation patterns of FPR1 or FPR2 are thought to mediate the infllamatory response of *S. aureus*, depending on the pathogenicity of the corresponding bacteria strain. Moreover, inhibitory proteins such as CHIPS and FLIPr are released by *S. aureus* to mediate the host reaction to invading bacteria.

Additionally, FPR2 was shown to be modulated by a plethora of exogenous and endogenous human proteins and molecules (132) including the anti-inflammatory LXA_4 (131,184). In our experiments, PSM-induced LT formation remained unaffected from LXA_4 presence. This data thereby supplements the controversial discussion about the modulatory effect of LXA_4 on FPR2 activation by peptide ligands (170,217), but also implies a distinct activation of FPR2 by peptides and small molecules that has already been demonstrated for other GPCRs (218).

Another key feature of FPRs is to mediate chemotaxis, and PSMs have been shown to induce neutrophil migration in a dose-dependent manner (129,131,168). Although the subsequent induction of chemotactic LTB_4 appears to be a conceivable mechanism to explain these observations, our data indicate a subordinated role of LMs in this respect, at least in our experimental setting. In line, PSM-induced neutrophil chemotaxis could be significantly inhibited by FPR2-antagonism but remained unaffected from inhibition of the LTB_4 receptor by LY293111. Accordingly, a hierarchy of chemotactic signals was discussed previously and postulated a preferential activity of bacteria-derived molecules over intermediate mediators such as LTB_4, which might explain the findings here (17,219). However, PSM-mediated LT formation of tissue-resident or infiltrated neutrophils might intensify a sufficient immune response upon staphylococcal infections by recruiting additional leukocytes to the damaged tissue (17,220).

Taken together, here we highlight secreted exotoxins as pivotal determinants for immune responses upon staphylococcal infections. In detail, we substantiate PSMs and the subsequent activation of the FPR2 receptor as crucial factors for LT formation in neutrophils, which should be considered for further studies directing the role of LMs during bacteria challenge. However, it remains elusive whether increases in intracellular Ca^{2+}, phosphorylation of 5-LOX and $cPLA_{2\alpha}$ or all in conjunction are the key mechanism for LT formation upon stimulation with PSMs.

5.3 FLAP mutagenesis affects the assembly of the LT-synthetic protein complex

In humans, approximately 30% of all genes encode for integral membrane proteins. Nevertheless, only a limited number of high-resolution crystal structures have been described to date (93). A three-dimensional structure of FLAP was first published by Ferguson and co-workers in 2007 and revealed four membrane embedded helices (α1-α4), two cytosolic (C1, C2) and one lumenal loop (L1) as well as the N- and C-terminal parts that face the inner side of lipid-bilayers (91). Interestingly, although FLAP is considered as promising pharmacological target, a clinically applied inhibitor could not reach the pharmaceutical market so far (10). Thus, intensive focus was set on mutational studies addressing distinct binding sites of the FLAP inhibitor MK-591, without considering LT formation or interaction-properties of mutated FLAP isoforms with 5-LOX (221). Here we asked whether mutation of distinct residues would alter FLAP-mediated LT biosynthesis in a HEK293 cell model.

Table 5.1 Effect of FLAP mutagenesis on 5-LOX activity and subcellular organization of the LT-synthetic protein complex. Unless stated different, arrows are indicating the alteration of each mutated residue compared to wildtype FLAP.

FLAP	*wt*	*I119A*	*Y112A*	*T66A*	*A27L*	*S41A*	*S41D*	*S108A*	*S108D*	*S108Δ*
Location of mutated residue	-	α4	C2	α2	α1	C1	C1	C2	C2	C2
Overall product formation	88.9 ng/10^6 cells	→	→	→	→	↘	↘	→	→	→
Ratio 5-HpETE vs. LTB_4 + *vehicle*	1.2	→	→	↘	→	→	↗	→	↗	↗
Ratio 5-HpETE vs LTB_4 + *MK886* (compared to vehicle)	↗	→	→	↗	↗	↗	↗	↗	→	→
Remaining activity upon MK886	61	82	94	74	62	54	74	79	103	108
5-LOX-translocation	✓	✓	✓	✓	✓	✓	✓	✓	✓	✓
In situ 5-LOX/FLAP interaction	✓	(✓)	(✓)	✓	✓	✓	✓	✓	x	x

In order to overcome the lack of enzymatic activity of FLAP (222), we stably co-expressed FLAP isoforms with 5-LOX as published recently (98), and determined overall 5-LOX product formation and inhibition by MK886, interaction of 5-LOX and FLAP as well as subcellular

localization of 5-LOX upon A23187 stimulation in order to assess the effects of FLAP mutagenesis. The results are summarized in **Table 5.1**.

Variations within the second cytosolic loop and the intersection to α4 remarkably altered LT formation, while mutation of additional residues barely influenced 5-LOX activity. Noticeably, the overall 5-LOX product formation was generally unaffected from FLAP mutations, which might result from exogenous AA addition and related, partially FLAP-independent 5-LOX activity. We therefore calculated the ratio of 5-H(p)ETE versus LTB_4-isomers, since it was discussed previously that FLAP enhances the second catalytic step of the 5-LOX reaction to support LTA_4 formation from 5-HpETE in HEK293 cells (98). Increased ratios, indicating a subordinated role of FLAP for LT biosynthesis compared to wildtype cells, were found for mutations located on the cytosolic surface of FLAP (*i.e.* for *S41D* and *S108D* or *S108*Δ) that in turn remained unaffected from FLAP inhibition by MK886. Moreover, interactions with 5-LOX appeared to be absent after mutagenesis of distinct cytosolic residues (*S108D* and *S108*Δ) of FLAP, even though replacement of all selected amino acids within FLAP could not diminish 5-LOX subcellular translocation upon stimulation. Our data thereby differs from early findings that discussed a supportive role of FLAP for 5-LOX membrane binding (85,96), but reflect a more recent opinion that 5-LOX redistribution is not altered by FLAP inhibition in human leukocytes (12). Interestingly, contrary effects have been shown for 5-LOX, since mutation of the residues corking the active site delayed 5-LOX membrane association, which in turn could be rescued by co-expression with FLAP (60). Here, we show that 5-LOX/FLAP co-localization is not influenced by FLAP mutagenesis, while protein complex assembly strongly depended on a correct FLAP structure, mainly in view of the conformation of the cytosolic loops. In line with this, we hypothesize that sufficient 5-LOX/FLAP interaction is necessary to complete the second step of LT biosynthesis from 5-HpETE to LTA_4, and that *in situ* interaction of 5-LOX and FLAP might be crucial for the activity of FLAP inhibitors, at least in our cell model and upon exogenous FA supply.

Considering the molecular properties of FLAP, several explanations appear to be conceivable for an altered 5-LOX/FLAP interaction and varied 5-LOX product formation in our study:

(I) Mutagenesis of amino acids located on the protein surface might **cause steric hindrance** that in turn prevents a direct physical interaction of 5-LOX and FLAP detectable by PLA. Accordingly, it was hypothesized that one 5-LOX molecule binds to each trimer of FLAP and that both the C-terminal domain of 5-LOX and the cytosolic loops of FLAP might be important in this respect (91). However, although intensive efforts focused on the activities of both proteins, exact residues mediating their direct interaction are still elusive. Interestingly, both lumenal and cytosolic loops of FLAP were found to be dynamic and flexible (221), which could be important for *in situ* protein complex assembly. The mobility of the loops could likewise support the recent hypothesis of a time-dependent formation of the 5-LOX/FLAP complex, which was found delayed compared to the co-localization of both proteins in neutrophils and monocytes (12). In parallel, a previous discovery of our group highlighted Cys^{159}, located on the surface of 5-LOX, as essential residue for the interaction with FLAP, supporting the present findings here (223). Moreover, our data are in agreement with earlier studies demonstrating a FLAP

mutant that lacks cytosolic residues 106 to 108 to result in increased ratios of 5-HpETE versus LTA_4 (224). In line with our hypothesis, diminished 5-LOX/FLAP complex assembly and insufficient AA transfer were discussed but not verified as possible explanation for these observations (221,224).

A structure alignment of monomeric FLAP and LTC_4S (**Fig. 5.3A**) revealed marked differences in their three-dimensional configurations, and variations were primarily found in the length of helix α4 and cytosolic loop C2 (221). Accordingly, a direct physical interaction of 5-LOX and LTC_4S remains controversial, although only co-localization of both proteins appears to be related to LTC_4 formation (75,225,226). Together, these findings confirm the crucial role of cytosolic loop C2 within FLAP to interact with 5-LOX during LTA_4 formation.

(II) Next, variations of residues located within the lipid-exposed domains of FLAP might **affect binding of AA or the intermediate 5-HpETE**, respectively. Along these lines, it was shown that 5-LOX/FLAP complex assembly is prevented by inhibition of endogenous FA release but can be rescued in presence of exogenous AA or 5-HpETE, whereas 5-LOX translocation to the nuclear envelope remained unaffected at the same time (12,227). Although a concrete mechanism of how FLAP binds and transfers AA still remains unknown, it has been postulated that AA diffuses through the membrane and enters FLAP within its lipid-exposed grooves. Finally, the *in situ* 5-LOX/FLAP interaction is mediating a reorientation of AA from FLAP to the active site of 5-LOX (221). Consequently, FLAP mutations affecting the binding of FA or oxidized lipids would alter these processes. However, a concrete crystal structure of FA-bound FLAP is elusive. Since binding of AA is prevented by FLAP inhibitors, at least an overlap of lipid and inhibitor binding sites within FLAP was assumed (221). Among mammalian species, two highly conserved regions in FLAP spanning from residues 39 to 68 and residues 74 to 128 have been revealed and short deletions within the former domain have been related to diminished inhibitor binding (228,229). Nonetheless, FAs appeared to occupy additional FLAP regions apart from those responsible for inhibitor binding, including cytosolic domains (224).

However, one major drawback of the HEK293 cell model is that AA has to be added exogenously to achieve sufficient LT formation, as reported for artificial cell models before (224,230). Accordingly, is has to be noted that 5-LOX product formation might just partially depend on FLAP and the related FA transfer in our setting, resulting in subordinated effects for lipid-exposed residue mutations. Nevertheless, we assume that lipid-exposed domains are less important for the formation of the LT-synthetic protein complex.

(III) Besides direct effects of the mutagenesis, **insufficient inhibitor binding** might likewise affect the results presented here. In detail, comparison of vehicle and inhibitor incubations has been utilized to evaluate the consequences of mutations on LT formation due to the lack of a proper enzymatic activity of FLAP (222). Accordingly, an attenuated inhibition by MK886 might dissemble FLAP to be less operative. The first crystal structure of FLAP was originally performed in presence of MK-591 and revealed distinct amino acids to be involved in inhibitor binding (including Ala^{27}, Thr^{66}, Tyr^{112}, and Ile^{119} (91)), which appeared to be analogue for

MK886 that has been used in our study (221). Moreover, although apparently not directly involved in inhibitor binding (224,228), variations within the cytosolic loops have been discussed to affect inhibitor access to the lipid-exposed binding pocket (221). However, a PyMOL animation of FLAP(*S108D*) revealed the highest probability score for an aspartate conformer that faces the external flank of FLAP without corking the entrance to the inhibitor binding site from the cytosol (**Fig. 5.3B**). Thus, we conclude that our findings for modifications of C2 do not result from insufficient inhibitor activity.

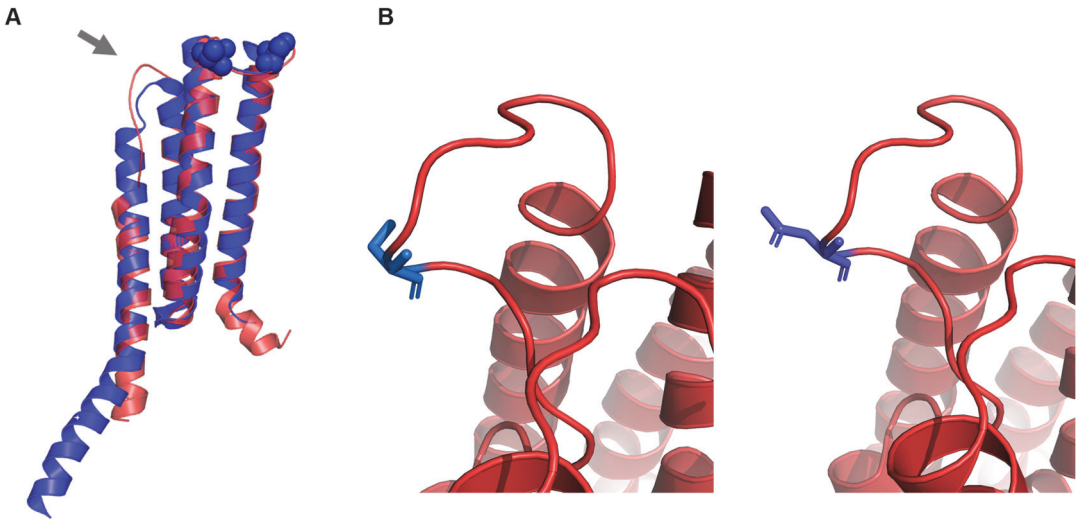

Fig. 5.3 A Crystal structure alignment of FLAP and LTC_4S. Monomeric FLAP (red, PDB accession number: 2q7m) and LTC_4S (blue, 2pno) are presented as cartoon rendering. The grey arrow highlights the main structural variations at cytosolic loop C2. Phosphorylation sites of LTC_4S (Ser^{36} and Thr^{40}) according to Ahmad et al. (13) are given as blue spheres. **B Mutagenesis of Ser^{108}.** FLAP (PDB accession number: 2q7m) is presented as cartoon rendering, while Ser^{108} (left hand site) and the corresponding aspartate mutant *S108D* (right) are given as blue sticks. Simulation of mutagenesis was performed with PyMOL Software and indicates a conceivable extension of the amino acid side-chain after mutation. Note, that the configuration with the highest probability has been chosen for presentation of FLAP(*S108D*) here, but that other conformers might be possible as well.

Phosphorylation is a common cellular mechanism to regulate the activity of enzymes and proteins, and serine, threonine, and tyrosine were found to be frequently phosphorylated residues (186). In fact, various enzymes participating in the biosynthesis of LTs are regulated by protein kinases, including 5-LOX, $cPLA_2$ and LTC_4S (6,13,33,69,70,171). Considering the structural homology with LTC_4S, we here asked whether FLAP serves as target for phosphoregulatory mechanisms in a comparable manner. *In silico* phospho-prediction tools revealed two FLAP residues, namely Ser^{41} and Ser^{108}, with high phosphorylation probability scores, and their localization on the cytosol-facing loops C1 and C2 might allow an interaction with soluble kinases. Both LT formation and 5-LOX-interaction of phosphomimetic FLAP(*S41D*) and non-phosphorylatable FLAP(*S41A*) as well as FLAP(*S108A*) widely corresponded with wildtype FLAP, whereas FLAP(*S108D*) was found to lack *in situ* complex assembly with 5-LOX. Indeed, product formation of HEK_5-LOX_FLAP(*S108D*) showed increased amounts of 5-H(p)ETE compared to LTB_4-isomers, underlining a subordinated effect of this FLAP mutant on 5-LOX product formation. These findings are in contrast to the study

of Ahmad et al. who demonstrated preferential phosphorylation of LTC_4S on cytosolic loop C1 instead of loop C2 (**Fig. 5.3A**). Phosphorylation of LTC_4S at Ser^{36} was thereby discussed to disturb the protein's active site by intermonomer-interactions (13). When FLAP(*S108D*) mutagenesis is simulated with PyMOL software, interactions with other subunits cannot be observed since the aspartate moiety is facing the cytosolic site of FLAP (**Fig. 5.3B**). However, despite intensive efforts, *in vitro* phosphorylation of FLAP could not be detected by phospho-proteomic approaches in our study. Interestingly, several challenges have been related to the detection of integral phospho-proteomes before, including insolubility, low abundance or the complexity of fragmentation and ionization of membrane proteins (231). Hence, we do not finally exclude the possibility of phosphorylatable residues within FLAP.

Taken together, we here identified the second cytosolic loop C2, and in particular Ser^{108} of FLAP as crucial determinant for sufficient 5-LOX/FLAP complex assembly and concurrent LT formation. Further studies should focus on this structural element to evaluate the consequences of its mutagenesis for the overall crystal structure of FLAP as well as for inhibitor and FA substrate binding, which has not been considered here. Moreover, it might be of interest whether loop C2 in general could serve as alternative pharmacological target to modulate LT biosynthesis, since the recently discovered FLAP inhibitors bind to lipid-exposed parts of the protein, and all exhibit high lipophilicity and thus inappropriate pharmacokinetic properties (10,221).

6 CONCLUSIONS

LMs derived from AA and related FAs exert diverse biological activities during the progression and resolution of inflammation (27). However, although discovered several decades ago, the knowledge about the activation and regulation of the enzymes involved in LM biosynthesis remains far from completion. This thesis first aimed at investigating the molecular mechanism of bacteria-induced LT formation and unveiled exotoxins secreted from pathogenic bacteria as determining factors for *in cellulo* 5-LOX activation. In case of *S. aureus*, a human commensal associated to both community- and health care-associated infections of diverse severity (4), we identified PSMs and their receptor FPR2 as critical factors capable to induce LM biosynthesis in neutrophils. Activation of FPR2, phosphorylation of ERK1/2 as well as an increase of intracellular Ca^{2+} are clearly involved in PSM-mediated 5-LOX activation. Together, we here present the release of LMs and the stimulation of 5-LOX as novel biological properties of PSMs. Moreover, our findings might encourage ongoing efforts to develop alternative anti-microbial strategies focusing on exotoxin secretion, since the rise of antibiotic resistant bacteria is becoming a progressive, relevant threat to humans (3,141). Our data likewise support manifold publications about FPR2 activation and the resulting potential to be modulated by anti-inflammatory therapies (135).

In addition, we here addressed structural elements of the integral membrane protein FLAP that acts as unique helper for cellular 5-LOX product formation (85,222). Our results uncover the second cytosolic loop (C2) of FLAP as crucial domain for sufficient assembly of the LT-synthetic protein complex at the nuclear membrane. Prospective studies and the development of FLAP inhibitors should therefore consider loop C2 as novel binding site, since previous compounds solely target lipid-exposed domains of FLAP, resulting in highly lipophilic drugs and thus inappropriate pharmacokinetic properties (8,10). Accordingly, our results shed light on the unresolved question of amino acids that are involved in the *in situ* 5-LOX/FLAP interaction. Moreover, although indications were found for a putative phosphorylation of Ser^{108} within FLAP, further investigations are needed to evaluate whether the discussed residue is indeed phosphorylated *in cellulo*.

Taken together, our results significantly contribute to the expansive field of LM research and provide novel insights into the signaling and molecular determinants of LT biosynthesis upon bacterial stimulation as well as its dependency on FLAP.

7 REFERENCES

1. Haeggstrom, J. Z., and Funk, C. D. (2011) Lipoxygenase and leukotriene pathways: biochemistry, biology, and roles in disease. *Chemical reviews* **111**, 5866-5898
2. Harizi, H., Corcuff, J. B., and Gualde, N. (2008) Arachidonic-acid-derived eicosanoids: roles in biology and immunopathology. *Trends Mol Med* **14**, 461-469
3. Infectious Diseases Society of, A., Spellberg, B., Blaser, M., Guidos, R. J., Boucher, H. W., Bradley, J. S., Eisenstein, B. I., Gerding, D., Lynfield, R., Reller, L. B., Rex, J., Schwartz, D., Septimus, E., Tenover, F. C., and Gilbert, D. N. (2011) Combating antimicrobial resistance: policy recommendations to save lives. *Clin Infect Dis* **52 Suppl 5**, S397-428
4. Tong, S. Y., Davis, J. S., Eichenberger, E., Holland, T. L., and Fowler, V. G., Jr. (2015) Staphylococcus aureus infections: epidemiology, pathophysiology, clinical manifestations, and management. *Clinical microbiology reviews* **28**, 603-661
5. Werz, O. (2002) 5-lipoxygenase: cellular biology and molecular pharmacology. *Current drug targets. Inflammation and allergy* **1**, 23-44
6. Werz, O., Burkert, E., Fischer, L., Szellas, D., Dishart, D., Samuelsson, B., Radmark, O., and Steinhilber, D. (2002) Extracellular signal-regulated kinases phosphorylate 5-lipoxygenase and stimulate 5-lipoxygenase product formation in leukocytes. *FASEB J* **16**, 1441-1443
7. Hammarberg, T., Provost, P., Persson, B., and Radmark, O. (2000) The N-terminal domain of 5-lipoxygenase binds calcium and mediates calcium stimulation of enzyme activity. *The Journal of biological chemistry* **275**, 38787-38793
8. Pettersen, D., Davidsson, O., and Whatling, C. (2015) Recent advances for FLAP inhibitors. *Bioorg Med Chem Lett* **25**, 2607-2612
9. Berger, W., De Chandt, M. T., and Cairns, C. B. (2007) Zileuton: clinical implications of 5-Lipoxygenase inhibition in severe airway disease. *International journal of clinical practice* **61**, 663-676
10. Werz, O., Gerstmeier, J., and Garscha, U. (2017) Novel leukotriene biosynthesis inhibitors (2012-2016) as anti-inflammatory agents. *Expert Opin Ther Pat* **27**, 607-620
11. Werz, O. (2007) Inhibition of 5-lipoxygenase product synthesis by natural compounds of plant origin. *Planta Med* **73**, 1331-1357
12. Gerstmeier, J., Weinigel, C., Rummler, S., Radmark, O., Werz, O., and Garscha, U. (2016) Time-resolved in situ assembly of the leukotriene-synthetic 5-lipoxygenase/5-lipoxygenase-activating protein complex in blood leukocytes. *FASEB journal : official publication of the Federation of American Societies for Experimental Biology* **30**, 276-285
13. Ahmad, S., Ytterberg, A. J., Thulasingam, M., Tholander, F., Bergman, T., Zubarev, R., Wetterholm, A., Rinaldo-Matthis, A., and Haeggstrom, J. Z. (2016) Phosphorylation of Leukotriene C4 Synthase at Serine 36 Impairs Catalytic Activity. *The Journal of biological chemistry* **291**, 18410-18418
14. Barton, G. M. (2008) A calculated response: control of inflammation by the innate immune system. *J Clin Invest* **118**, 413-420
15. Medzhitov, R. (2008) Origin and physiological roles of inflammation. *Nature* **454**, 428-435
16. Soehnlein, O., and Lindbom, L. (2010) Phagocyte partnership during the onset and resolution of inflammation. *Nature reviews. Immunology* **10**, 427-439
17. Kolaczkowska, E., and Kubes, P. (2013) Neutrophil recruitment and function in health and inflammation. *Nature reviews. Immunology* **13**, 159-175
18. Dempsey, P. W., Vaidya, S. A., and Cheng, G. (2003) The art of war: Innate and adaptive immune responses. *Cell Mol Life Sci* **60**, 2604-2621
19. Punchard, N. A., Whelan, C. J., and Adcock, I. (2004) The Journal of Inflammation. *Journal of inflammation* **1**, 1

20. Netea, M. G., Balkwill, F., Chonchol, M., Cominelli, F., Donath, M. Y., Giamarellos-Bourboulis, E. J., Golenbock, D., Gresnigt, M. S., Heneka, M. T., Hoffman, H. M., Hotchkiss, R., Joosten, L. A. B., Kastner, D. L., Korte, M., Latz, E., Libby, P., Mandrup-Poulsen, T., Mantovani, A., Mills, K. H. G., Nowak, K. L., O'Neill, L. A., Pickkers, P., van der Poll, T., Ridker, P. M., Schalkwijk, J., Schwartz, D. A., Siegmund, B., Steer, C. J., Tilg, H., van der Meer, J. W. M., van de Veerdonk, F. L., and Dinarello, C. A. (2017) A guiding map for inflammation. *Nature immunology* **18**, 826-831
21. Ortega-Gomez, A., Perretti, M., and Soehnlein, O. (2013) Resolution of inflammation: an integrated view. *EMBO Mol Med* **5**, 661-674
22. Bannenberg, G., and Serhan, C. N. (2010) Specialized pro-resolving lipid mediators in the inflammatory response: An update. *Biochim Biophys Acta* **1801**, 1260-1273
23. Sugimoto, M. A., Sousa, L. P., Pinho, V., Perretti, M., and Teixeira, M. M. (2016) Resolution of inflammation: what Controls its Onset? *Frontiers in Immunology* **7**
24. Mantovani, A., Bonecchi, R., and Locati, M. (2006) Tuning inflammation and immunity by chemokine sequestration: decoys and more. *Nature reviews. Immunology* **6**, 907-918
25. Fadok, V. A., Bratton, D. L., Konowal, A., Freed, P. W., Westcott, J. Y., and Henson, P. M. (1998) Macrophages that have ingested apoptotic cells in vitro inhibit proinflammatory cytokine production through autocrine/paracrine mechanisms involving TGF-beta, PGE2, and PAF. *J Clin Invest* **101**, 890-898
26. Shimizu, T. (2009) Lipid Mediators in Health and Disease: Enzymes and Receptors as Therapeutic Targets for the Regulation of Immunity and Inflammation. *Annu Rev Pharmacol* **49**, 123-150
27. Dennis, E. A., and Norris, P. C. (2015) Eicosanoid storm in infection and inflammation. *Nature reviews. Immunology* **15**, 511-523
28. Serhan, C. N., Hong, S., Gronert, K., Colgan, S. P., Devchand, P. R., Mirick, G., and Moussignac, R. L. (2002) Resolvins: a family of bioactive products of omega-3 fatty acid transformation circuits initiated by aspirin treatment that counter proinflammation signals. *J Exp Med* **196**, 1025-1037
29. Ricciotti, E., and FitzGerald, G. A. (2011) Prostaglandins and inflammation. *Arterioscler Thromb Vasc Biol* **31**, 986-1000
30. Panigrahy, D., Kaipainen, A., Greene, E. R., and Huang, S. (2010) Cytochrome P450-derived eicosanoids: the neglected pathway in cancer. *Cancer Metast Rev* **29**, 723-735
31. Macdonald, J. I. S., and Sprecher, H. (1991) Phospholipid Fatty-Acid Remodeling in Mammalian-Cells. *Biochimica Et Biophysica Acta* **1084**, 105-121
32. Leslie, C. C. (2015) Cytosolic phospholipase A(2): physiological function and role in disease. *J Lipid Res* **56**, 1386-1402
33. Murakami, M., and Kudo, I. (2002) Phospholipase A2. *J Biochem* **131**, 285-292
34. Schievella, A. R., Regier, M. K., Smith, W. L., and Lin, L. L. (1995) Calcium-mediated translocation of cytosolic phospholipase A2 to the nuclear envelope and endoplasmic reticulum. *J Biol Chem* **270**, 30749-30754
35. Lone, A. M., and Tasken, K. (2013) Proinflammatory and immunoregulatory roles of eicosanoids in T cells. *Front Immunol* **4**, 130
36. Kuhn, H., Banthiya, S., and van Leyen, K. (2015) Mammalian lipoxygenases and their biological relevance. *Biochim Biophys Acta* **1851**, 308-330
37. Rouzer, C. A., and Marnett, L. J. (2009) Cyclooxygenases: structural and functional insights. *J Lipid Res* **50 Suppl**, S29-34
38. Stables, M. J., and Gilroy, D. W. (2011) Old and new generation lipid mediators in acute inflammation and resolution. *Progress in lipid research* **50**, 35-51
39. Chandrasekharan, N. V., and Simmons, D. L. (2004) The cyclooxygenases. *Genome biology* **5**, 241
40. Mashima, R., and Okuyama, T. (2015) The role of lipoxygenases in pathophysiology; new insights and future perspectives. *Redox biology* **6**, 297-310

41. Manikandan, P., and Nagini, S. (2018) Cytochrome P450 Structure, Function and Clinical Significance: A Review. *Current drug targets* **19**, 38-54
42. Imig, J. D., and Hammock, B. D. (2009) Soluble epoxide hydrolase as a therapeutic target for cardiovascular diseases. *Nat Rev Drug Discov* **8**, 794-805
43. Shen, H. C., and Hammock, B. D. (2012) Discovery of Inhibitors of Soluble Epoxide Hydrolase: A Target with Multiple Potential Therapeutic Indications. *Journal of Medicinal Chemistry* **55**, 1789-1808
44. Folco, G., and Murphy, R. C. (2006) Eicosanoid transcellular biosynthesis: from cell-cell interactions to in vivo tissue responses. *Pharmacological reviews* **58**, 375-388
45. Lopez-Vicario, C., Rius, B., Alcaraz-Quiles, J., Garcia-Alonso, V., Lopategi, A., Titos, E., and Claria, J. (2016) Pro-resolving mediators produced from EPA and DHA: Overview of the pathways involved and their mechanisms in metabolic syndrome and related liver diseases. *Eur J Pharmacol* **785**, 133-143
46. Dahlen, S. E., Hedqvist, P., Hammarstrom, S., and Samuelsson, B. (1980) Leukotrienes are potent constrictors of human bronchi. *Nature* **288**, 484-486
47. Dalli, J., Ramon, S., Norris, P. C., Colas, R. A., and Serhan, C. N. (2015) Novel proresolving and tissue-regenerative resolvin and protectin sulfido-conjugated pathways. *FASEB J* **29**, 2120-2136
48. Dalli, J., Chiang, N., and Serhan, C. N. (2014) Identification of 14-series sulfido-conjugated mediators that promote resolution of infection and organ protection. *Proc Natl Acad Sci U S A* **111**, E4753-4761
49. Serhan, C. N., and Chiang, N. (2013) Resolution phase lipid mediators of inflammation: agonists of resolution. *Current opinion in pharmacology* **13**, 632-640
50. Lee, T. H., Horton, C. E., Kyanaung, U., Haskard, D., Crea, A. E. G., and Spur, B. W. (1989) Lipoxin-A4 and Lipoxin-B4 Inhibit Chemotactic Responses of Human-Neutrophils Stimulated by Leukotriene-B4 and N-Formyl-L-Methionyl-L-Leucyl-L-Phenylalanine. *Clinical science* **77**, 195-203
51. Papayianni, A., Serhan, C. N., and Brady, H. R. (1996) Lipoxin A4 and B4 inhibit leukotriene-stimulated interactions of human neutrophils and endothelial cells. *J Immunol* **156**, 2264-2272
52. Godson, C., Mitchell, S., Harvey, K., Petasis, N. A., Hogg, N., and Brady, H. R. (2000) Cutting edge: lipoxins rapidly stimulate nonphlogistic phagocytosis of apoptotic neutrophils by monocyte-derived macrophages. *J Immunol* **164**, 1663-1667
53. Radmark, O., Werz, O., Steinhilber, D., and Samuelsson, B. (2015) 5-Lipoxygenase, a key enzyme for leukotriene biosynthesis in health and disease. *Biochimica et biophysica acta* **1851**, 331-339
54. Uhl, J., Klan, N., Rose, M., Entian, K. D., Werz, O., and Steinhilber, D. (2002) The 5-lipoxygenase promoter is regulated by DNA methylation. *J Biol Chem* **277**, 4374-4379
55. Coffey, M. J., Gyetko, M., and Petersgolden, M. (1993) 1,25-Dihydroxyvitamin-D(3) up-Regulates 5-Lipoxygenase Metabolism and 5-Lipoxygenase Activating Protein in Peripheral-Blood Monocytes as They Differentiate into Mature Macrophages. *J Lipid Mediator* **6**, 43-51
56. Pouliot, M., McDonald, P. P., Khamzina, L., Borgeat, P., and McColl, S. R. (1994) Granulocyte-macrophage colony-stimulating factor enhances 5-lipoxygenase levels in human polymorphonuclear leukocytes. *J Immunol* **152**, 851-858
57. Murakami, M., Austen, K. F., Bingham, C. O., Friend, D. S., Penrose, J. F., and Arm, J. P. (1995) Interleukin-3 Regulates Development of the 5-Lipoxygenase/Leukotriene C-4 Synthase Pathway in Mouse Mast-Cells. *Journal of Biological Chemistry* **270**, 22653-22656
58. Matsumoto, T., Funk, C. D., Radmark, O., Hoog, J. O., Jornvall, H., and Samuelsson, B. (1988) Molecular cloning and amino acid sequence of human 5-lipoxygenase. *Proc Natl Acad Sci U S A* **85**, 26-30
59. Gilbert, N. C., Bartlett, S. G., Waight, M. T., Neau, D. B., Boeglin, W. E., Brash, A. R., and Newcomer, M. E. (2011) The structure of human 5-lipoxygenase. *Science* **331**, 217-219

60. Gerstmeier, J., Newcomer, M. E., Dennhardt, S., Romp, E., Fischer, J., Werz, O., and Garscha, U. (2016) 5-Lipoxygenase-activating protein rescues activity of 5-lipoxygenase mutations that delay nuclear membrane association and disrupt product formation. *FASEB journal : official publication of the Federation of American Societies for Experimental Biology* **30**, 1892-1900
61. Chen, X. S., and Funk, C. D. (2001) The N-terminal "beta-barrel" domain of 5-lipoxygenase is essential for nuclear membrane translocation. *J Biol Chem* **276**, 811-818
62. Hafner, A. K., Cernescu, M., Hofmann, B., Ermisch, M., Hornig, M., Metzner, J., Schneider, G., Brutschy, B., and Steinhilber, D. (2011) Dimerization of human 5-lipoxygenase. *Biological chemistry* **392**, 1097-1111
63. Radmark, O. (2002) Arachidonate 5-lipoxygenase. *Prostaglandins Other Lipid Mediat* **68-69**, 211-234
64. Ford-Hutchinson, A. W. (1981) Leukotriene B4 and neutrophil function: a review. *J R Soc Med* **74**, 831-833
65. Haeggstrom, J. Z. (2000) Structure, function, and regulation of leukotriene A4 hydrolase. *Am J Respir Crit Care Med* **161**, S25-31
66. Lam, B. K., and Austen, K. F. (2002) Leukotriene C4 synthase: a pivotal enzyme in cellular biosynthesis of the cysteinyl leukotrienes. *Prostaglandins Other Lipid Mediat* **68-69**, 511-520
67. Hammarberg, T., and Radmark, O. (1999) 5-lipoxygenase binds calcium. *Biochemistry* **38**, 4441-4447
68. Werz, O., Burkert, E., Samuelsson, B., Radmark, O., and Steinhilber, D. (2002) Activation of 5-lipoxygenase by cell stress is calcium independent in human polymorphonuclear leukocytes. *Blood* **99**, 1044-1052
69. Werz, O., Szellas, D., Steinhilber, D., and Radmark, O. (2002) Arachidonic acid promotes phosphorylation of 5-lipoxygenase at Ser-271 by MAPK-activated protein kinase 2 (MK2). *The Journal of biological chemistry* **277**, 14793-14800
70. Luo, M., Jones, S. M., Phare, S. M., Coffey, M. J., Peters-Golden, M., and Brock, T. G. (2004) Protein kinase A inhibits leukotriene synthesis by phosphorylation of 5-lipoxygenase on serine 523. *The Journal of biological chemistry* **279**, 41512-41520
71. Radmark, O., and Samuelsson, B. (2009) 5-Lipoxygenase: mechanisms of regulation. *J Lipid Res* **50 Suppl**, S40-45
72. Peters-Golden, M., and Brock, T. G. (2003) 5-lipoxygenase and FLAP. *Prostaglandins Leukot Essent Fatty Acids* **69**, 99-109
73. Hanaka, H., Shimizu, T., and Izumi, T. (2002) Nuclear-localization-signal-dependent and nuclear-export-signal-dependent mechanisms determine the localization of 5-lipoxygenase. *Biochem J* **361**, 505-514
74. Brock, T. G., McNish, R. W., Bailie, M. B., and Peters-Golden, M. (1997) Rapid import of cytosolic 5-lipoxygenase into the nucleus of neutrophils after in vivo recruitment and in vitro adherence. *J Biol Chem* **272**, 8276-8280
75. Mandal, A. K., Jones, P. B., Bair, A. M., Christmas, P., Miller, D., Yamin, T. T., Wisniewski, D., Menke, J., Evans, J. F., Hyman, B. T., Bacskai, B., Chen, M., Lee, D. M., Nikolic, B., and Soberman, R. J. (2008) The nuclear membrane organization of leukotriene synthesis. *Proc Natl Acad Sci U S A* **105**, 20434-20439
76. Pouliot, M., McDonald, P. P., Krump, E., Mancini, J. A., McColl, S. R., Weech, P. K., and Borgeat, P. (1996) Colocalization of cytosolic phospholipase A2, 5-lipoxygenase, and 5-lipoxygenase-activating protein at the nuclear membrane of A23187-stimulated human neutrophils. *Eur J Biochem* **238**, 250-258
77. Newcomer, M. E., and Gilbert, N. C. (2010) Location, location, location: compartmentalization of early events in leukotriene biosynthesis. *The Journal of biological chemistry* **285**, 25109-25114
78. Provost, P., Samuelsson, B., and Radmark, O. (1999) Interaction of 5-lipoxygenase with cellular proteins. *Proc Natl Acad Sci U S A* **96**, 1881-1885

79. Borgeat, P., and Samuelsson, B. (1979) Arachidonic acid metabolism in polymorphonuclear leukocytes: effects of ionophore A23187. *Proceedings of the National Academy of Sciences of the United States of America* **76**, 2148-2152
80. Salari, H., Braquet, P., Naccache, P., and Borgeat, P. (1985) Characterization of effect of N-formyl-methionyl-leucyl-phenylalanine on leukotriene synthesis in human polymorphonuclear leukocytes. *Inflammation* **9**, 127-138
81. Clancy, R. M., Dahinden, C. A., and Hugli, T. E. (1983) Arachidonate metabolism by human polymorphonuclear leukocytes stimulated by N-formyl-Met-Leu-Phe or complement component C5a is independent of phospholipase activation. *Proceedings of the National Academy of Sciences of the United States of America* **80**, 7200-7204
82. Chilton, F. H., O'Flaherty, J. T., Walsh, C. E., Thomas, M. J., Wykle, R. L., DeChatelet, L. R., and Waite, B. M. (1982) Platelet activating factor. Stimulation of the lipoxygenase pathway in polymorphonuclear leukocytes by 1-O-alkyl-2-O-acetyl-sn-glycero-3-phosphocholine. *J Biol Chem* **257**, 5402-5407
83. Schroder, J. M. (1989) The monocyte-derived neutrophil activating peptide (NAP/interleukin 8) stimulates human neutrophil arachidonate-5-lipoxygenase, but not the release of cellular arachidonate. *The Journal of experimental medicine* **170**, 847-863
84. Claesson, H. E., Lundberg, U., and Malmsten, C. (1981) Serum-coated zymosan stimulates the synthesis of leukotriene B4 in human polymorphonuclear leukocytes. Inhibition by cyclic AMP. *Biochem Biophys Res Commun* **99**, 1230-1237
85. Dixon, R. A., Diehl, R. E., Opas, E., Rands, E., Vickers, P. J., Evans, J. F., Gillard, J. W., and Miller, D. K. (1990) Requirement of a 5-lipoxygenase-activating protein for leukotriene synthesis. *Nature* **343**, 282-284
86. Gillard, J., Ford-Hutchinson, A. W., Chan, C., Charleson, S., Denis, D., Foster, A., Fortin, R., Leger, S., McFarlane, C. S., Morton, H., and et al. (1989) L-663,536 (MK-886) (3-[1-(4-chlorobenzyl)-3-t-butyl-thio-5-isopropylindol-2-yl]-2,2 - dimethylpropanoic acid), a novel, orally active leukotriene biosynthesis inhibitor. *Canadian journal of physiology and pharmacology* **67**, 456-464
87. Miller, D. K., Gillard, J. W., Vickers, P. J., Sadowski, S., Leveille, C., Mancini, J. A., Charleson, P., Dixon, R. A. F., Fordhutchinson, A. W., Fortin, R., Gauthier, J. Y., Rodkey, J., Rosen, R., Rouzer, C., Sigal, I. S., Strader, C. D., and Evans, J. F. (1990) Identification and Isolation of a Membrane-Protein Necessary for Leukotriene Production. *Nature* **343**, 278-281
88. Martinez Molina, D., Eshaghi, S., and Nordlund, P. (2008) Catalysis within the lipid bilayer-structure and mechanism of the MAPEG family of integral membrane proteins. *Current opinion in structural biology* **18**, 442-449
89. Pouliot, M., McDonald, P. P., Borgeat, P., and McColl, S. R. (1994) Granulocyte/macrophage colony-stimulating factor stimulates the expression of the 5-lipoxygenase-activating protein (FLAP) in human neutrophils. *The Journal of experimental medicine* **179**, 1225-1232
90. Chen, X. S., Naumann, T. A., Kurre, U., Jenkins, N. A., Copeland, N. G., and Funk, C. D. (1995) cDNA cloning, expression, mutagenesis, intracellular localization, and gene chromosomal assignment of mouse 5-lipoxygenase. *J Biol Chem* **270**, 17993-17999
91. Ferguson, A. D., McKeever, B. M., Xu, S., Wisniewski, D., Miller, D. K., Yamin, T. T., Spencer, R. H., Chu, L., Ujjainwalla, F., Cunningham, B. R., Evans, J. F., and Becker, J. W. (2007) Crystal structure of inhibitor-bound human 5-lipoxygenase-activating protein. *Science* **317**, 510-512
92. Newport, T. D., Sansom, M. S. P., and Stansfeld, P. J. (2019) The MemProtMD database: a resource for membrane-embedded protein structures and their lipid interactions. *Nucleic acids research* **47**, D390-D397
93. Cordes, F. S., Bright, J. N., and Sansom, M. S. (2002) Proline-induced distortions of transmembrane helices. *J Mol Biol* **323**, 951-960

94. Mancini, J. A., Abramovitz, M., Cox, M. E., Wong, E., Charleson, S., Perrier, H., Wang, Z., Prasit, P., and Vickers, P. J. (1993) 5-lipoxygenase-activating protein is an arachidonate binding protein. *FEBS letters* **318**, 277-281
95. Charleson, S., Evans, J. F., Leger, S., Perrier, H., Prasit, P., Wang, Z., and Vickers, P. J. (1994) Structural requirements for the binding of fatty acids to 5-lipoxygenase-activating protein. *Eur J Pharmacol* **267**, 275-280
96. Rouzer, C. A., Fordhutchinson, A. W., Morton, H. E., and Gillard, J. W. (1990) Mk886, a Potent and Specific Leukotriene Biosynthesis Inhibitor Blocks and Reverses the Membrane Association of 5-Lipoxygenase in Ionophore-Challenged Leukocytes. *Journal of Biological Chemistry* **265**, 1436-1442
97. Brock, T. G., McNish, R. W., and Peters-Golden, M. (1998) Capacity for repeatable leukotriene generation after transient stimulation of mast cells and macrophages. *Biochemical Journal* **329**, 519-525
98. Gerstmeier, J., Weinigel, C., Barz, D., Werz, O., and Garscha, U. (2014) An experimental cell-based model for studying the cell biology and molecular pharmacology of 5-lipoxygenase-activating protein in leukotriene biosynthesis. *Biochimica et biophysica acta* **1840**, 2961-2969
99. Werner, M., Jordan, P. M., Romp, E., Czapka, A., Rao, Z., Kretzer, C., Koeberle, A., Garscha, U., Pace, S., Claesson, H. E., Serhan, C. N., Werz, O., and Gerstmeier, J. (2019) Targeting biosynthetic networks of the proinflammatory and proresolving lipid metabolome. *FASEB J*, fj201802509R
100. Byrum, R. S., Goulet, J. L., Griffiths, R. J., and Koller, B. H. (1997) Role of the 5-lipoxygenase-activating protein (FLAP) in murine acute inflammatory responses. *The Journal of experimental medicine* **185**, 1065-1075
101. Jawien, J., Gajda, M., Rudling, M., Mateuszuk, L., Olszanecki, R., Guzik, T. J., Cichocki, T., Chlopicki, S., and Korbut, R. (2006) Inhibition of five lipoxygenase activating protein (FLAP) by MK-886 decreases atherosclerosis in apoE/LDLR-double knockout mice. *European journal of clinical investigation* **36**, 141-146
102. Jawien, J., Gajda, M., Olszanecki, R., and Korbut, R. (2007) BAY x 1005 attenuates atherosclerosis in apoE/LDLR - double knockout mice. *J Physiol Pharmacol* **58**, 583-588
103. Giannopoulos, P. F., Chu, J., Joshi, Y. B., Sperow, M., Li, J. G., Kirby, L. G., and Pratico, D. (2013) 5-lipoxygenase activating protein reduction ameliorates cognitive deficit, synaptic dysfunction, and neuropathology in a mouse model of Alzheimer's disease. *Biological psychiatry* **74**, 348-356
104. Helgadottir, A., Manolescu, A., Thorleifsson, G., Gretarsdottir, S., Jonsdottir, H., Thorsteinsdottir, U., Samani, N. J., Gudmundsson, G., Grant, S. F., Thorgeirsson, G., Sveinbjornsdottir, S., Valdimarsson, E. M., Matthiasson, S. E., Johannsson, H., Gudmundsdottir, O., Gurney, M. E., Sainz, J., Thorhallsdottir, M., Andresdottir, M., Frigge, M. L., Topol, E. J., Kong, A., Gudnason, V., Hakonarson, H., Gulcher, J. R., and Stefansson, K. (2004) The gene encoding 5-lipoxygenase activating protein confers risk of myocardial infarction and stroke. *Nature genetics* **36**, 233-239
105. Lowy, F. D. (1998) Staphylococcus aureus infections. *N Engl J Med* **339**, 520-532
106. Arciola, C. R., Campoccia, D., Speziale, P., Montanaro, L., and Costerton, J. W. (2012) Biofilm formation in Staphylococcus implant infections. A review of molecular mechanisms and implications for biofilm-resistant materials. *Biomaterials* **33**, 5967-5982
107. Verdrengh, M., and Tarkowski, A. (1997) Role of neutrophils in experimental septicemia and septic arthritis induced by Staphylococcus aureus. *Infect Immun* **65**, 2517-2521
108. Balaban, N., Goldkorn, T., Nhan, R. T., Dang, L. B., Scott, S., Ridgley, R. M., Rasooly, A., Wright, S. C., Larrick, J. W., Rasooly, R., and Carlson, J. R. (1998) Autoinducer of virulence as a target for vaccine and therapy against Staphylococcus aureus. *Science* **280**, 438-440

109. Le, K. Y., and Otto, M. (2015) Quorum-sensing regulation in staphylococci-an overview. *Frontiers in Microbiology* **6**
110. George, E. A., and Muir, T. W. (2007) Molecular mechanisms of agr quorum sensing in virulent staphylococci. *Chembiochem : a European journal of chemical biology* **8**, 847-855
111. Queck, S. Y., Jameson-Lee, M., Villaruz, A. E., Bach, T. H., Khan, B. A., Sturdevant, D. E., Ricklefs, S. M., Li, M., and Otto, M. (2008) RNAIII-independent target gene control by the agr quorum-sensing system: insight into the evolution of virulence regulation in Staphylococcus aureus. *Molecular cell* **32**, 150-158
112. Cheung, A. L., Koomey, J. M., Butler, C. A., Projan, S. J., and Fischetti, V. A. (1992) Regulation of exoprotein expression in Staphylococcus aureus by a locus (sar) distinct from agr. *Proc Natl Acad Sci U S A* **89**, 6462-6466
113. Dunman, P. M., Murphy, E., Haney, S., Palacios, D., Tucker-Kellogg, G., Wu, S., Brown, E. L., Zagursky, R. J., Shlaes, D., and Projan, S. J. (2001) Transcription profiling-based identification of Staphylococcus aureus genes regulated by the agr and/or sarA loci. *J Bacteriol* **183**, 7341-7353
114. Vandenesch, F., Lina, G., and Henry, T. (2012) Staphylococcus aureus hemolysins, bi-component leukocidins, and cytolytic peptides: a redundant arsenal of membrane-damaging virulence factors? *Frontiers in cellular and infection microbiology* **2**, 12
115. Cheung, G. Y., Joo, H. S., Chatterjee, S. S., and Otto, M. (2014) Phenol-soluble modulins--critical determinants of staphylococcal virulence. *FEMS Microbiol Rev* **38**, 698-719
116. DeLeo, F. R., Otto, M., Kreiswirth, B. N., and Chambers, H. F. (2010) Community-associated meticillin-resistant Staphylococcus aureus. *Lancet* **375**, 1557-1568
117. Bubeck Wardenburg, J., Bae, T., Otto, M., Deleo, F. R., and Schneewind, O. (2007) Poring over pores: alpha-hemolysin and Panton-Valentine leukocidin in Staphylococcus aureus pneumonia. *Nature medicine* **13**, 1405-1406
118. Bubeck Wardenburg, J., Patel, R. J., and Schneewind, O. (2007) Surface proteins and exotoxins are required for the pathogenesis of Staphylococcus aureus pneumonia. *Infect Immun* **75**, 1040-1044
119. Bhakdi, S., and Tranum-Jensen, J. (1991) Alpha-toxin of Staphylococcus aureus. *Microbiological reviews* **55**, 733-751
120. Wilke, G. A., and Bubeck Wardenburg, J. (2010) Role of a disintegrin and metalloprotease 10 in Staphylococcus aureus alpha-hemolysin-mediated cellular injury. *Proc Natl Acad Sci U S A* **107**, 13473-13478
121. Pany, S., Vijayvargia, R., and Krishnasastry, M. V. (2004) Caveolin-1 binding motif of alpha-hemolysin: its role in stability and pore formation. *Biochem Biophys Res Commun* **322**, 29-36
122. Valeva, A., Walev, I., Pinkernell, M., Walker, B., Bayley, H., Palmer, M., and Bhakdi, S. (1997) Transmembrane beta-barrel of staphylococcal alpha-toxin forms in sensitive but not in resistant cells. *Proceedings of the National Academy of Sciences of the United States of America* **94**, 11607-11611
123. Spaan, A. N., van Strijp, J. A. G., and Torres, V. J. (2017) Leukocidins: staphylococcal bi-component pore-forming toxins find their receptors. *Nature Reviews Microbiology* **15**, 435-447
124. Said-Salim, B., Dunman, P. M., McAleese, F. M., Macapagal, D., Murphy, E., McNamara, P. J., Arvidson, S., Foster, T. J., Projan, S. J., and Kreiswirth, B. N. (2003) Global regulation of Staphylococcus aureus genes by Rot. *J Bacteriol* **185**, 610-619
125. Huseby, M., Shi, K., Brown, C. K., Digre, J., Mengistu, F., Seo, K. S., Bohach, G. A., Schlievert, P. M., Ohlendorf, D. H., and Earhart, C. A. (2007) Structure and biological activities of beta toxin from Staphylococcus aureus. *J Bacteriol* **189**, 8719-8726
126. Walev, I., Weller, U., Strauch, S., Foster, T., and Bhakdi, S. (1996) Selective killing of human monocytes and cytokine release provoked by sphingomyelinase (beta-toxin) of Staphylococcus aureus. *Infect Immun* **64**, 2974-2979

127. Mehlin, C., Headley, C. M., and Klebanoff, S. J. (1999) An inflammatory polypeptide complex from Staphylococcus epidermidis: isolation and characterization. *J Exp Med* **189**, 907-918
128. Rautenberg, M., Joo, H. S., Otto, M., and Peschel, A. (2011) Neutrophil responses to staphylococcal pathogens and commensals via the formyl peptide receptor 2 relates to phenol-soluble modulin release and virulence. *FASEB journal : official publication of the Federation of American Societies for Experimental Biology* **25**, 1254-1263
129. Kretschmer, D., Gleske, A. K., Rautenberg, M., Wang, R., Koberle, M., Bohn, E., Schoneberg, T., Rabiet, M. J., Boulay, F., Klebanoff, S. J., van Kessel, K. A., van Strijp, J. A., Otto, M., and Peschel, A. (2010) Human formyl peptide receptor 2 senses highly pathogenic Staphylococcus aureus. *Cell Host Microbe* **7**, 463-473
130. Weiss, E., and Kretschmer, D. (2018) Formyl-Peptide Receptors in Infection, Inflammation, and Cancer. *Trends Immunol*
131. Ye, R. D., Boulay, F., Wang, J. M., Dahlgren, C., Gerard, C., Parmentier, M., Serhan, C. N., and Murphy, P. M. (2009) International Union of Basic and Clinical Pharmacology. LXXIII. Nomenclature for the formyl peptide receptor (FPR) family. *Pharmacological reviews* **61**, 119-161
132. He, H. Q., and Ye, R. D. (2017) The Formyl Peptide Receptors: Diversity of Ligands and Mechanism for Recognition. *Molecules* **22**
133. Dorward, D. A., Lucas, C. D., Chapman, G. B., Haslet, C., Dhaliwal, K., and Rossi, A. G. (2015) The Role of Formylated Peptides and Formyl Peptide Receptor 1 in Governing Neutrophil Function during Acute Inflammation. *American Journal of Pathology* **185**, 1172-1184
134. Postma, B., Poppelier, M. J., van Galen, J. C., Prossnitz, E. R., van Strijp, J. A., de Haas, C. J., and van Kessel, K. P. (2004) Chemotaxis inhibitory protein of Staphylococcus aureus binds specifically to the C5a and formylated peptide receptor. *J Immunol* **172**, 6994-7001
135. Dufton, N., and Perretti, M. (2010) Therapeutic anti-inflammatory potential of formyl-peptide receptor agonists. *Pharmacol Ther* **127**, 175-188
136. Cooray, S. N., Gobbetti, T., Montero-Melendez, T., McArthur, S., Thompson, D., Clark, A. J. L., Flower, R. J., and Perretti, M. (2013) Ligand-specific conformational change of the G-protein-coupled receptor ALX/FPR2 determines proresolving functional responses. *P Natl Acad Sci USA* **110**, 18232-18237
137. Bae, Y. S., Lee, H. Y., Jo, E. J., Kim, J. I., Kang, H. K., Ye, R. D., Kwak, J. Y., and Ryu, S. H. (2004) Identification of peptides that antagonize formyl peptide receptor-like 1-mediated signaling. *J Immunol* **173**, 607-614
138. Prat, C., Bestebroer, J., de Haas, C. J., van Strijp, J. A., and van Kessel, K. P. (2006) A new staphylococcal anti-inflammatory protein that antagonizes the formyl peptide receptor-like 1. *J Immunol* **177**, 8017-8026
139. Palmer, R. M., and Salmon, J. A. (1983) Release of leukotriene B4 from human neutrophils and its relationship to degranulation induced by N-formyl-methionyl-leucyl-phenylalanine, serum-treated zymosan and the ionophore A23187. *Immunology* **50**, 65-73
140. Werz, O., Gerstmeier, J., Libreros, S., De la Rosa, X., Werner, M., Norris, P. C., Chiang, N., and Serhan, C. N. (2018) Human macrophages differentially produce specific resolvin or leukotriene signals that depend on bacterial pathogenicity. *Nature Communications* **9**, 59
141. Prestinaci, F., Pezzotti, P., and Pantosti, A. (2015) Antimicrobial resistance: a global multifaceted phenomenon. *Pathog Glob Health* **109**, 309-318
142. Meirer, K., Steinhilber, D., and Proschak, E. (2014) Inhibitors of the arachidonic acid cascade: interfering with multiple pathways. *Basic Clin Pharmacol Toxicol* **114**, 83-91
143. Haeggstrom, J. Z. (2018) Leukotriene biosynthetic enzymes as therapeutic targets. *J Clin Invest* **128**, 2680-2690

144. Mazaleuskaya, L. L., Lawson, J. A., Li, X., Grant, G., Mesaros, C., Grosser, T., Blair, I. A., Ricciotti, E., and FitzGerald, G. A. (2016) A broad-spectrum lipidomics screen of antiinflammatory drug combinations in human blood. *JCI insight* **1**
145. Boyum, A. (1968) Isolation of mononuclear cells and granulocytes from human blood. Isolation of monuclear cells by one centrifugation, and of granulocytes by combining centrifugation and sedimentation at 1 g. *Scand J Clin Lab Invest Suppl* **97**, 77-89
146. Bremell, T., Lange, S., Svensson, L., Jennische, E., Grondahl, K., Carlsten, H., and Tarkowski, A. (1990) Outbreak of spontaneous staphylococcal arthritis and osteitis in mice. *Arthritis Rheum* **33**, 1739-1744
147. Tuchscherr, L., Bischoff, M., Lattar, S. M., Noto Llana, M., Pfortner, H., Niemann, S., Geraci, J., Van de Vyver, H., Fraunholz, M. J., Cheung, A. L., Herrmann, M., Volker, U., Sordelli, D. O., Peters, G., and Loffler, B. (2015) Sigma Factor SigB Is Crucial to Mediate Staphylococcus aureus Adaptation during Chronic Infections. *PLoS pathogens* **11**, e1004870
148. Schmitt, J., Joost, I., Skaar, E. P., Herrmann, M., and Bischoff, M. (2012) Haemin represses the haemolytic activity of Staphylococcus aureus in an Sae-dependent manner. *Microbiol-Sgm* **158**, 2619-2631
149. Geiger, T., Francois, P., Liebeke, M., Fraunholz, M., Goerke, C., Krismer, B., Schrenzel, J., Lalk, M., and Wolz, C. (2012) The stringent response of Staphylococcus aureus and its impact on survival after phagocytosis through the induction of intracellular PSMs expression. *PLoS Pathog* **8**, e1003016
150. Voyich, J. M., Otto, M., Mathema, B., Braughton, K. R., Whitney, A. R., Welty, D., Long, R. D., Dorward, D. W., Gardner, D. J., Lina, G., Kreiswirth, B. N., and DeLeo, F. R. (2006) Is Panton-Valentine leukocidin the major virulence determinant in community-associated methicillin-resistant Staphylococcus aureus disease? *The Journal of infectious diseases* **194**, 1761-1770
151. Grosz, M., Kolter, J., Paprotka, K., Winkler, A. C., Schafer, D., Chatterjee, S. S., Geiger, T., Wolz, C., Ohlsen, K., Otto, M., Rudel, T., Sinha, B., and Fraunholz, M. (2014) Cytoplasmic replication of Staphylococcus aureus upon phagosomal escape triggered by phenol-soluble modulin alpha. *Cell Microbiol* **16**, 451-465
152. Lauderdale, K. J., Boles, B. R., Cheung, A. L., and Horswill, A. R. (2009) Interconnections between Sigma B, agr, and proteolytic activity in Staphylococcus aureus biofilm maturation. *Infect Immun* **77**, 1623-1635
153. Schleifer, K. H., and Fischer, U. (1982) Description of a New Species of the Genus Staphylococcus - Staphylococcus-Carnosus. *International Journal of Systematic Bacteriology* **32**, 153-156
154. Nippe, N., Varga, G., Holzinger, D., Loffler, B., Medina, E., Becker, K., Roth, J., Ehrchen, J. M., and Sunderkotter, C. (2011) Subcutaneous infection with S. aureus in mice reveals association of resistance with influx of neutrophils and Th2 response. *J Invest Dermatol* **131**, 125-132
155. Romp, E., Arakandy, V., Fischer, J., Wolz, C., Siegmund, A., Loffler, B., Tuchscherr, L., Werz, O., and Garscha, U. (2019) Exotoxins from Staphylococcus aureus activate 5-lipoxygenase and induce leukotriene biosynthesis. *Cell Mol Life Sci*
156. Brzuszkiewicz, E., Bruggemann, H., Liesegang, H., Emmerth, M., Oschlager, T., Nagy, G., Albermann, K., Wagner, C., Buchrieser, C., Emody, L., Gottschalk, G., Hackert, J., and Dobrindt, U. (2006) How to become a uropathogen: Comparative genomic analysis of extraintestinal pathogenic Escherichia coli strains. *P Natl Acad Sci USA* **103**, 12879-12884
157. Chart, H., Smith, H. R., La Ragione, R. M., and Woodward, M. J. (2000) An investigation into the pathogenic properties of Escherichia coli strains BLR, BL21, DH5alpha and EQ1. *J Appl Microbiol* **89**, 1048-1058
158. Gotz, F., and Schumacher, B. (1987) Improvements of Protoplast Transformation in Staphylococcus-Carnosus. *Fems Microbiol Lett* **40**, 285-288
159. Rosenstein, R., and Götz, F. (2013) What Distinguishes Highly Pathogenic Staphylococci from Medium- and Non-pathogenic? in *Between Pathogenicity and*

Commensalism (Dobrindt, U., Hacker, J. H., and Svanborg, C. eds.), Springer Berlin Heidelberg, Berlin, Heidelberg. pp 33-89
160. Wu, H. J., Wang, A. H., and Jennings, M. P. (2008) Discovery of virulence factors of pathogenic bacteria. *Current opinion in chemical biology* **12**, 93-101
161. DuMont, A. L., and Torres, V. J. (2014) Cell targeting by the Staphylococcus aureus pore-forming toxins: it's not just about lipids. *Trends Microbiol* **22**, 21-27
162. Porta, H., Cancino-Rodezno, A., Soberon, M., and Bravo, A. (2011) Role of MAPK p38 in the cellular responses to pore-forming toxins. *Peptides* **32**, 601-606
163. Werz, O., Klemm, J., Samuelsson, B., and Radmark, O. (2000) 5-lipoxygenase is phosphorylated by p38 kinase-dependent MAPKAP kinases. *Proceedings of the National Academy of Sciences of the United States of America* **97**, 5261-5266
164. Koeberle, S. C., Romir, J., Fischer, S., Koeberle, A., Schattel, V., Albrecht, W., Grutter, C., Werz, O., Rauh, D., Stehle, T., and Laufer, S. A. (2011) Skepinone-L is a selective p38 mitogen-activated protein kinase inhibitor. *Nature chemical biology* **8**, 141-143
165. Cheung, G. Y. C., Rigby, K., Wang, R., Queck, S. Y., Braughton, K. R., Whitney, A. R., Teintze, M., Deleo, F. R., and Otto, M. (2010) Staphylococcus epidermidis Strategies to Avoid Killing by Human Neutrophils. *Plos Pathogens* **6**
166. Weiss, E., Hanzelmann, D., Fehlhaber, B., Klos, A., von Loewenich, F. D., Liese, J., Peschel, A., and Kretschmer, D. (2018) Formyl-peptide receptor 2 governs leukocyte influx in local Staphylococcus aureus infections. *FASEB J* **32**, 26-36
167. Surette, M. E., Dallaire, N., Jean, N., Picard, S., and Borgeat, P. (1998) Mechanisms of the priming effect of lipopolysaccharides on the biosynthesis of leukotriene B4 in chemotactic peptide-stimulated human neutrophils. *FASEB journal : official publication of the Federation of American Societies for Experimental Biology* **12**, 1521-1531
168. Christophe, T., Karlsson, A., Dugave, C., Rabiet, M. J., Boulay, F., and Dahlgren, C. (2001) The synthetic peptide Trp-Lys-Tyr-Met-Val-Met-NH2 specifically activates neutrophils through FPRL1/lipoxin A(4) receptors and is an agonist for the orphan monocyte-expressed chemoattractant receptor FPRL2. *Journal of Biological Chemistry* **276**, 21585-21593
169. Dahlgren, C., Christophe, T., Boulay, F., Madianos, P. N., Rabiet, M. J., and Karlsson, A. (2000) The synthetic chemoattractant Trp-Lys-Tyr-Met-Val-DMet activates neutrophils preferentially through the lipoxin A(4) receptor. *Blood* **95**, 1810-1818
170. Cattaneo, F., Parisi, M., and Ammendola, R. (2013) Distinct Signaling Cascades Elicited by Different Formyl Peptide Receptor 2 (FPR2) Agonists. *International journal of molecular sciences* **14**, 7193-7230
171. Radmark, O., Werz, O., Steinhilber, D., and Samuelsson, B. (2007) 5-Lipoxygenase: regulation of expression and enzyme activity. *Trends Biochem Sci* **32**, 332-341
172. Raingeaud, J., Gupta, S., Rogers, J. S., Dickens, M., Han, J., Ulevitch, R. J., and Davis, R. J. (1995) Pro-inflammatory cytokines and environmental stress cause p38 mitogen-activated protein kinase activation by dual phosphorylation on tyrosine and threonine. *J Biol Chem* **270**, 7420-7426
173. Roskoski, R., Jr. (2012) ERK1/2 MAP kinases: structure, function, and regulation. *Pharmacol Res* **66**, 105-143
174. Favata, M. F., Horiuchi, K. Y., Manos, E. J., Daulerio, A. J., Stradley, D. A., Feeser, W. S., Van Dyk, D. E., Pitts, W. J., Earl, R. A., Hobbs, F., Copeland, R. A., Magolda, R. L., Scherle, P. A., and Trzaskos, J. M. (1998) Identification of a novel inhibitor of mitogen-activated protein kinase kinase. *Journal of Biological Chemistry* **273**, 18623-18632
175. Vlahos, C. J., Matter, W. F., and Brown, R. F. (1994) A Specific Inhibitor of Phosphatidylinositol 3-Kinase. *Journal of Cellular Biochemistry*, 274-274
176. Beltman, J., McCormick, F., and Cook, S. J. (1996) The selective protein kinase C inhibitor, Ro-31-8220, inhibits mitogen-activated protein kinase phosphatase-1 (MKP-

1) expression, induces c-Jun expression, and activates Jun N-terminal kinase. *Journal of Biological Chemistry* **271**, 27018-27024
177. Hiller, G., and Sundler, R. (1999) Activation of arachidonate release and cytosolic phospholipase A2 via extracellular signal-regulated kinase and p38 mitogen-activated protein kinase in macrophages stimulated by bacteria or zymosan. *Cell Signal* **11**, 863-869
178. Seno, K., Okuno, T., Nishi, K., Murakami, Y., Yamada, K., Nakamoto, S., and Ono, T. (2001) Pyrrolidine inhibitors of human cytosolic phospholipase A2. Part 2: synthesis of potent and crystallized 4-triphenylmethylthio derivative 'pyrrophenone'. *Bioorg Med Chem Lett* **11**, 587-590
179. Yamamoto, M., Haruna, T., Imura, K., Hikita, I., Furue, Y., Higashino, K., Gahara, Y., Deguchi, M., Yasui, K., and Arimura, A. (2008) Inhibitory effect of a potent and selective cytosolic phospholipase A2alpha inhibitor RSC-3388 on skin inflammation in mice. *Pharmacology* **81**, 301-311
180. Thomas, J. M., Chap, H., and Douste-Blazy, L. (1981) Calcium ionophore A 23187 induces arachidonic acid release from phosphatidylcholine in cultured human endothelial cells. *Biochemical and biophysical research communications* **103**, 819-824
181. Saeki, K., and Yokomizo, T. (2017) Identification, signaling, and functions of LTB4 receptors. *Seminars in Immunology* **33**, 30-36
182. Jackson, W. T., Froelich, L. L., Boyd, R. J., Schrementi, J. P., Saussy, D. L., Schultz, R. M., Sawyer, J. S., Sofia, M. J., Herron, D. K., Goodson, T., Snyder, D. W., Pechous, P. A., Spaethe, S. M., Roman, C. R., and Fleisch, J. H. (1999) Pharmacologic actions of the second-generation leukotriene B-4 receptor antagonist LY293111: In vitro studies. *Journal of Pharmacology and Experimental Therapeutics* **288**, 286-294
183. Chiang, N., Serhan, C. N., Dahlen, S. E., Drazen, J. M., Hay, D. W., Rovati, G. E., Shimizu, T., Yokomizo, T., and Brink, C. (2006) The lipoxin receptor ALX: potent ligand-specific and stereoselective actions in vivo. *Pharmacological reviews* **58**, 463-487
184. Fiore, S., Maddox, J. F., Perez, H. D., and Serhan, C. N. (1994) Identification of a human cDNA encoding a functional high affinity lipoxin A4 receptor. *J Exp Med* **180**, 253-260
185. Chen, Z., and Cole, P. A. (2015) Synthetic approaches to protein phosphorylation. *Current opinion in chemical biology* **28**, 115-122
186. Ardito, F., Giuliani, M., Perrone, D., Troiano, G., and Lo Muzio, L. (2017) The crucial role of protein phosphorylation in cell signaling and its use as targeted therapy (Review). *International journal of molecular medicine* **40**, 271-280
187. Flannagan, R. S., Jaumouille, V., and Grinstein, S. (2012) The cell biology of phagocytosis. *Annual review of pathology* **7**, 61-98
188. Mancuso, P., Standiford, T. J., Marshall, T., and Peters-Golden, M. (1998) 5-Lipoxygenase reaction products modulate alveolar macrophage phagocytosis of Klebsiella pneumoniae. *Infect Immun* **66**, 5140-5146
189. Czop, J. K., and Austen, K. F. (1985) Generation of leukotrienes by human monocytes upon stimulation of their beta-glucan receptor during phagocytosis. *Proc Natl Acad Sci U S A* **82**, 2751-2755
190. Peters-Golden, M., Canetti, C., Mancuso, P., and Coffey, M. J. (2005) Leukotrienes: underappreciated mediators of innate immune responses. *J Immunol* **174**, 589-594
191. Mogensen, T. H. (2009) Pathogen Recognition and Inflammatory Signaling in Innate Immune Defenses. *Clinical microbiology reviews* **22**, 240-+
192. Licona-Limon, I., Garay-Canales, C. A., Munoz-Paleta, O., and Ortega, E. (2015) CD13 mediates phagocytosis in human monocytic cells. *J Leukoc Biol* **98**, 85-98
193. Baranova, I. N., Kurlander, R., Bocharov, A. V., Vishnyakova, T. G., Chen, Z., Remaley, A. T., Csako, G., Patterson, A. P., and Eggerman, T. L. (2008) Role of

human CD36 in bacterial recognition, phagocytosis, and pathogen-induced JNK-mediated signaling. *J Immunol* **181**, 7147-7156
194. Uhlen, M., Fagerberg, L., Hallstrom, B. M., Lindskog, C., Oksvold, P., Mardinoglu, A., Sivertsson, A., Kampf, C., Sjostedt, E., Asplund, A., Olsson, I., Edlund, K., Lundberg, E., Navani, S., Szigyarto, C. A., Odeberg, J., Djureinovic, D., Takanen, J. O., Hober, S., Alm, T., Edqvist, P. H., Berling, H., Tegel, H., Mulder, J., Rockberg, J., Nilsson, P., Schwenk, J. M., Hamsten, M., von Feilitzen, K., Forsberg, M., Persson, L., Johansson, F., Zwahlen, M., von Heijne, G., Nielsen, J., and Ponten, F. (2015) Proteomics. Tissue-based map of the human proteome. *Science* **347**, 1260419
195. Wang, R., Braughton, K. R., Kretschmer, D., Bach, T. H., Queck, S. Y., Li, M., Kennedy, A. D., Dorward, D. W., Klebanoff, S. J., Peschel, A., DeLeo, F. R., and Otto, M. (2007) Identification of novel cytolytic peptides as key virulence determinants for community-associated MRSA. *Nature medicine* **13**, 1510-1514
196. Borgeat, P., and Samuelsson, B. (1979) Transformation of arachidonic acid by rabbit polymorphonuclear leukocytes. Formation of a novel dihydroxyeicosatetraenoic acid. *The Journal of biological chemistry* **254**, 2643-2646
197. Hansson, G., Lindgren, J. A., Dahlen, S. E., Hedqvist, P., and Samuelsson, B. (1981) Identification and biological activity of novel omega-oxidized metabolites of leukotriene B4 from human leukocytes. *FEBS letters* **130**, 107-112
198. Guerra, F. E., Borgogna, T. R., Patel, D. M., Sward, E. W., and Voyich, J. M. (2017) Epic Immune Battles of History: Neutrophils vs. Staphylococcus aureus. *Frontiers in cellular and infection microbiology* **7**, 286
199. Bhakdi, S., Muhly, M., Korom, S., and Hugo, F. (1989) Release of interleukin-1 beta associated with potent cytocidal action of staphylococcal alpha-toxin on human monocytes. *Infect Immun* **57**, 3512-3519
200. Nygaard, T. K., Pallister, K. B., Zurek, O. W., and Voyich, J. M. (2013) The impact of alpha-toxin on host cell plasma membrane permeability and cytokine expression during human blood infection by CA-MRSA USA300. *Journal of leukocyte biology* **94**, 971-979
201. Suttorp, N., Seeger, W., Zucker-Reimann, J., Roka, L., and Bhakdi, S. (1987) Mechanism of leukotriene generation in polymorphonuclear leukocytes by staphylococcal alpha-toxin. *Infection and immunity* **55**, 104-110
202. Rose, F., Dahlem, G., Guthmann, B., Grimminger, F., Maus, U., Hanze, J., Duemmer, N., Grandel, U., Seeger, W., and Ghofrani, H. A. (2002) Mediator generation and signaling events in alveolar epithelial cells attacked by S-aureus alpha-toxin. *Am J Physiol-Lung C* **282**, L207-L214
203. Otto, M. (2011) A MRSA-terious enemy among us: end of the PVL controversy? *Nature medicine* **17**, 169-170
204. Tsuda, Y., Takahashi, H., Kobayashi, M., Hanafusa, T., Herndon, D. N., and Suzuki, F. (2004) Three different neutrophil subsets exhibited in mice with different susceptibilities to infection by methicillin-resistant Staphylococcus aureus. *Immunity* **21**, 215-226
205. Bremm, K. D., Konig, W., Thelestam, M., and Alouf, J. E. (1987) Modulation of granulocyte functions by bacterial exotoxin and endotoxins. *Immunology* **62**, 363-371
206. Hensler, T., Konig, B., Prevost, G., Piemont, Y., Koller, M., and Konig, W. (1994) Leukotriene B4 generation and DNA fragmentation induced by leukocidin from Staphylococcus aureus: protective role of granulocyte-macrophage colony-stimulating factor (GM-CSF) and G-CSF for human neutrophils. *Infect Immun* **62**, 2529-2535
207. Finck-Barbancon, V., Prevost, G., and Piemont, Y. (1991) Improved purification of leukocidin from Staphylococcus aureus and toxin distribution among hospital strains. *Research in microbiology* **142**, 75-85
208. Forsman, H., Christenson, K., Bylund, J., and Dahlgren, C. (2012) Receptor-dependent and -independent immunomodulatory effects of phenol-soluble modulin peptides from Staphylococcus aureus on human neutrophils are abrogated through peptide inactivation by reactive oxygen species. *Infect Immun* **80**, 1987-1995

209. Wan, M., Godson, C., Guiry, P. J., Agerberth, B., and Haeggstrom, J. Z. (2011) Leukotriene B4/antimicrobial peptide LL-37 proinflammatory circuits are mediated by BLT1 and FPR2/ALX and are counterregulated by lipoxin A4 and resolvin E1. *FASEB journal : official publication of the Federation of American Societies for Experimental Biology* **25**, 1697-1705
210. Lee, H. Y., Jo, S. H., Lee, C., Baek, S. H., and Bae, Y. S. (2006) Differential production of leukotriene B4 or prostaglandin E-2 by WKYMVm or serum amyloid A via formyl peptide receptor-like 1. *Biochemical Pharmacology* **72**, 860-868
211. Buczynski, M. W., Stephens, D. L., Bowers-Gentry, R. C., Grkovich, A., Deems, R. A., and Dennis, E. A. (2007) TLR-4 and sustained calcium agonists synergistically produce eicosanoids independent of protein synthesis in RAW264.7 cells. *J Biol Chem* **282**, 22834-22847
212. Verdon, J., Girardin, N., Lacombe, C., Berjeaud, J. M., and Hechard, Y. (2009) delta-hemolysin, an update on a membrane-interacting peptide. *Peptides* **30**, 817-823
213. Karlsson, J., Stenfeldt, A. L., Rabiet, M. J., Bylund, J., Forsman, H. F., and Dahlgren, C. (2009) The FPR2-specific ligand MMK-1 activates the neutrophil NADPH-oxidase, but triggers no unique pathway for opening of plasma membrane calcium channels. *Cell Calcium* **45**, 431-438
214. Bjorstad, A., Askarieh, G., Brown, K. L., Christenson, K., Forsman, H., Onnheim, K., Li, H. N., Teneberg, S., Maier, O., Hoekstra, D., Dahlgren, C., Davidson, D. J., and Bylund, J. (2009) The host defense peptide LL-37 selectively permeabilizes apoptotic leukocytes. *Antimicrob Agents Chemother* **53**, 1027-1038
215. Malishev, R., Tayeb-Fligelman, E., David, S., Meijler, M. M., Landau, M., and Jelinek, R. (2018) Reciprocal Interactions between Membrane Bilayers and S. aureus PSM alpha 3 Cross-alpha Amyloid Fibrils Account for Species-Specific Cytotoxicity. *Journal of Molecular Biology* **430**, 1431-1441
216. Evans, J. H., Spencer, D. M., Zweifach, A., and Leslie, C. C. (2001) Intracellular calcium signals regulating cytosolic phospholipase A2 translocation to internal membranes. *J Biol Chem* **276**, 30150-30160
217. Christophe, T., Karlsson, A., Rabiet, M. J., Boulay, F., and Dahlgren, C. (2002) Phagocyte activation by Trp-Lys-Tyr-Met-Val-Met, acting through FPRL1/LXA4R, is not affected by lipoxin A4. *Scand J Immunol* **56**, 470-476
218. Cash, J. L., Norling, L. V., and Perretti, M. (2014) Resolution of inflammation: targeting GPCRs that interact with lipids and peptides. *Drug Discovery Today* **19**, 1186-1192
219. Foxman, E. F., Campbell, J. J., and Butcher, E. C. (1997) Multistep navigation and the combinatorial control of leukocyte chemotaxis. *Journal of Cell Biology* **139**, 1349-1360
220. Ng, L. G., Qin, J. S., Roediger, B., Wang, Y., Jain, R., Cavanagh, L. L., Smith, A. L., Jones, C. A., de Veer, M., Grimbaldeston, M. A., Meeusen, E. N., and Weninger, W. (2011) Visualizing the neutrophil response to sterile tissue injury in mouse dermis reveals a three-phase cascade of events. *J Invest Dermatol* **131**, 2058-2068
221. Ferguson, A. D. (2012) Structure-based drug design on membrane protein targets: human integral membrane protein 5-lipoxygenase-activating protein. *Methods Mol Biol* **841**, 267-290
222. Evans, J. F., Ferguson, A. D., Mosley, R. T., and Hutchinson, J. H. (2008) What's all the FLAP about?: 5-lipoxygenase-activating protein inhibitors for inflammatory diseases. *Trends Pharmacol Sci* **29**, 72-78
223. Konig, S., Romp, E., Krauth, V., Ruhl, M., Dorfer, M., Liening, S., Hofmann, B., Hafner, A. K., Steinhilber, D., Karas, M., Garscha, U., Hoffmeister, D., and Werz, O. (2018) Melleolides from Honey Mushroom Inhibit 5-Lipoxygenase via Cys159. *Cell chemical biology*
224. Mancini, J. A., Waterman, H., and Riendeau, D. (1998) Cellular oxygenation of 12-hydroxyeicosatetraenoic acid and 15-hydroxyeicosatetraenoic acid by 5-lipoxygenase

is stimulated by 5-lipoxygenase-activating protein. *The Journal of biological chemistry* **273**, 32842-32847
225. Liening, S., Scriba, G. K., Rummler, S., Weinigel, C., Kleinschmidt, T. K., Haeggstrom, J. Z., Werz, O., and Garscha, U. (2016) Development of smart cell-free and cell-based assay systems for investigation of leukotriene C4 synthase activity and evaluation of inhibitors. *Biochimica et biophysica acta* **1861**, 1605-1613
226. Strid, T., Svartz, J., Franck, N., Hallin, E., Ingelsson, B., Soderstrom, M., and Hammarstrom, S. (2009) Distinct parts of leukotriene C(4) synthase interact with 5-lipoxygenase and 5-lipoxygenase activating protein. *Biochem Biophys Res Commun* **381**, 518-522
227. Bair, A. M., Turman, M. V., Vaine, C. A., Panettieri, R. A., and Soberman, R. J. (2012) The nuclear membrane leukotriene synthetic complex is a signal integrator and transducer. *Mol Biol Cell* **23**, 4456-4464
228. Mancini, J. A., Coppolino, M. G., Klassen, J. H., Charleson, S., and Vickers, P. J. (1994) The binding of leukotriene biosynthesis inhibitors to site-directed mutants of human 5-lipoxygenase-activating protein. *Life sciences* **54**, PL137-142
229. Vickers, P. J., O'Neill, G. P., Mancini, J. A., Charleson, S., and Abramovitz, M. (1992) Cross-species comparison of 5-lipoxygenase-activating protein. *Mol Pharmacol* **42**, 1014-1019
230. Abramovitz, M., Wong, E., Cox, M. E., Richardson, C. D., Li, C., and Vickers, P. J. (1993) 5-lipoxygenase-activating protein stimulates the utilization of arachidonic acid by 5-lipoxygenase. *Eur J Biochem* **215**, 105-111
231. Orsburn, B. C., Stockwin, L. H., and Newton, D. L. (2011) Challenges in plasma membrane phosphoproteomics. *Expert review of proteomics* **8**, 483-494

APPENDIX 1: Curriculum Vitae

Persönliches

Dipl.-Pharm. Erik Romp

Geboren am 20.07.1990 in Arnstadt, Thüringen

Berufserfahrung

Jan. 2019 bis heute	Apotheker - Centrum Apotheke Jena
Jun. 2015 bis Dez. 2015	Vertretungsapotheker - Apotheke im Hauptbahnhof Leipzig

Akademischer Werdegang

Jun. 2015 bis Dez. 2018	wissenschaftlicher Mitarbeiter und Promotionsstudent Friedrich-Schiller-Universität Jena, Lehrstuhl für Pharmazeutische/ Medizinische Chemie unter Prof. Dr. O. Werz
Mai 2015	Approbation als Apotheker (3. Staatsexamen)
Nov. 2014 bis Mai 2015	Pharmazeut im Praktikum - 3. Halbjahr: Apotheke im Hauptbahnhof Leipzig
Mai 2014 bis Okt. 2014	Pharmazeut im Praktikum - 2. Halbjahr: Apotheke im Uniklinikum Leipzig
Nov. 2013 bis Apr. 2014	Pharmazeut im Praktikum - 1. Halbjahr: Diplom am Lehrstuhl für Pharmazeutische/Medizinische Chemie der Friedrich-Schiller-Universität Jena (*Charakterisierung des dualen sEH und FLAP-Inhibitors I-12 / In-vitro-Testung angewandter Pharmaka auf sEH-Inhibition*)
Okt. 2009 bis Sep. 2013	Studium der Pharmazie - Friedrich-Schiller-Universität Jena

Schulbildung

Aug. 2001 bis Jul. 2009	Neideck Gymnasium Arnstadt (seit 2007 Staatliches Gymnasium Arnstadt)
Aug. 1997 bis Jul. 2001	Grundschule II in Arnstadt

Lehrerfahrungen

Jun. 2015 bis Jul. 2018	Betreuung des Studentenpraktikums *„Arzneimittelanalytik, Drug Monitoring, toxikologische und umweltrelevante Untersuchungen“*
März 2017	Antrittskolloquium und Seminar im Studentenpraktikum *„Quantitative Bestimmung von Arznei-, Hilfs- und Schadstoffen (unter Einbeziehung von Arzneibuchmethoden)“*
Jun. 2015 bis Dez. 2018	Betreuung diverser Masteranden, Diplomanden und Wahlpflichtfachstudenten

APPENDIX 2: List of publications and conference contributions

List of publications

1. *Exotoxins from Staphylococcus aureus activate 5-lipoxygenase and induce leukotriene biosynthesis.* **Romp E**, Arakandy V, Fischer J, Wolz C, Siegmund A, Löffler B, Tuchscherr L, Werz O, and Garscha U. Cell Mol Life Sci. 2019, in press
2. *Liquid chromatography-coupled mass spectrometry analysis of glutathione conjugates of oxygenated polyunsaturated fatty acids.* Liening S, **Romp E**, Werz O, Scriba GKE, and Garscha U. Prostaglandins Other Lipid Mediat. 2019 Oct 144:106350
3. *Targeting biosynthetic networks of the proinflammatory and proresolving lipid metabolome.* Werner M, Jordan PM, **Romp E**, Czapka A, Rao Z, Kretzer C, Koeberle A, Garscha U, Pace S, Claesson HE, Serhan CN, Werz O, and Gerstmeier J. FASEB J. 2019 May 33 (5):6140-6153
4. *Gliotoxin from Aspergillus fumigatus abrogates the biosynthesis of neutrophil chemotactic leukotriene B_4 through inhibition of leukotriene A_4 hydrolase.* König S, Pace S, Pein H, Heinekamp T, Kramer J, **Romp E**, Straßburger M, Troisi F, Proschak A, Scherlach K, Rossi A, Sautebin L, Haeggström JZ, Hertweck C, Brakhage AA, Gerstmeier J, Proschak E, and Werz O. Cell Chem Biol. 2019 Apr 18 26 (4):524-534
5. *Melleolides from honey mushroom inhibit 5-lipoxygenase via Cys159.* König S, **Romp E**, Krauth V, Rühl M, Dörfer M, Hofmann B, Häfner A, Steinhilber D, Karas M, Garscha U, Hoffmeister D, and Werz O. Cell Chem Biol. 2019 Jan 17 26 (1):60-70
6. *Synthesis, Biological Evaluation and Structure-Activity Relationships of Diflapolin Analogues as Dual sEH/FLAP Inhibitors.* Vieider L, **Romp E**, Temml V, Fischer J, Kretzer C, Schoenthaler M, Taha A, Hernández-Olmos V, Sturm S, Schuster D, Werz O, Garscha U, and Matuszczak B. ACS Med Chem Lett. 2018 Nov 29 10 (1):62-66
7. *Pharmacological profile and efficiency in vivo of diflapolin, the first dual inhibitor of 5-lipoxygenase-activating protein and soluble epoxide hydrolase.* Garscha U, **Romp E**, Pace S, Rossi A, Temml V, Schuster D, König S, Gerstmeier J, Liening S, Werner M, Atze H, Wittmann S, Weinigel C, Rummler S, Scriba GK, Sautebin L, and Werz O. Sci Rep. 2017 Aug 24 7 (1):9398
8. *Discovery of the first dual inhibitor of the 5-lipoxygenase-activating protein and soluble epoxide hydrolase using pharmacophore-based virtual screening*. Temml V, Garscha U, **Romp E**, Schubert G, Gerstmeier J, Kutil Z, Matuszczak B, Waltenberger B, Stuppner H, Werz O, and Schuster D. Sci Rep. 2017 Feb 20 (7):42751
9. *5-Lipoxygenase-activating protein rescues activity of 5-lipoxygenase mutations that delay nuclear membrane association and disrupt product formation.* Gerstmeier J, Newcomer ME, Dennhardt S, **Romp E**, Fischer J, Werz O, and Garscha U. FASEB J. 2016 May 30 (5):1892-90

Conference contributions

- *Bioactive Lipids: From Chemistry to Biology and Medicine,* Athens, Greece, 29. - 31.03.2018, Oral presentation: Pathogenic bacteria and their pore-forming toxins induce 5-lipoxygenase activation via elevation of $[Ca^{2+}]_i$ in human cells
- *DPhG Annual Meeting 2017, Novel Therapies for Future Challenges*, Saarbrücken, Germany, 26. – 29.09.2017 Poster presentation: Diflapolin, a novel dual inhibitor of 5-lipoxygenase-activating protein (FLAP) and soluble epoxide hydrolase (sEH)

APPENDIX 3: Eigenständigkeitserklärung

Hiermit bestätige ich, Erik Romp, dass mir die gültige Promotionsordnung der Fakultät für Biowissenschaften der Friedrich-Schiller-Universität Jena bekannt ist und ich diese Dissertation selbstständig angefertigt habe. Des Weiteren habe ich keine Textabschnitte eines Dritten oder eigene Prüfungsarbeiten ohne Kennzeichnung übernommen und alle verwendeten Hilfsmittel, persönlichen Mitteilungen und Quellen in meiner Arbeit angegeben.

Zur Erarbeitung dieser Dissertation und zur Auswahl und Auswertung der Materialien sowie zur Erstellung des Manuskriptes habe ich weiterhin nur die Hilfe von Prof. Dr. O. Werz und Prof. Dr. U. Garscha in Anspruch genommen und Dritten weder unmittelbare noch mittelbare geldwerte Leistungen im Zusammenhang mit den Inhalten dieser Arbeit gezahlt. Darüber hinaus habe ich keine Hilfe einer kommerziellen Promotionsvermittlung in Anspruch genommen.

Ich versichere, dass die hier vorgelegte Dissertation zuvor weder für eine staatliche noch eine andere wissenschaftliche Prüfung eingereicht wurde. Zudem habe ich weder diese Arbeit, noch eine gleiche oder in wesentlichen Teilen ähnliche Version oder eine andere Abhandlung bei einer anderen Hochschule oder Fakultät vorgelegt.

_____ _____

Ort, Datum Unterschrift

Um ganz wir selbst zu sein, müssen wir unser wahres Selbst zulassen.
So einfach ist das. Es liegt nur an uns, wenn es schwer erscheint.
John Strelecky